UC Berkeley
UC Berkeley Electronic Theses and Dissertations

Title

Phytochemical Disruption of Hormone Receptor Expression and Intracellular Signaling in Human Reproductive Cancer Cells

Permalink
https://escholarship.org/uc/item/9jh0t9c5

Author
Marconett, Crystal Nicole

Publication Date
2009

Peer reviewed|Thesis/dissertation

eScholarship.org Powered by the California Digital Library
University of California

Phytochemical Disruption of Hormone Receptor Expression and Intracellular Signaling in Human Reproductive Cancer Cells

By

Crystal Nicole Marconett

B.S. (University of California, Santa Cruz) 2005

A dissertation submitted in partial satisfaction of the

Requirements for the degree of

Doctor of Philosophy

In

Molecular and Cell Biology

in the

Graduate Division

of the

University of California, Berkeley

Committee in charge:

Professor Gary L. Firestone, Chair

Professor Len F. Bjeldanes

Professor G. Steven Martin

Professor Lin He

Fall 2009

ABSTRACT

Phytochemical Disruption of Hormone Receptor Expression and Intracellular Signaling in Human Reproductive Cancer Cells

By

Crystal Nicole Marconett

Doctor of Philosophy in Molecular and Cell Biology

University of California, Berkeley

Professor Gary Firestone, Chair

ERα is a critical target of therapeutic strategies to control the proliferation of hormone dependent breast cancers. Preferred clinical options have significant adverse side effects that can lead to treatment resistance due to the persistence of active estrogen receptors. This thesis details the molecular mechanism indole-3-carbinol (I3C) initiates to ablate ERα expression and subsequent downstream targets of ERα transcriptional activity; IRS1, IGF1R, and hTERT and the ability of an aqueous mixture from the *Scutellaria Barbata* plant, BZL101, to arrest the proliferation of human reproductive cancer cells, regardless of hormonal status. I3C dependent activation of the aryl hydrocarbon receptor (AhR) initiates Rbx-1 E3 ligase-mediated ubiquitination and proteasomal degradation of ERα protein. I3C disrupts endogenous GATA3 interactions with the ERα promoter, leading to a loss of GATA3 and ERα expression. Ectopic expression of GATA3 has no effect on I3C induced ERα protein degradation but does prevent I3C inhibition of ERα promoter activity, demonstrating the importance of GATA3 in this I3C triggered cascade. Our preclinical results implicate I3C as a novel anti-cancer agent in human cancers that co-express ERα, GATA3 and AhR, a

combination found in a large percentage of breast cancers but not in other critical ERα target tissues essential to patient health. Estrogen signaling stimulates growth and proliferation of these cells by activation of key downstream targets, such as Insulin-like Growth Factor Receptor-1 (IGF1R) and Insulin Receptor Substrate-1 (IRS1) of the Insulin-like Growth Factor (IGF1) signaling pathway. We show that I3C downregulates both IGF1R and IRS1 RNA and protein expression. We established that this decrease in expression was contingent upon Estrogen Receptor-α (ERα) ablation by I3C. I3C is able to block hTERT expression through a loss of transcriptional activation. I3C mediated loss of hTERT expression was attributed to disrupted endogenous binding to a composite ERα -Sp1 site. The block in hTERT expression disrupted telomerase activity, and ectopic expression of hTERT was able to restore telomerase activity. We have uncovered a critical role I3C employs to block the proproliferative activities of IGF signaling and telomerase activity in hormone sensitive breast cancer cells. Aqueous extracts from BZL101 were able to disrupt estrogen expression in the hormone MCF7 cell line. Specifically, BZL101 induced a G1 cell cycle arrest and ablation of Cyclin D, CDK2, and CDK4 expression in MCF7 cells. MDA-MB-231 and PC3 cells arrested in S phase with corresponding ablations in Cyclin A2 and CDK2. LNCaP cells arrested in G2/M phase upon exposure to BZL101 with a corresponding decrease in Cyclin B1 and CDK1. Our results indicate that BZL101 exerts cell type specific molecular changes that lead to arrest of reproductive cancer proliferation and the general disruption of ERα by phytochemicals is a potent disruptor of hormone sensitive cancer growth and proliferation.

_____

Gary Firestone, PhD

ACKNOWLEDGEMENTS

First and foremost I would like to thank Professor Gary Firestone for believing in me when no one else within the department would. Gary, I will never be able to thank you enough for taking me into your lab, knowing I was a risk, and allowing me the freedom and flexibility within my research to thrive. Thank you also for allowing me to train members of the lab, letting me gain valuable experience and interpersonal skills. I also wanted to thank you for never giving up on me, even after my qualifying exam. I'll never forget the spirited discussions in lab meeting, which have made me a more discerning and thoughtful scientist. After all, "Nothing is etched in stone"

Second, I would like to thank my parents, Sean K. Lynch and Vickie Ann Lynch. You both taught be to strive for success, encouraged and supported me through this difficult process, and believed in me. You helped me in every way possible, from the purchase of my computer to the washing of my unmentionables, all so I could focus on my research.

Third, I would like to thank Doctor Shyam Sundar. Shyam, you bequeathed me three thesis projects, which have led to the three chapters within this thesis. Thank you for everything you have done, all of the thoughtful scientific discussions, the voice of experience, and yes, the drama too. Life would be too boring without it! I wish you, Nithya, and Shiva the best wherever you go.

My undergraduates and group members have made this thesis possible through their sheer determination and tireless effort.

-Kevin Poindexter- You made the AhR paper possible! Working side-by-side with you for a whole year, I felt like I really got to know you. I saw your many great strengths, the compassion for others, your kind and selfless nature. Your cooperative spirit and technical prowess aided me greatly. I was so happy for you when you were accepted to graduate school. I believe Karma will give you many rewards for your hard work.

-Travis Morgenstern- The BZL man! You're tireless effort on an impossible task has brought coherency to this project. Thank you for staying with my group so long and enduring the drug shortages, cell contaminations, batch inconsistencies, and all manner of difficulties that you effortlessly rise above.

-Ankur Singhal- My master's Student! It seems like yesterday Gary introduced you to me and we did immunofluorescence together, and since then you've grown to become a critical and intelligent scientist. Your collaboration with the IGF project has expanded the scope of the project into new uncharted territory. Thank you for all your effort.

I would also like to thank my committee members; Len Bjeldanes, Steve Martin, and Lin He, who inspired confidence in me and my research while providing alternate fresh ideas.

In addition, I would like to thank all the undergraduates I had the pleasure of mentoring. The time we shared together was dynamic, at times stressful, fruitful, and

ultimately special. Adrianna San Ramon, Gretchen Arnason, Tuff Witarama, Shreya Ramesh, and my adopted undergrad Vickie Aivaliotis, I wish you all health and happiness.

My colleagues in the Firestone lab have shared more with me than any other group of friends I have ever had. I would like to specially acknowledge Andrea, Jamin, and Theresa for your impact upon me. You were all mentors and sources of inspiration, not only as scientists but also as friends.

Lastly, I would like to thank my husband Pat for putting up with me and all of my late nights in lab.

This work is dedicated to my grandmother

Beryl Whitaker

Who lost her courageous battle with

malignant melanoma

on

February 10th, 1990.

Your struggle inspired my life's passion

TABLE OF CONTENTS

List of Figures ……viii

General Introduction…….....xiii

Chapter I

Indole-3-carbinol disrupts an ERα-GATA3 transcriptional cross-regulatory loop by triggering AhR-dependent ERα protein degradation in breast cancer cells……..1

Abstract…….....2

Introduction……..3

Materials and Methods…….....8

Results……....15

Discussion……..56

Chapter II

A. Indole-3-Carbinol (I3C) abrogates mitogenic cell growth in hormone sensitive human breast cancer by ablating estrogen-dependent expression of Insulin-Like Growth Factor Receptor (IGF1R) and Insulin Receptor Substrate-1 (IRS-1)……..62

Abstract…….…63

Introduction……64

Materials and Methods……..….67

Results……....71

Discussion……..91

B. I3C ablates expression and activity of the catalytic TERT subunit of the telomerase enzyme through ablation of ER α expression and Sp1 activity……...93

Abstract……..94

Introduction……....95

Materials and Methods…….…..97

Results…….....100

Discussion……...….109

<u>Chapter III</u>

Ban Zhu Lain (BZL), a natural herbal mixture derived from the Scuttelaria Barbata plant, is able to inhibit breast and prostate cancer cell cycle progression by multiple mechanisms……...111

Abstract…….…...112

Introduction…….….113

Materials and Methods…….……116

Results…….….122

Discussion……154

Chapter IV

Conclusions and Future Directions…….…….158

Conclusion……...159

Future Directions…….162

References……...166

LIST OF FIGURES

General Introduction Figures

Figure 1: Classical mode of ERα action……...…….…..xvi

Figure 2: Classical model of xenbiotic activation of AhR……..…..xx

Figure 3: Insulin-like growth factor receptor signaling…….xxvi

Figure 4: Cell Cycle…….…xxxiii

Chapter I Figures

Figure 5: Effects on kinetics of ERα expression……..……..16

Figure 6: I3C downregulation of ERα protein is blocked by the proteasome inhibitor MG132……19

Figure 7: I3C induces the ubiquitination and 26S proteasome degradation of ERα protein and requirement of the Rbx1 E3 ubiquitin ligase in this degradative process…….21

Figure 8: I3C mediated degradation of ERα protein requires AhR…….…….24

Figure 9: I3C induces the nuclear localization of AhR…….27

Figure 10: DIM and Tryptophol fail to induce the downregulation of ERα seen with I3C and its chemically modified derivatives…….30

Figure 11: Effects of I3C on the expression of GATA3 protein and transcripts…....33

Figure 12: The observed half-maximal downregulation of GATA3 is 150 μM

I3C and involvement of GATA3 in ERα regulation…….……36

Figure 13: GATA3 is expressed in hormone sensitive breast cancer cell lines and I3C disrupts this expression……38

Figure 14: I3C disrupts ERα protein interaction with GATA3 regulatory regions....40

Figure 15: I3C downregulation of GATA3 gene expression requires the I3C mediated loss of ERα protein……...….43

Figure 16: I3C inhibition of ERα transcript levels requires the downregulation of GATA3 gene expression…….……46

Figure 17: The I3C inhibition of ERα promoter activity requires the downregulation of GATA3 gene expression…….……48

Figure 18: Identification of the I3C responsive region of the ERα promoter and the I3C responsive transcription factor…….……..51

Figure 19: GATA3 endogenous binding to the ERα promoter decreases with I3C...54

Figure 20: Proposed mechanism for the I3C disruption of a cross-regulatory positive feedback loop involving expression of GATA3 and ERα by stimulating the degradation of ERα protein…….57

Chapter IIA Figures

Figure 21: The observed half maximal downregulation of IGF1R and IRS1 is 150 μM I3C……...….72

Figure 22: Effect of I3C on the expression of IGF1R and IRS1 protein and transcripts……....74

Figure 23: IGF1R and IRS1 are expressed in hormone sensitive breast cancer cell lines and I3C disrupts this expression……...…..77

Figure 24: DIM and Tryptophol fail to induce the downregulation of IGF1R and IRS1 seen with I3C…….……80

Figure 25: I3C blocks estrogen dependent expression of IGF1R and IRS1 protein and transcript expression……...82

Figure 26: I3C disrupts ERα protein interaction with IGF1R and IRS1 regulatory regions……..86

Figure 27: I3C downregulation of IGF1R and IRS1 gene expression requires the I3C mediated loss of ERα protein…….……..89

Chapter II-B Figures

Figure 28: I3C is able to disrupt the estrogen dependent stimulation of hTERT expression and increase Sp1 phosphorylation……101

Figure 29: I3C disrupts endogenous binding of ERα and Sp1 at a critical regulatory site within the hTERT promoter ……...…….104

Figure 30: I3C dependent inhibition of telomerase activity is overcome by exogenous expression of hTERT…….…107

Chapter III Figures

Figure 31: BZL101 inhibits proliferation of human breast and prostate cancer cells…….……..123

Figure 32: Dependence of BZL101 concentration on increased cellular debris…...126

Figure 33: BZL101 increases the amount of cellular debris in hormone dependent and independent breast and prostate cancer cell lines……....128

Figure 34: Comparison of BZL101 induced cellular debris to cell cycle arrest in MDA-MB-231 cells……..….131

Figure 35: BZL101 induction of cell cycle arrest in hormone sensitive and insensitive breast and prostate cancer cell lines…….……..133

Figure 36: Protein levels of cell cycle regulators exhibit downregulation with BZL101……136

Figure 37: BZL101 disrupts RNA levels of key cell cycle regulatory components and steroid receptors……140

Figure 38: BZL101 sustained loss of cell cycle component expression over time……143

Figure 39: BZL101 sustained loss of cell cycle component and steroid receptor expression over time…….….146

Figure 40: BZL101 alters growth factor receptor expression and intracellular signaling in hormone sensitive MCF7 breast cancer cells……...……149

Figure 41: BZL101 alters cellular morphology…….....152

Figure 42: Proposed model for the BZL101 disruption of cell cycle progression in hormone sensitive and insensitive breast and prostate cancer cell lines……..…155

INTRODUCTION

Normal estrogen action within the breast

Mammary gland development and function is regulated by complex signaling networks requiring the concerted action of growth factors and hormones. Estrogen and progesterone are hormones identified as critical for the development of the breast. These hormones act at a cellular level to increase expression of cell cycle progression factors that allow for the normal proliferation of the mammary gland. Estrogen binds to one of several congnate receptors to exert its cellular action.

There are two major subtypes of estrogen receptor, estrogen receptor alpha (ERα) and estrogen receptor beta (ERβ). 17-β-estradiol (E_2) binding to ERα induces the hormone receptor complex to bind to DNA sequences termed estrogen-response elements (EREs) present in the cis regulatory regions of genes. EREs are short consensus palindromic sequences with a variable sequence spacer. The hormone receptor interaction with ERE allows for enhanced recruitment of the basal transcription machinery and increased rates of transcription. Conversely, when estrogen binds to ERβ in estrogen sensitive tissues, it represses downstream target gene transcription. The dichotomy between ERα and ERβ allows for the proliferative action of estrogens to take place through ERα, but also inhibits overactivity through ERβ mediated repression. This introduces negative feedback to modulate the activation of gene expression of

downstream targets, including protein factors involved in the specification of cell fate. This is shown in figure 1.

Figure 1:

Classical mode of estrogen action. Estrogenic activities in breast cancer are mediated by 17-β-estradiol binding to one of two receptor subtypes, ERα and ERβ. Once activated, they can form homodimers or heterodimers with each other, each of these complexes can bind to estrogen response elements on DNA and modulate transcription of target genes. ERa can also heterodimerize with other transcription factors and bind to composite DNA elements, or act through protein-protein interactions with other transcription factors bound to DNA.

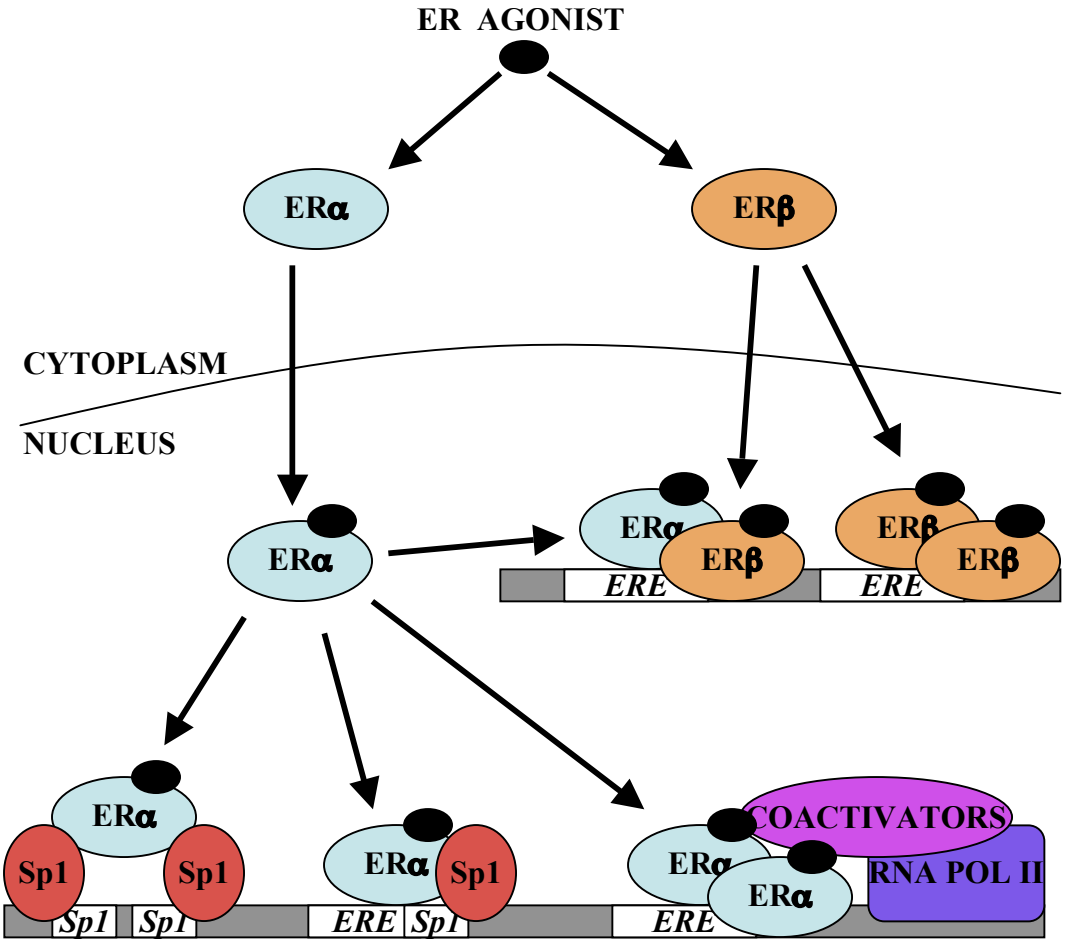
ER AGONIST
ERα
ERβ
CYTOPLASM
NUCLEUS
ERα
ERα
ERβ
ERβ
ERβ
ERE
ERE
ERα
Sp1
Sp1
Sp1
Sp1
ERα
Sp1
ERE
Sp1
ERα
ERα
COACTIVATORS
RNA POL II
ERE

Studies have demonstrated a multitude of transcription factors acting in concert to regulate the transcription of ERα mRNA from the estrogen receptor-1 (*ESR1*) gene. *ESR1* gene transcription initiates from at least six separate promoters (A-F) spanning over 50kB of upstream regulatory sequence, each of which splices into a common 5' UTR. Expression of ERα at each of these promoters differs according to tissue specificity and malignancy, with promoter B identified with abberant expression in human carcinoma. Additionally, mRNA levels can be regulated by microRNAs, which bind to the 3' UTR of *ESR1* mRNA and block efficient translation, effectively shutting off ERα protein production.

Direct effects on the rate on protein degradation also regulate ERα expression. Protein degradation occurs through a highly conserved sequence of events. Ubiquitin, a short protein sequence, serves as the signal for degradation by the proteasome when attached as a post-translational modification to the target protein. Increased degradation of ERα occurs in response to multiple stimuli. Estrogen binding to ERα increases the receptor's degradation through conformational shifts that allow E3 ubiquitin ligase binding to occur in addition to DNA binding. This process is thought to increase overall gene transcription by displacing older ERα protein-protein complexes, allowing for tighter regulation of target gene transcription.

Aryl Hydrocarbon Receptor Signaling

Xenobiotic chemicals are also implicated to increase ERα degradation through activation of the aryl hydrocarbon receptor (AhR), a protein involved in the metabolism of foreign compounds. Ligand binding causes AhR to adopt an active conformation allowing it to complex with aryl hydrocarbon receptor nuclear translocator (ARNT), which translocates activated AhR to the nucleus (figure 2). Translocated AhR can then bind to consensus dioxin response elements (DREs), also known as xenobiotic response elements (XREs), and activate downstream target gene transcription. DRE's were discovered through the activation of AhR by the highest affinity AhR ligand known to date, 2, 3, 7, 8-tetrochlorodibenzo-p-dioxin, a particular example of the wider halogenated polycyclic aromatic hydrocarbon family commonly referred to as "dioxins". Genes required for the metabolism of xenobiotic compounds contain DRE elements. Therefore, activation of AhR by xenobiotic ligands allows for the metabolism of ligands, removing them as a potential hazard from the body.

Figure 2:

Classical model of xenobiotic activation of AhR. Xenobiotic ligand binding to AhR induces association with ARNT, causeing the AhR-ARNT complex to nuclear translocated and bind consensus DRE sequence elements, which allows AhR to modulate target gene expression.

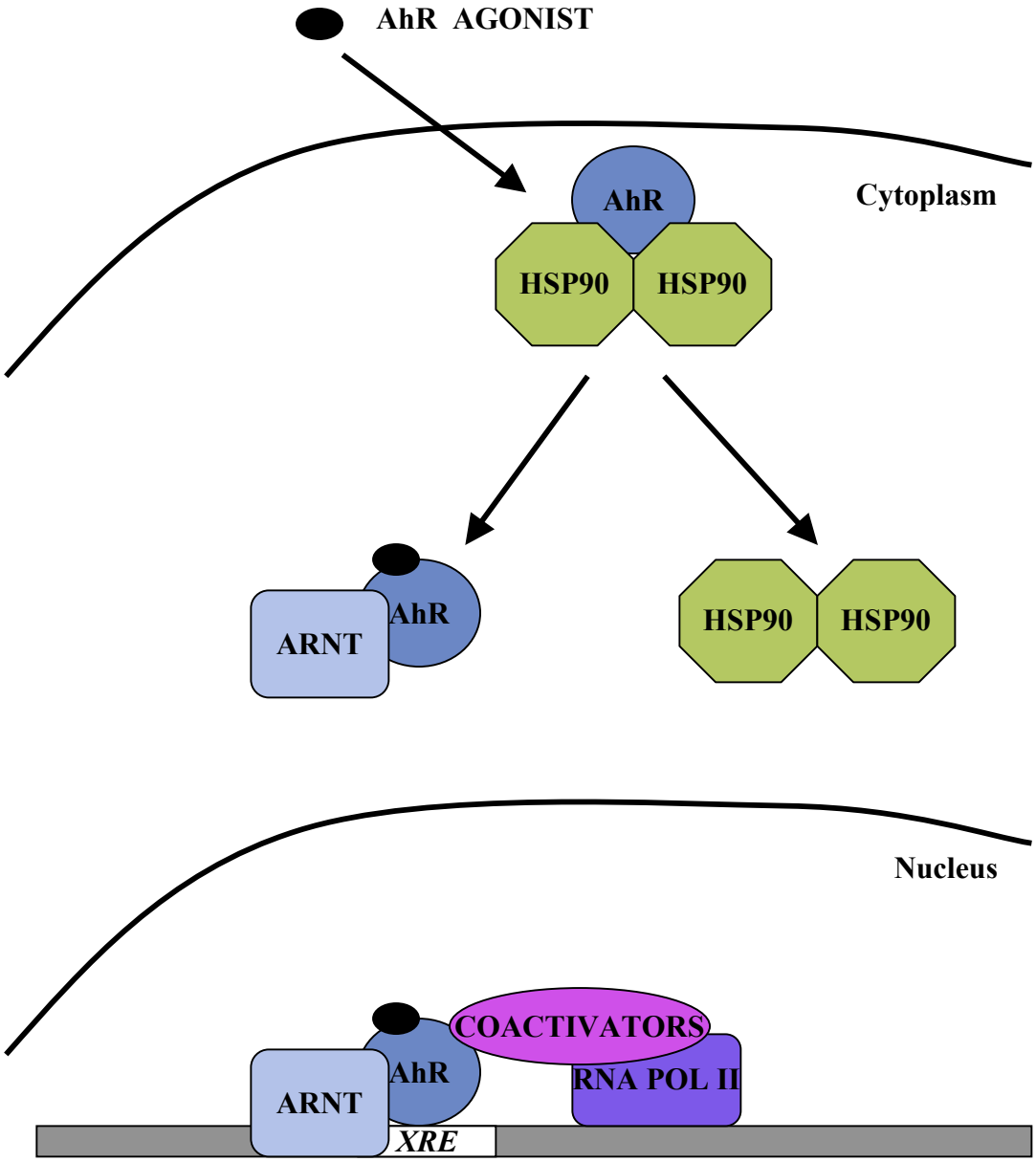

Drugs Fut 2004, 29(5): 479

Xenobiotic chemicals introduced into the body are not limited to the liver and can penetrate a variety of tissues. As a result, AhR is normally expressed in a wide variety of tissues, suggesting a larger role in cellular regulation. In breast cancer not only is AhR expressed, but AhR activation leads to both classical metabolism target expression as well as non-classical protein degradative effects on ERα. AhR does this by recruiting the E3 ubiquitin ligase Rbx1 complexed with accessory Cullin proteins serving as scaffolds to attach ubiquitin to the ERα substrate. Therefore, AhR activation antagonizes estrogen signaling in breast cancer. Conversely, it has been reported that activation of estrogen signaling can block expression of specific downstream targets of AhR signaling. Therefore a complex interplay between these two signaling pathways exists in which activation of AhR antagonizes ERα and inversely activation of ERα suppresses AhR. This negative regulation may contribute to the balance of hormone signaling with environmental cues in the breast.

Estrogen receptor transcriptional activation

Association of ERα with DNA allows for the recruitment of accessory proteins, which increase the rate of recruitment of the transcription machinery allowing for increased activation of target gene expression. Classical targets of ERα include pS2, which is highly expressed in breast cancer and correlated to ER status, Cathepsin D, a lysosomal protease involved in cellular invasion and apoptosis, and Progesterone

Receptor (PR), itself a steroid receptor whose activity is necessary temporally after ERα signaling during the menstrual cycle. Conformational changes associated with ligand binding to ERα also allow for the binding of other proteins through two distinct trans-activation domains present in ERα; AF1 and AF2. E_2 induced activation of ERα causes the formation of ERα-ERα homodimers, which are able to bind to the palindromic repeat sequence of the classical ERE.

The AF1 and AF2 domains also allow for complex formation with other DNA binding transcription factors, such as Stable Protein 1 (Sp1) and FBJ murine osteosarcoma viral oncogene (Fos), known commonly as a component of the AP1 transcription complex. These heterodimers bind to composite sequence elements present in target gene regulatory regions. In the case of ER-Sp1, the Sp1 protein binds to a consensus CG rich sequence and ERα binds an adjacent half ERE site composed of half the ERE sequence and without the linker bases. ERα can also stimulate downstream target expression solely through protein interactions and without DNA binding. The discovery of estrogen regulated genes without canonical ERE or composite element sites have shown ERα playing a role in protein recruitment and activation without DNA binding.

Genome-wide sequence analysis has revealed the presence of EREs throughout the genome. This has led to the molecular characterization of genes previously thought to be regulated by estrogen including Insulin-like Growth Factor-1 (IGF1), the mitogenic

ligand initiating downstream MAPK signaling, and GATA3, a zinc finger containing transcription factor important for T cell lineage and breast development.

The GATA3 transcription factor in breast cancer

GATA3 is one of six members of the GATA binding protein family, so named for their zinc finger domains' ability to bind conserved GATA DNA elements within the regulatory regions of target genes. Each GATA is expressed in a conserved pattern during development. GATA1, GATA2, and GATA3 are responsible for hematopoetic differentiation, with GATA1/GATA2 involved in leukocyte differentiation and GATA3 critical for lymphocyte fate. GATA4, GATA5, and GATA6 are involved in muscle and skeletal tissue development, with GATA4 being involved in cardiomyocyte differentiation and GATA5/GATA6 responsible for smooth muscle development. GATA3 activity as a transcription factor is ascribed to a specific subset of downstream target genes, including the TCRα enhancer region, Interleukin 4 (IL4), and Interleukin 18 receptor accessory protein (IL19RAP), which are involved in T cell differentiation.

Deregulated expression of GATA factors has been characterized in several types of cancer. For example, aberrant expression of GATA4/GATA5 has been demonstrated in ovarian cancer, while hypermethylation of GATA4/GATA5 regulatory regions, which results in epigenetic silencing, has been observed in colorectal and gastric cancer. GATA3 expression has been intimately tied to estrogen sensitive breast cancer, with ninety seven percent of ERα positive breast cancers coexpressing GATA3 and eighty two

percent of GATA3 positive breast cancers expressing ERα. This high level of correlation between ERα and GATA3 expression patterns has been characterized to a functional level, with increased ERα binding to ERE elements within GATA3 regulatory regions upon E_2 activation.

Insulin-like growth factor receptor signaling in hormone sensitive breast cancer

Another pathway regulated by estrogen signaling is the Insulin-like growth factor mitogen pathway. Insulin-like growth factor receptor (IGF1R) is a receptor tyrosine kinase that once bound by Insulin-like growth factor (IGF1) autophosphorylates its intracellular domain, recruiting the insulin receptor substrate (IRS1) through binding of the phosphtyrosine binding (PTB) domain to the phosphorylated sites. Phosphorylation of IRS1 in turn activates downstream PI3K and Ras signaling to increase cellular survival and proliferation, respectively (figure 3).

Figure 3:

Insulin-like growth factor receptor signaling. IGF1 ligand binding to one of three receptor tyrosine kinase family members (IR, IGF1R, IGFF2R) induces downstream autophosphorylation and activation of IRS1. Pathway branching occurs at this point, with activation of Ras-MAPK signaling leading to proliferation or differentiation or activation of AKT signaling leasing to enhanced survival by blocking apoptosis.

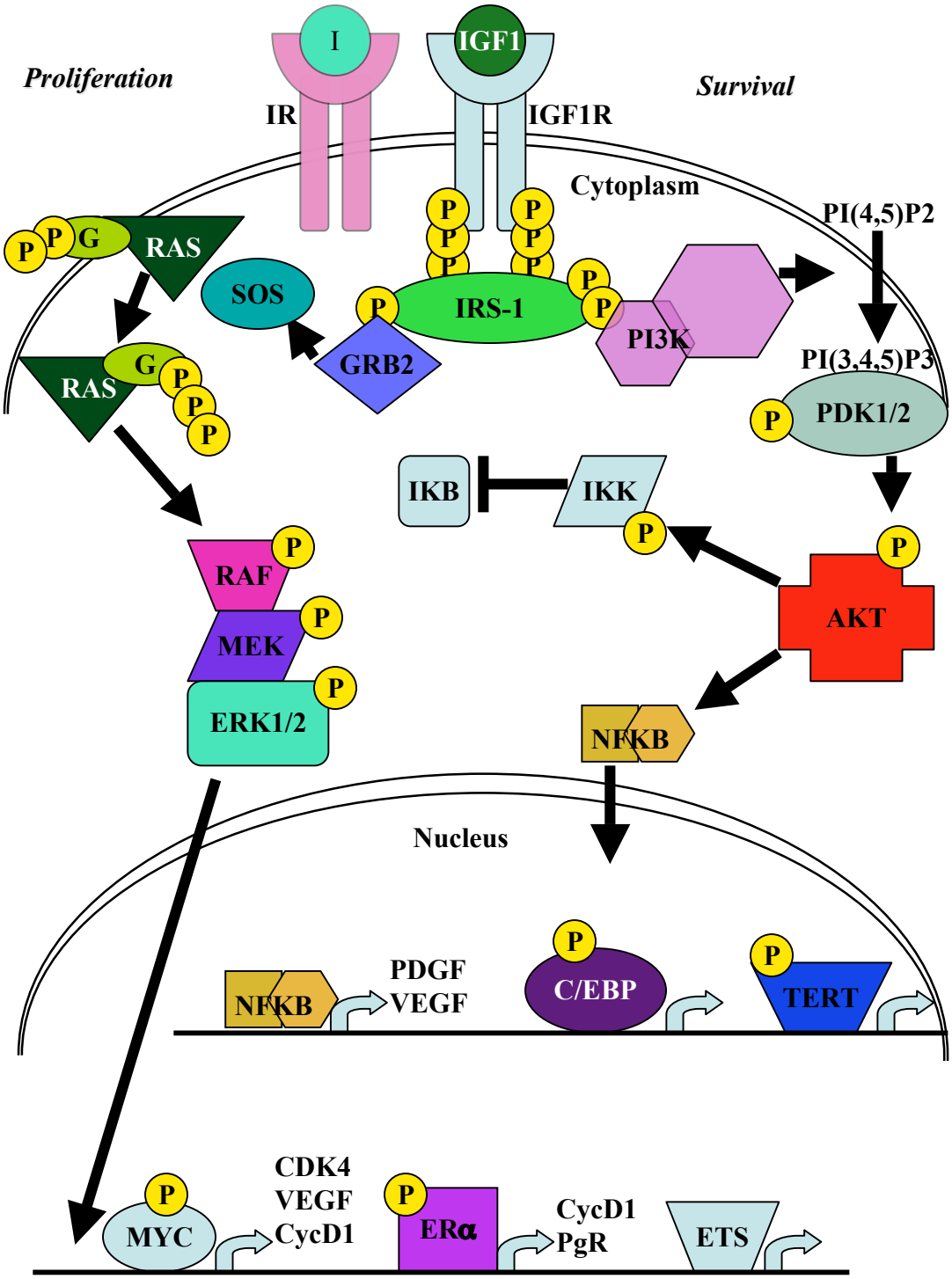
Proliferation
Survival
I
IGF1
IR
IGF1R
Cytoplasm
PI(4,5)P2
P
G
RAS
SOS
IRS-1
GRB2
PI3K
PI(3,4,5)P3
PDK1/2
IKB
IKK
RAF
MEK
ERK1/2
AKT
NFKB
Nucleus
PDGF
VEGF
C/EBP
TERT
CDK4
VEGF
CycD1
MYC
ERα
CycD1
PgR
ETS

During development growth hormone secretion activates the expression of IGF1 in the liver, which results in high levels of circulating IGF1. This then affects the processes associated with growth, such as bone growth from the epiphyseal plate during adolescence. Increased levels of circulating IGF1 are observed in women with hormone sensitive breast cancer, with on average a nine-fold increase in IGF1R expression in these cancers. Mechanistic studies have determined that E2 is able to stimulate expression of IGF1R and IRS1 in hormone sensitive breast cancers. Conversely, IGF1R activation can induce the phosphorylation of ERα at Ser118. This cross-talk between pathways has been observed in hormone sensitive breast cancers treated with selective estrogen receptor modulators (SERMs) and has spurred investigation into possible synergistic effects of combination ERα antagonists and IGF inhibitors. Combination therapies have demonstrated enhanced antiproliferative and signaling inhibition in hormone sensitive breast cancers leading to decreased reoccurrence.

Telomerase activity in hormone sensitive breast cancer

The constant division of cancerous cells puts enormous replicative stress on the cell, inducing DNA damage. Maintenance of DNA structure is aided by the telomerase ribonucleoprotein enzyme. Telomerase was initially discovered as the enzyme capable of extenting repeat DNA sequences at the telomeric end region of chromosomes, but has

recently ascribed activity in DNA damage repair and blocking cellular scenescence. Telmorease is composed of both RNA and protein components. Telomerase RNA (TR) serves as a template for the extension of telomeric DNA sequence. Telomerase protein (TERT) maintains RNA structure and houses the catalytic activity of telomerase.

Cells regulate the activity of telomerase by tightly controlled expression of the TERT protein component. Constitutive expression of TR RNA allows for immediate assembly of the telomerase complex upon expression of TERT protein. Normal expression of TERT occurs during development in specific tissues such as the neural tube, and the expression is highly regulated in adult tissues. Abberant TERT expression occurs in upwards of ninety five percent of breast cancers, making telomerase, and therefore ablation of TERT, an attractive target for new therapeutics. Estradiol is able to stimulate TERT expression, which is attributed to increased binding of ERα to a composite ERα-Sp1 element within the TERT promoter. This contributes to the increased expression of TERT and therefore to telomere extention, repair of DNA damage, and blocking cellular scenescense, allowing the abberant immortalization of breast cancer cells.

Indole-3-carbinol and breast cancer

Epidemiological evidence has shown that diets with increased cruciferous vegetable consumption have decreased cancer incidence. Cruciferous vegetables contain glucobrassicin, a precursor that when ingested is broken down into indole-3-carbinol.

I3C has demonstrated antiproliferative activity in human reproductive cancer cells, specifically in prostate and breast. I3C is able to induce a G1 cell cycle arrest, which can be attributed to specific molecular changes occurring within breast cancer cells, namely the ablation of CDK6 expression through modulation of Sp1 activity. More recently, elastase has been identified as a target of I3C small molecule binding. I3C-dependent inhibition of elastase activity blocks cyclinE processing and prevents nuclear transloaction of CDK2, a kinase critical to cell cycle progression.

I3C is not the only component from cruciferous vegetables able to block breast cancer cell proliferation. Once ingested I3C is subjected to acid condensation in the stomach, resulting in a plethora of acid condensation products, including 3, 3'-diindoylylmethane (DIM). DIM has demonstrated anticancer properties, which are distinct from I3C, including the stimulation of immune function in mice, activation of interferon gamma (IFNγ), and altered estrogen metabolite processing.

In addition to an overall effect of growth, I3C is able to specifically ablate ERα expression in hormone sensitive breast cancer cells. This is a property intrinsic to I3C and distinct from DIM, as DIM does not alter expression levels of ERα in hormone sensitive breast cancer cells and can lead to abberant activation of ERα in human endometrial tissue. Prior to this study the I3C disruption of ERα promoter activity was established, however the mechanism of action was undetermined.

Phytochemical anticancer compounds and the cancer cell cycle

Cellular proliferation is a multistep process requiring the concerted activities of a number of proteins involved in cell cycle progression. Induction of cellular growth through the activation of growth factor pathways or steroid receptors leads to increased expression of cyclinD1, which when complexed with cyclin dependent kinase 4 (CDK4) hypophosphorylates retinoblastoma protein. This permits the binding of cyclinE-CDK2 complexes to hyperphosphorylate Rb, releasing E2F1 from Rb's constraint. E2F1 activity as a transcription factor allows for expression of many S phase cell cycle components, including cyclinA, which in complexes of cyclinA-CDK2 phosphorylate and induce origin of replication opening and the initiation of S phase. Once DNA replication progresses cyclinB1-CDK1 complexes are able to initiate anaphase, which allow for mitosis and for the process to repeat (figure 4).

Cyclins are so named for their specific expression in certain phases of the cell cycle, ones in which their activities are required for cell cycle progression. Blocking expression of cell cycle components can block the ability of the cell to progress through the cell cycle, inducing a cell cycle arrest, which, if unable to be overcome can induce the cellular machinery to execute programmed cell death, or apoptosis. Blocking cell cycle progression is key to inhibition of breast cancer proliferation. Therefore the development of drugs which specifically disrupt the expression of key cell cycle components has been key to the development of chemotherapeutics.

Ban Zhi Lian (BZL101) an aqueous extract of the *Scutellaria barbata* plant has demonstrated antiproliferative effects in a limited number of cancers, including lung cancer and leukemia. It has been shown to affect glycolysis, and to disrupt cellular survival leading to apoptosis. These combined effects demonstrate potential for isolation of the active compounds within BZL101 and potential development as an anticancer compound.

Figure 4:

Cell cycle phases and select cell cycle regulators. Proliferation stimuli lead to increased G1-S phase cell cycle progression through hyperphosphorylation of Rb. Subsequent release of E2F1 transcription factor turns on expression of S phase regulatory proteins (Cyclin A, CDK2), allowing for origin firing and DNA replication. Cyclin B1-CDK1 activity allows for anaphase onset and chromatid separation, allowing the cycle to repeat.

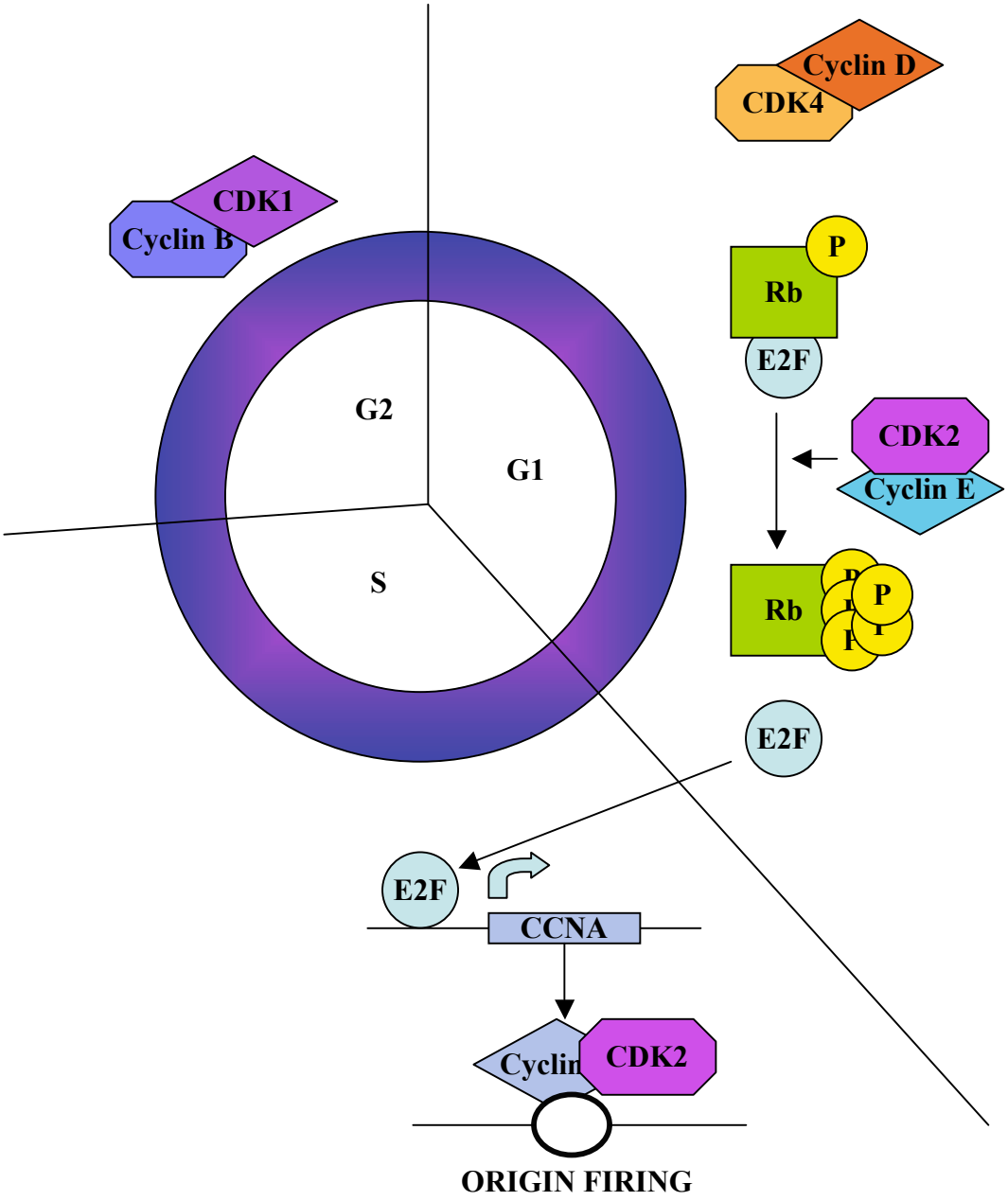
Cyclin D
CDK4
CDK1
Cyclin B
P
Rb
E2F
G2
G1
S
CDK2
Cyclin E
Rb
P
E2F
E2F
CCNA
Cyclin
CDK2
ORIGIN FIRING

Chapter I

Indole-3-carbinol triggers AhR-dependent ERα protein degradation in breast cancer cells disrupting an ERα-GATA3 transcriptional cross-regulatory loop

ABSTRACT

ERα is a critical target of therapeutic strategies to control the proliferation of hormone dependent breast cancers. Preferred clinical options have significant adverse side effects that can lead to treatment resistance due to the persistence of active estrogen receptors. We have established the cellular mechanism by which indole-3-carbinol (I3C), a promising anti-cancer phytochemical from Bassica genius vegetables, ablates ERα expression, and have uncovered a critical role for the GATA3 transcription factor in this indole-regulated cascade. I3C dependent activation of the aryl hydrocarbon receptor (AhR) initiates Rbx-1 E3 ligase-mediated ubiquitination and proteasomal degradation of ERα protein. I3C inhibits endogenous binding of ERα with the 3'-enhancer region of GATA3 and disrupts endogenous GATA3 interactions with the ERα promoter, leading to a loss of GATA3 and ERα expression. Ectopic expression of GATA3 has no effect on I3C induced ERα protein degradation but does prevent I3C inhibition of ERα promoter activity, demonstrating the importance of GATA3 in this I3C triggered cascade. Our preclinical results implicate I3C as a novel anti-cancer agent in human cancers that co-express ERα, GATA3 and AhR, a combination found in a large percentage of breast cancers but not in other critical ERα target tissues essential to patient health.

INTRODUCTION

One of the challenges in developing new therapeutic strategies for human breast cancer is the existence of several distinct classes of mammary tumors that differ in their phenotypes and proliferative responses to hormonal cues. It is critical to distinguish these properties in order to match the appropriate treatment to the corresponding tumor type (Brenton et al., 2005). Estrogens are a class of steroid hormones that play a critical role in the development of the normal breast and in the genesis of hormone-dependent and independent breast cancer (Fuqua et al., 1991; Pasqualini and Chetrite, 2005). The existing options for the clinical management of hormone-dependent breast cancers are the use of selective estrogen receptor modulators (SERMs), such as tamoxifen, that can block ligand-dependent receptor activation (Dutertre and Smith, 2000) or inhibitors of aromatase activity that prevent estrogen synthesis, such as exemestane and letrozole (Miller, 1999). Both classes of therapeutic agents are prescribed to treat hormone-dependent early stage breast cancer, however, a limitation of their effectiveness is the development of tumor resistance within approximately five years of initiating either therapy due to the persistence of functional estrogen receptors (Clarke et al., 2003). These treatments do not alter cellular levels of estrogen receptor protein and estrogen receptor activity is maintained by ligand-independent activation due to selective receptor phosphorylation, which can lead to more aggressive forms of hormone independent cancers (Badia et al., 2007).

A biological complexity in the development of more effective therapeutic strategies that target estrogen receptor expression in human cancers is the existence of two major estrogen receptor subtypes, estrogen receptor-alpha (ERα) and estrogen receptor-beta (ERβ). (Enmark and Gustafsson, 1999) Each receptor subtype is encoded by different genes that trigger distinct cellular and physiological responses (Chang et al., 2006). After ligand activation, ERα and ERβ regulate the transcription of unique but overlapping sets of target genes (Harris et al., 2002), although both receptors are capable of activating synthetic reporter plasmids driven by estrogen response elements (ERE). Normal and cancerous breast epithelium express both ERα and ERβ. A high ERα: ERβ ratio correlates positively with enhanced cellular proliferation (Ali and Coombes, 2000; Lee et al., 2008); whereas predominance of functional ERβ over ERα is associated decreased proliferation (Campbell-Thompson et al., 2001; Roger et al., 2001; Shaaban et al., 2003). Consistent with the proliferative effect of estrogens being mediated primarily by ERα, ablation of ERα in mouse mammary glands leads to a severely underdeveloped mammary epithelium. While ERβ expression is preserved in ERα null epithelium, the impaired mammary epithelial cell growth cannot be rescued by administration of pharmacological levels of estrogens (Bocchinfuso and Korach, 1997), suggesting that ERα mediates the proliferative effects of estrogens. This is further strengthened by clinical observations where high-risk precancerous breast lesions were shown to possess elevated ERα levels and declining ERβ expression (Roger et al., 2001; Shaaban et al., 2003), which implicates the direct involvement of ERα with the estrogen mediated increase in tumorigenicity in humans (Ali and Coombes, 2000).

The majority of ERα positive breast cancers respond well to anti-hormonal therapy (Colozza et al., 2008), although only fulvestrant (ICI-182780), a selective estrogen receptor down-regulator (SERD) used in clinical trials, has been shown to reduce the level of total ERα protein to block both ligand-dependent and -independent receptor activation (Osborne et al., 2004). Fulvestrant, similar to the currently used SERMs and aromatase inhibitors, has significant systemic side effects (Mercier et al., 2003), and an emerging priority is the development of new classes of SERDs that effectively target ERα expression selectively in human breast cancers with minimal to no side effects. Epidemiological and physiological studies have suggested that phytochemicals from vegetables and fruits represent intriguing natural sources for new classes of potential anti-cancer molecules with minimal adverse side effects that function as SERDs. One such phytochemical is indole-3-carbinol (I3C), a natural compound derived by hydrolysis from glucobrassicin produced in Brassica cruciferous vegetables such as cabbage, broccoli and Brussels sprouts.

I3C exhibits potent anti-carcinogenic properties in a wide range of human cancers such as lung, liver, colon, cervical, endometrial, prostate and breast cancer (Aggarwal and Ichikawa, 2005; Kim and Milner, 2005; Safe et al., 2008; Weng et al., 2008). Exposure of human cancer cells to I3C triggers complementary sets of transcriptional, cell signaling, enzymatic, and metabolic cascades that directly lead to cell cycle arrest and apoptosis (Cover *et al.*, 1999; Rahman *et al.*, 2004; Garcia *et al.*, 2005). Within the context of this anti-proliferative environment, there is compelling evidence in estrogen sensitive human breast cancer cell lines, such as MCF7 and T47D, that I3C treatment

disrupts estrogen responsive gene expression (Cover *et al.*, 1998; Auborn *et al.*, 2003; Wang *et al.*, 2006) and inhibits estrogen dependent proliferation. I3C does not bind to either ERα or ERβ (Cover et al., 1999); the endocrine disrupting effects of this indole are due to its strong downregulation of ERα protein and transcript expression, as well as the activation of ERβ (Sundar et al., 2006). Consistent with these effects on estrogen responsive proliferation, I3C cooperates with tamoxifen to more effectively ablate phosphorylation of retinoblastoma protein accompanied by a G1 cell cycle arrest of MCF7 cells (Cover et al., 1999). In addition, I3C disrupts the estrogenic responses of ERα selective agonists such as propyl pyrazole triol, and in transient transfections of human breast cancer cells, I3C strongly attenuated ERα gene (*ESR1*) promoter activity (Sundar et al., 2006). An understanding of the precise pathway by which I3C disrupts ERα expression will potentially lead to the design of new clinical applications for I3C and improve patient outcomes through targeted therapies of human breast cancers. However, identification of the I3C triggered cascade and the indole regulated transcription factors that direct the loss of ERα expression and responsiveness in human breast cancer cells has remained elusive.

One of the critical regulators of *ESR1* gene promoter activity that is involved in mammary gland development is the GATA3 transcription factor (Asselin-Labat et al., 2007). GATA3 expression is positively correlated with ERα expression in 97% of breast cancer biopsies (Hoch et al., 1999), suggesting a functional association between GATA3 status and the ER+ breast cancer phenotype. The physiological significance of GATA3 in ERα expression is further strengthened by studies showing that ERα and GATA3

knockout mice exhibit marked similarities in that both mouse mammary glands display severe developmental deficiencies in epithelial morphogenesis (Asselin-Labat et al., 2007). One explanation for these physiological observations is that GATA3 and ERα are involved in a cross-stimulatory positive feedback loop that helps to drive proliferation of estrogen-sensitive breast cancer cells (Eeckhoute et al., 2007). Activated ERα binds to a 3'-enhancer in the *GATA3* gene to activate its transcription, and the GATA3 transcription factor stimulates *ESR1* transcription through multiple binding sites in the *ESR1* gene promoter (Eeckhoute et al., 2007). We now demonstrate in estrogen responsive human breast cancer cells that I3C triggers the ubiquitin 26S proteasome mediated degradation of ERα protein in a cascade that requires the aryl hydrocarbon receptor (AhR) and the E3 ubiquitin ligase ring box-1 (Rbx1). This I3C triggered loss of ERα protein then directly disrupts the GATA3/ ERα cross-regulatory loop, which results in the downregulation of *ESR1* promoter activity leading to the ablation of ERα expression and loss of ERα responsive proliferation.

MATERIALS AND METHODS

Reagents

ERα, GATA3, AhR, and Rbx1 antibodies were purchased from Santa Cruz Biotechnology (Santa Cruz, CA). I3C, MG132, and DMSO were obtained from Sigma Chemical Company (St. Louis, MO). All other chemicals were of the highest quality available.

Cell Culture

MCF7 human breast cancer cells were obtained from American Type Culture Collection (Manassas, VA). Cells were grown in Dulbecco's Modified Eagles Medium (DMEM) from BioWhittaker (Walkersville, MD), supplemented with 10% fetal bovine serum from Mediatech (Manassas, VA), 10 μg/ml insulin, 50 U/ml penicillin, 50 U/ml streptomycin, and 2 mM L-glutamine from Sigma (St. Louis, MO). Cells were grown to subconfluency in a humidified chamber at 37°C containing 5% CO_2. A 200 mM stock solution of I3C was dissolved in DMSO. I3C was then diluted 1:1000 in media prior to culture plate application.

Western Blotting

After the indicated treatments, western blots were performed as previously indicated (Sundar et al., 2006). Mouse anti-ERα (sc-8005) and goat anti-Rbx1 (sc-5201) were diluted 1:200 in TBST. Rabbit anti GATA3 (sc-9009) was diluted 1:500 in TBST. Hsp90 (#610419 BD Transduction laboratories, Franklin Lakes, NJ) and actin (#AAN01 Cytoskeleton, Inc. Denver, CO) were used as loading controls, and antibodies for these were diluted 1:2000 and 1:1000 respectively, in TBST. Immunoreactive proteins were

detected after incubation with horseradish peroxidase-conjugated secondary antibodies diluted $3x10^{-4}$ in 1% NFDM in TBST. Blots were then treated with enhanced chemiluminescence reagents (Eastman Kodak, Rochester NY) visualization on film.

Immunoprecipitation

After the indicated treatments, immunoprecipitations were performed as previously described (Failor et al., 2007). Precleared samples were then incubated with 50 μg mouse anti-ERα or 50 μg rabbit anti-AhR overnight at 4°C. Immunoprecipitated protein was eluted from beads by addition of GLB and heating the sample at 100°C for 5 minutes. Samples were analyzed by Western blot as described before (Sundar et al., 2007).

siRNA, shRNA, and Overexpression Plasmid Transfection

Cells were grown and indicated treatments performed on 10 cm tissue culture plates from Nunc (Fisher Scientific, Rochester, NY). Once cells reached 50% confluency transfection with siRNA constructs was performed using siRNA transfection reagent (sc-29528) from Santa Cruz Biotechnology (Santa Cruz, CA) using control siRNA (#1022076) from Qiagen (Valencia, CA) or Rbx1-specific siRNA (sc-44072) from Santa Cruz Biotechnology following transfection reagent manufacturer protocol. Short-hairpin RNA plasmids directed against AhR (TI378261) or against GFP (TR30003) were obtained from Origene Technologies, Inc (Rockville, MD). Human CMV-GATA3 overexpression plasmid and CMV-GATA-KRR dominant negative plasmid were a kind gift from Dr. Astar Winoto, Dept. of Molecular and Cell Biology, University of California, Berkeley, CA. Human CMV-ERα was a kind gift from Dr. Benita Katzenellenbogen, University of Illinois at Urbana-Champagne. Transfection of

expression vectors and shRNA plasmids were performed using Polyfect transfection reagent from Qiagen (Valencia, California) per manufacturers' recommended protocol.

Immunofluorescence

Cells were grown and indicated treatments performed on 2 well chamber slides from Nunc (Fisher Scientific, Rochester, NY). The cells were fixed with 3.75% formaldehyde in PBS for 15 min at room temperature. After three additional washes with PBS, the plasma membrane was permeabilized with 0.1% Triton-X-100; 10 mM Tris-HCl at pH 7.5, 120 mM sodium chloride; 25 mM potassium chloride, 2 mM EGTA; and 2 mM EDTA) for 10 min at room temperature. Slides were incubated with 3% BSA (Sigma) before incubation with primary antibodies. Rabbit anti-AhR antibody (sc-8088 Santa Cruz Biotechnology, Santa Cruz, CA) was used at a 1:400 dilution. Secondary Alexa488 anti-rabbit and Texas Red-conjugated phalloidin were used at 1:400 dilutions each. Stained cells were mounted with Vectashield Mounting medium containing DAPI (Vector Laboratories, Burlingame, CA). Stained and mounted cells were then processed with a Zeiss Axioplan epiflourescence microscope (Carl Zeiss, Thornwood, NY).

RT-PCR

Total RNA from MCF7 cells treated with indicated compounds was isolated with TRI Reagent according to manufacturer's protocol from Sigma (St. Louis, MO). Total RNA (4 μg) was used to synthesize cDNA using Moloney murine leukemia virus-reverse transcriptase from Promega Corp (Madison, WI) with random hexamers as primers. The cDNA reaction product (200 ng) was amplified with primers of the following sequences:

ERα Forward: 5'-AGCACCCAGTGAAGCTACT-3',

ERα Reverse: 5'-TGAGGCACACAAACTCCT-3';

GATA3 Forward: 5'-CTCATTAAGCCCAAGCGAAG-3',

GATA3 Reverse 5'-TTTTTCGGTTTCTGGTCTGG -3';

GAPDH Forward 5'-TGAAGGTCGGAGTCAACGGATTTG-3',

GAPDH Reverse: 5'- CATGTGGGCCATGAGGTCCACCAC-3'. PCR products were analyzed on 1.2% agarose gel along with 1-kb Plus DNA ladder from Invitrogen (Carlsbad, CA) and the products were visualized with GelRed from Biotium (Hayward, CA).

ERα Promoter Fragment and Mutation generation

pERα-3794-pgl2 and pERα-860-pgl2 plasmids were kind gifts from Dr. Lisa McPherson, Stanford University. pERα-2294, pERα-1892, and pERα-985 were amplified from purified genomic DNA isolated from LNCaP prostate cancer cells using the restriction enzymes MluI and BglII from New England Biolabs (Ipswich, MA). Restriction sites were engineered into the following PCR primers:

-2294: 5'-CTCGAGTCGGCCCTTGACTTCTACA-3', and

+46: 5'-GGCGCCTTGCTGCTGTCCAGGTACA-3';

-1892: 5'-TGCCATTCCACGCACAAACACATC-3', and

+109: 5'-TAAGTACTGGTCTCCCGA'-3;

-985, 5'-ATGTGTGTGTGTATGTGCGTGT-3' and

+285, 5'-AAAGAGCACAGCCCGAGGTTAGA-3'.

For PCR amplification a 50 μl PCR reaction (1xVENT polymerase buffer Mg^{2+} free, 0.2 mM dNTPs, 1U of VENT Polymerase (NEB), 1.5 mM $MgCl_2$, 0.2 μM each primer) was amplified for 38 cycles (30sec/94°C, 30sec/58°C, 2.5min/72°C) with a 94°C 1-min hot start. Sequence was confirmed by automated DNA sequencing (UC Berkeley

Sequencing Facility). PCR products from all constructs were purified using QIAEXII Gel Extraction Kit from Qiagen (Valencia, CA), digested with MluI and BglII, and subcloned into PGL2-basic from Promega (Madison WI).

Mutations in the predicted transcription factor binding sites were introduced using the pERα-2294-pgl2 construct as a template. Primer sequences with the indicated mutations were as follows;

GATA3-1 Forward:

5'-GGCATTTGATCCACATGGCGCCCAGAAGGCTTTTATTG-3',

GATA3-1 Reverse:

5'-CAATAAAAGCCTTCTGGGCGCCATGTGGATCAAATGCC-3';

GATA3-2 Forward:

5'-GTCCTATTTTGTAAACTTGGCGCCCATACACTTTTGACTGG-3',

GATA3-2 Reverse:

5'-CCAGTCAAAAGTGTATGGGCGCCAAGTTTACAAAATAGGAC-3';

Ap1 Forward:

5'-CTATTTTAGCCGTAAGACTATTGATCACAGCAAGCCTGTTTTTCCTC-3',

Ap1 Reverse:

5'-GAGGAAAAACAGGCTTGCTGTGATCAATAGTCTTACGGCTAAAATAG-3'.

pERα-2294-pgl2 was used as a template for the mutagenesis reactions. Template DNA (5ng) was mixed with 125 ng of each primer and mutagenesis was performed using the Stratagene Lighting QuickChange mutagenesis kit per the manufacturer's instructions.

Luciferase Assays

MCF7 cells grown to 70% confluency in six-well Nunc plates were transfected with 2 μg/well of the indicated plasmid construct. Transfections were performed in serum-free medium using Superfect (Qiagen) transfection reagent as per manufacturer's instructions. Cells were treated 24 hr post-transfection with DMSO or 200 μM I3C for 24 hr. Cells were then lysed and relative luciferase activity was evaluated using the Promega Luciferase Assay kit (Promega Corp., Madison, WI). Relative luciferase activities were normalized to protein input and pERα-3794-pgl2 construct activity with standard error. Reproducibility of these results was verified by three independent experiments performed with triplicate samples of each treatment.

Chromatin Immunoprecipitation (ChIP) Assays

MCF7 cells were grown to subconfluency and treated for 48 hr with 200 μM I3C or DMSO vehicle control. ChIP was performed as previously described (Sundar et al, 2008). Primers for ChIP experiments were as follows:

pERα-GATA3-2207 site Forward: 5'-AATGCCTCTGTTCAGAGACTGGG-3',

Reverse: 5'-GCTTGCTGTGAATCATAGTCTTACGGC-3';

pERα-GATA3-3812 site Forward: 5'-TTTAATCTGGGTGGCTGGAG-3',

Reverse: 5'-CTCAACTTCCCCGTGTCTGT-3'

GATA3 3'Enhancer-ERα site Forward: 5'- GATGTTAGGGAGTGACCAAAGAGG-3',

Reverse: 5'- GTGGACAAGTTTGATCCTTTAAGCTCTG-3'.

MCF7 cells were grown to subconfluency and treated for 48 hr with 200 μM I3C or DMSO vehicle control. ChIP was performed as previously described (Sundar et al, 2008). Primers for ChIP experiments were as follows:

pERα-GATA3-2207 site Forward: 5'-AATGCCTCTGTTCAGAGACTGGG-3',

Reverse: 5'-GCTTGCTGTGAATCATAGTCTTACGGC-3';

pERα-GATA3-3812 site Forward: 5'-TTTAATCTGGGTGGCTGGAG-3',

Reverse: 5'-CTCAACTTCCCCGTGTCTGT-3'

GATA3 3'Enhancer-ERα site Forward: 5'- GATGTTAGGGAGTGACCAAAGAGG-3',

Reverse: 5'- GTGGACAAGTTTGATCCTTTAAGCTCTG-3'.

Products were visualized on a 1.5% agarose gel buffered with TBE.

RESULTS

I3C induces the ubiquitination and proteasome-mediated degradation of ERα protein prior to downregulation of ERα transcripts

The effects of I3C on the kinetics of ERα transcript and protein downregulation were examined in a 24 hr time course of MCF7 human breast cancer cells treated with or without 200 μM I3C. This concentration of I3C causes the maximal inhibition of estrogen dependent proliferation without any apoptotic effects (Sundar et al., 2006). Total ERα protein levels at each time point were determined by western blot analysis of electrophoretically fractionated cell extracts, and the corresponding levels of ERα transcripts were analyzed by RT-PCR analysis of isolated total RNA. As shown in Figure 5A and quantified in Figure 5B, I3C treatment caused a rapid downregulation of ERα protein prior to any effect on ERα-transcript levels. A significant reduction in ERα protein levels was observed within 6 hr of indole treatment, and ablation of detectable ERα protein occurred by 24 hr. In contrast, the earliest time point in which a significant decrease in ERα transcripts occurred was 12 hr (Figure 5A and 5B). No changes were observed for gel loading control genes actin (protein) or GAPDH (mRNA) throughout the time course. Thus, I3C exerts a rapid and direct effect on ERα protein levels, which is followed kinetically by the attenuation of ERα transcription.

Figure 5:

Effects of I3C on kinetics of ERα Expression. (A) MCF-7 human breast cancer cells were treated with or without 200 μM I3C through a 24-hour time course. At the indicated time points, the levels of ERα protein were monitored by western blots and the levels of ERα transcripts determined by RT-PCR. Actin was used as protein loading control, and GAPDH was used as a RNA loading control. PCR products were visualized on a 1% agarose gel stained with ethidium bromide. (B) The levels of ERα protein and transcripts were quantified by densitometry of the western blots and RT-PCR gels shown in Fig. 5A. The relative levels of ERα gene products were compared to the respective actin or GAPDH gel loading controls, and normalized to DMSO at each time point. Results were repeated three times to verify statistical significance.

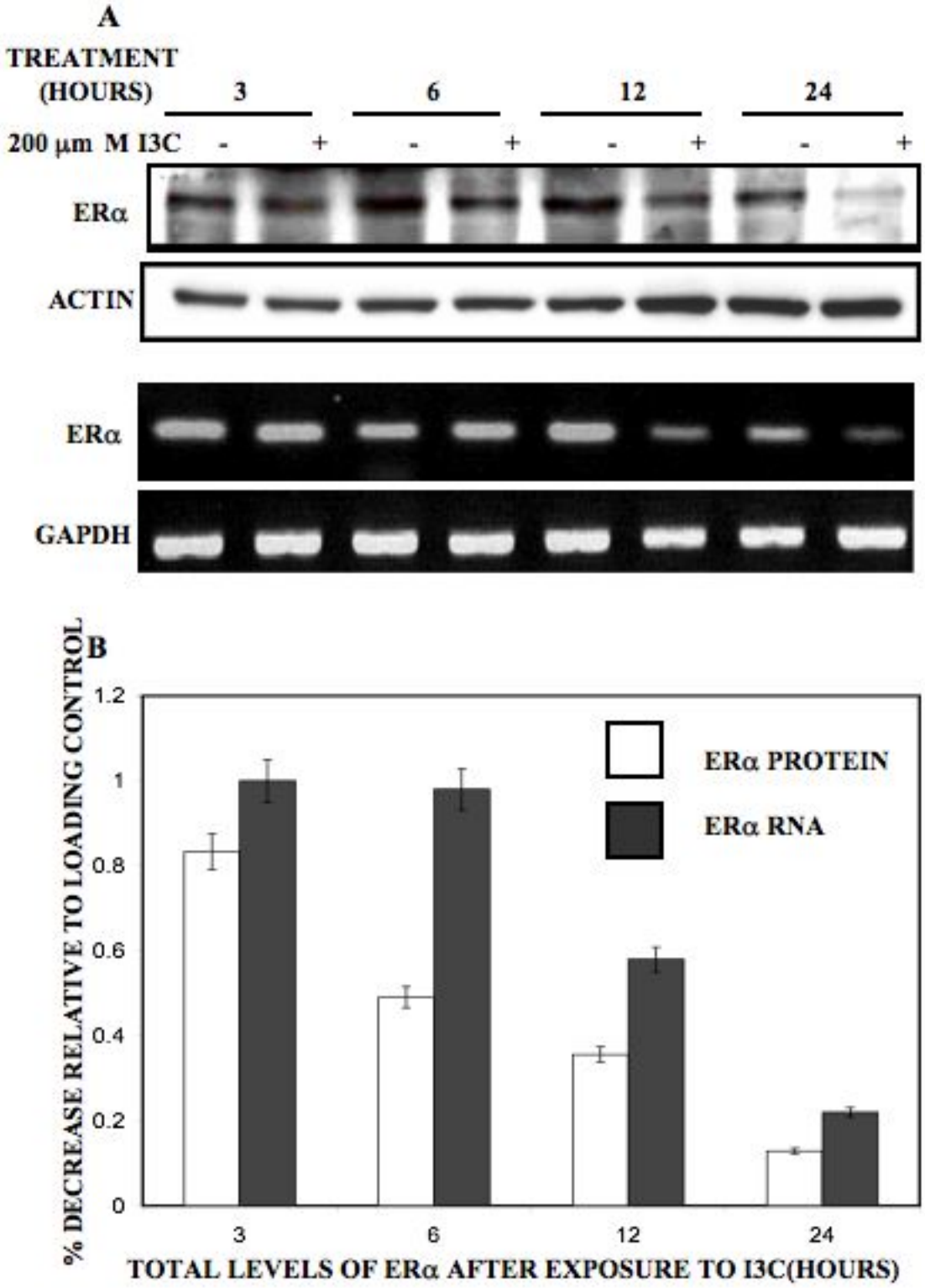
A
TREATMENT (HOURS)
3
6
12
24
200 µm M I3C
-
+
-
+
-
+
-
+
ERα
ACTIN
ERα
GAPDH
B
% DECREASE RELATIVE TO LOADING CONTROL
1.2
1
0.8
0.6
0.4
0.2
0
ERα PROTEIN
ERα RNA
3
6
12
24
TOTAL LEVELS OF ERα AFTER EXPOSURE TO I3C(HOURS)

To determine if the I3C downregulation of ERα protein was due to induced ubiquitination and 26S proteasome-mediated degradation, MCF7 cells were treated with or without 200 μM I3C for 6 hr in the presence or absence of MG132, an inhibitor of proteasome peptidase enzymatic activity. As shown in figure 6, immunoblot analysis revealed that MG132 treatment completely rescued ERα protein from the I3C-induced degradation. MG132 blocked I3C-dependent degradation in the hormone sensitive T47D cell line as well (figure 6). Attachment of ubiquitin to ERα protein was examined by western blot analysis of immunoprecipitated ERα protein in cells treated with or without 200 μM I3C for 6 hr in the presence of MG132. As shown in Figure 7A, I3C treatment resulted in a significant increase in ubiquitinated ERα protein levels. Thus, I3C-induced degradation of ERα protein is triggered by ubiquitination that targets ERα for destruction by the 26S proteasome.

Several E3 ubiquitin ligases are involved in ERα protein degradation in different cell systems (Osborne *et al.*, 2004; Eakin *et al.*, 2007). The potential role of Rbx1, a RING-domain E3 ligase, in I3C induced-destruction of ERα protein was examined because this E3 ligase has been implicated in xenobiotic-mediated degradation of ERα protein (Ohtake et al., 2007). Rbx1 expression was selectively ablated in MCF7 cells by transfection of Rbx1 specific small interfering RNA (siRNA). Control cells were either transfected with scrambled siRNA or remained untransfected. As shown in Figure 7B, I3C treatment failed to induce ERα protein degradation in cells expressing Rbx1 siRNA. In contrast, in control cells expressing scrambled siRNA or in those that remained

Figure 6:

I3C downregulation of ERα protein is blocked by the proteasomal inhbitor MG132. MCF-7 and T47D cells were treated with the indicated combinations of 200 μM I3C and 5 mM MG132 (a 26S proteasome inhibitor) for 6 hours, and the level of ERα protein monitored by western blots. HSP90 was used as gel loading control. Representative blots from three independent experiments shown.

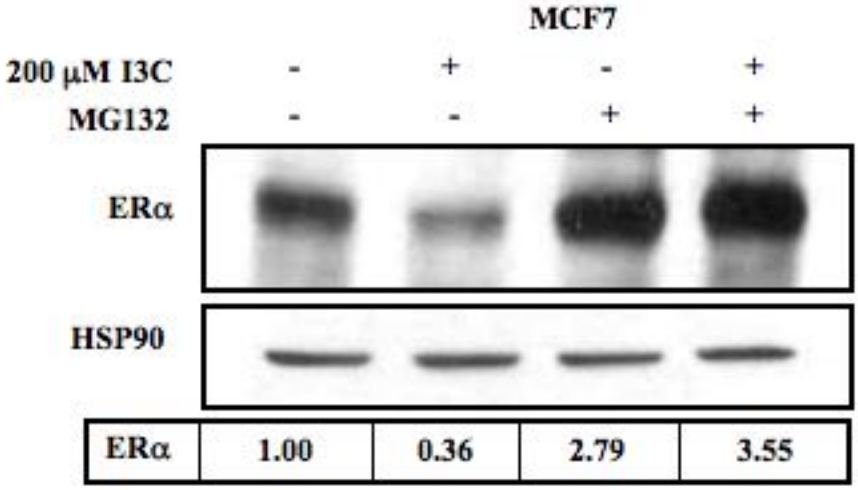

ERα	1.00	0.36	2.79	3.55

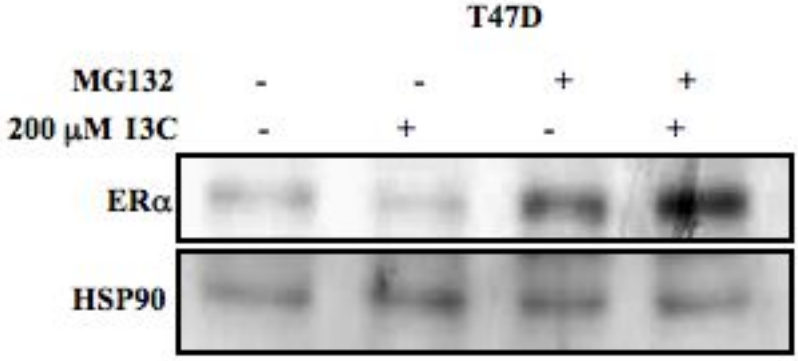

ERα	1.00	0.44	3.16	4.59

Figure 7:

I3C induces the ubiquitination and 26S proteasome degradation of ERα protein and requirement of the Rbx1 E3 ubiquitin ligase this degradative process. (A) In MCF-7 cells were treated with the indicated combinations of 200 μM I3C and 5 mM MG132. Total cell extracts were immunoprecipitated with mouse-anti-ERα antibodies and electrophoretically fractionated samples blotted with either rabbit-anti-ERα or rabbit-anti-Ubiquitin antibodies (ERα-UB). Result was repeated four times, representative blot shown. (B) MCF-7 cells were transfected with control scrambled siRNA or Rbx1-specific siRNA, or remained untransfected for 24 hours. Cells were then treated with or without 200 μM I3C for 6 hours, and the level of ERα protein determined by western blot analysis. Result was repeated twice. Densitometry numbers are the ratio of ERα to loading control, normalized to the DMSO ratio.

A

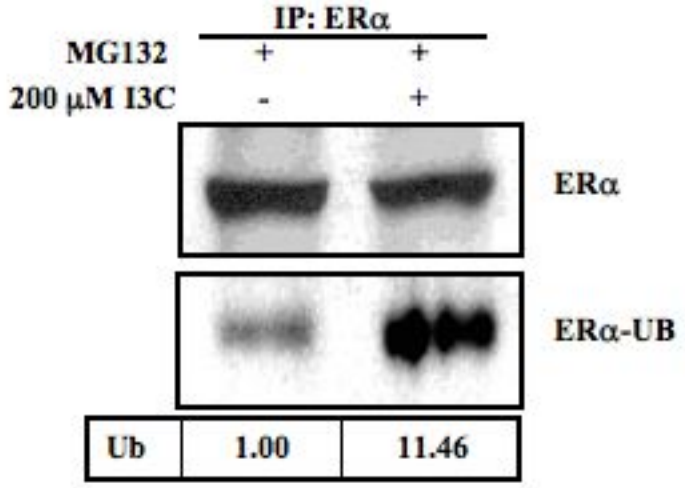
IP: ERα
MG132 + +
200 μM I3C - +
ERα
ERα-UB
Ub 1.00 11.46

B

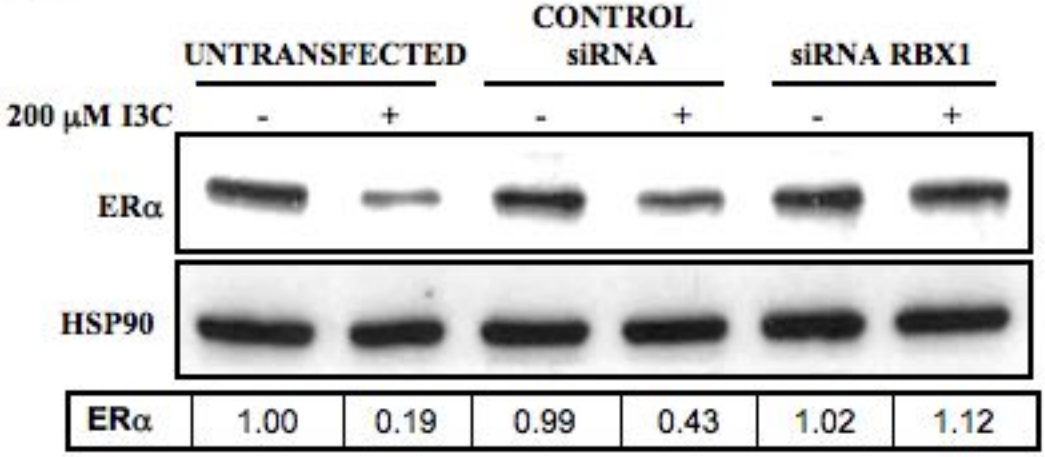
UNTRANSFECTED
CONTROL siRNA
siRNA RBX1
200 μM I3C - + - + - +
ERα
HSP90
ERα 1.00 0.19 0.99 0.43 1.02 1.12

untransfected this indole efficaciously triggered the degradation of ERα protein. These results demonstrate that Rbx1 is required for the I3C induced degradation of ERα protein in MCF7 human breast cancer cells. Furthermore, this result differentiates the degradative mechanism of I3C from that of fulvestrant, which is a SERD that binds directly to ERα and causes the receptor to localize to the nuclear periphery and recruit the NEDD8 E3 ligase for receptor degradation (Fan et al., 2003).

Activated aryl hydrocarbon receptor (AhR) is required for I3C-induced ERα protein degradation

Previous studies have determined that treatment of estrogen responsive human breast or prostate human cancer cells with the 3-MC or TCDD high-affinity xenobiotic ligands for the aryl hydrocarbon receptor (AhR) can cause ERα degradation (Wormke et al., 2003) through recruitment of Rbx-1 (Ohtake et al., 2009). Although I3C has relatively low affinity for AhR (Jellinck et al., 1993), we examined whether the I3C degradation of ERα protein is dependent on AhR in MCF7 human breast cancer cells by disrupting its expression with AhR-specific shRNA. Expression of shRNA to green fluorescence protein (shGFP) provided a control for the transfection procedure. Transfected MCF7 cells were treated with or without 200 μM I3C for 6 hr, and ERα protein was examined by western blots. As shown in Figure 8, shRNA targeted to AhR effectively blocked ERα ubiquitination and subsequent protein degradation by I3C, demonstrating the AhR dependence on this process.

Figure 8:

I3C-mediated degradation of ERα protein requires AhR. MCF-7 cells were transfected with shAhR or shGFP (control plasmid) and then treated with or without or 200 μM I3C for 6 hours. Total cell extracts were electrophoretically fractionated and the levels of ERα, AhR and Actin (loading control) analyzed by Western blots. Densitometry numbers are the ratio of ERα to loading control, normalized to the DMSO ratio.

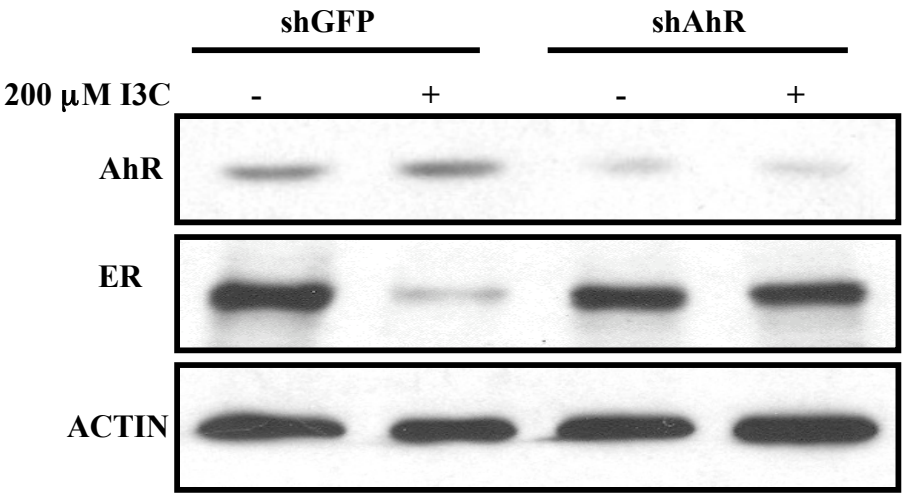

AhR	1.00	1.05	0.23	0.21
ERα	1.00	0.06	0.79	0.76

The ligand dependent activation of AhR leads to its nuclear translocation, which provides access to its gene targets (Richter et al., 2001). To determine if I3C activates AhR, the nuclear translocation of AhR was examined by indirect immunofluorescence in 6 hr I3C treated and untreated MCF7 cells. As shown in figure 9, I3C treatment significantly increased nuclear staining of AhR, whereas, in untreated cells AhR was distributed more uniformly throughout the cell. These results suggest that I3C activates AhR, a process that is required for its nuclear translocation, which in turn triggers the Rbx1 mediated ubiquitination and proteasomal degradation of ERα protein.

The I3C induced nuclear localization of AhR was confirmed by biochemical fractionation of the MCF7 cells into nuclear and cytoplasmic fractions. As shown in Figure 9, AhR was highly enriched in the cytoplasmic fraction of untreated cells, whereas, in 24 hr I3C treated cells, the majority of AhR co-fractionated with the nuclei. Furthermore, Rbx1, the E3 ubiquitin ligase that is required for the indole induced ERα degradation, also co-fractionates with the nuclear compartment in I3C treated cells, but not in untreated cells. The efficiency of the nuclear fractionation in both I3C treated and untreated cells were verified using lamin as a nuclear marker (Fig. 9).

Figure 9:

I3C induces the nuclear localization of AhR. MCF-7 cells were treated with or without 200 μM I3C for 6 hours, and the subcellular localization of AhR determined by indirect immunofluorescence microscopy. DAPI staining was used to visualize DNA stained nuclei (top panels). MCF-7 cells treated with 200 μM I3C or with the DMSO (vehicle control) for 24 hr, and cell extracts fractionated into cytoplasmic and nuclear fractions (bottom panels). Each set of subcellular fractions were electrophoretically fractionated and analyzed by Western blot for the levels of AhR, Rbx1, nuclear lamin (fractionation control), and Actin (loading control) in each cellular compartment.

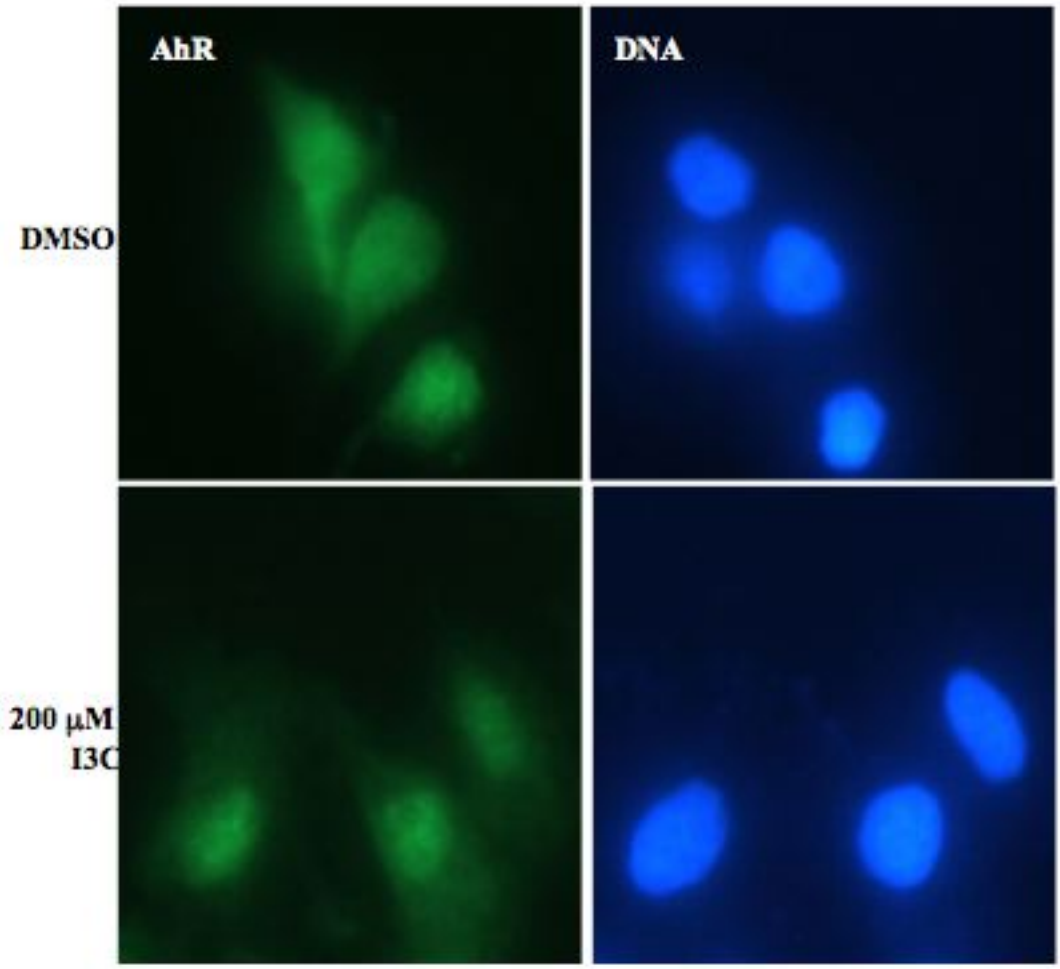
AhR
DNA
DMSO
200 μM
I3C

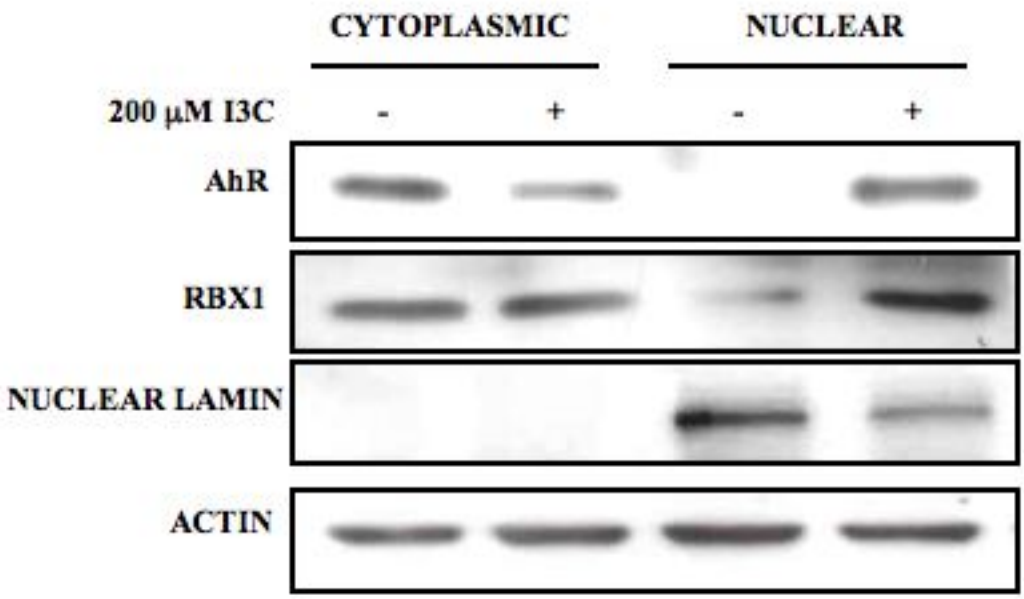
CYTOPLASMIC
NUCLEAR
200 μM I3C
-
+
-
+
AhR
RBX1
NUCLEAR LAMIN
ACTIN

The downregulation of ERα protein is an intrinsic property of I3C and it's derivatives

The activation of AhR to induce ERα protein degradation raises the possibility that this is a generalized property of AhR activation, rather than a specific activity associated with this indole. In order to test whether general activation of AhR can induce proteolytic degradation of ERα we subjected MCF7 cells to 6 hr treatments of 200 μM I3C, DMSO vehicle control, or 30 μM 3, 3'-diindoylylmethane (DIM), the acid condensation dimer of I3C which has been previously demonstrated as a ligand for AhR. In addition, we tested the ability of chemically modified versions of I3C to induce ERα proteolytic degradation. This included 1-benzyl I3C at 20 μM and N-butoxy-I3C at 4 μM, the lowest concentration necessary to induce G1 cell cycle arrest. Because all of the above mentioned indole derivatives induce a G1 cell cycle arrest, an indole derivative without the ability to arrest cellular growth, tryptophol, was tested as well. As shown in figure 10, I3C and its derivatives 1-benzyl I3C and N-butoxy-I3C were able to induce ERα downregulation, whereas the acid condensation dimmer DIM and tryptophol were unable to induce proteolytic degradation of ERα. Therefore the activation of AhR dependent proteolytic degradation of ERα is a specific property of I3C and derivatives rather than a generalized response to xenobiotic ligand binding.

Figure 10:

DIM and Tryptophol fail to induce the downregulation of ERα seen with I3C and its chemically modified derivatives. MCF7 cells were treated with the indicated concentrations of indoles for 6 hours, and the level of ERα protein monitored by western blots. HSP90 was used as gel loading control. Representative blot of three independent experiments shown. MCF7 cells were treated with increasing concentration of 1-Benzyl-I3C or chemically unmodified I3C for 24 hr, and the level of ERα protein monitored by western blots. Actin was used as a gel loading control.

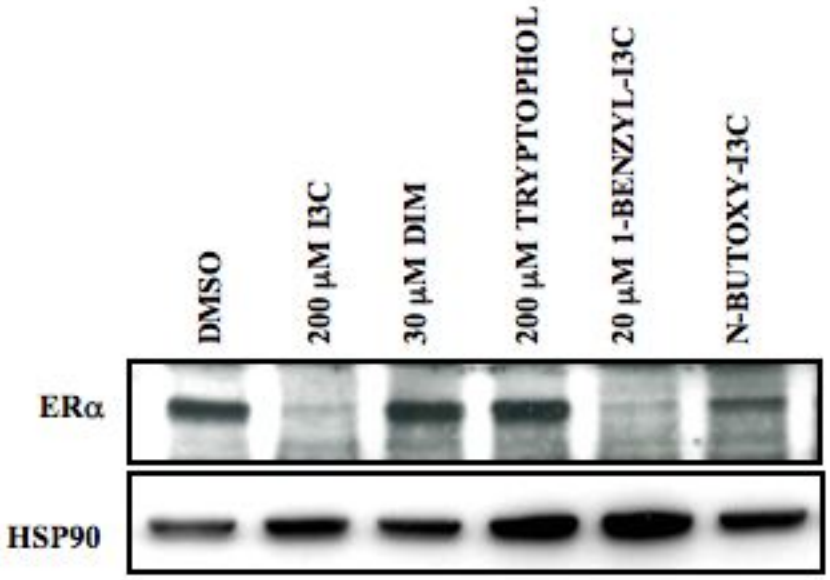

N-Benzyl-I3C

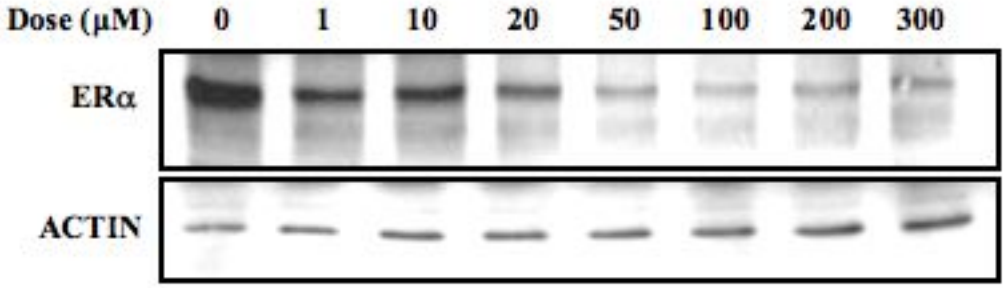

I3C

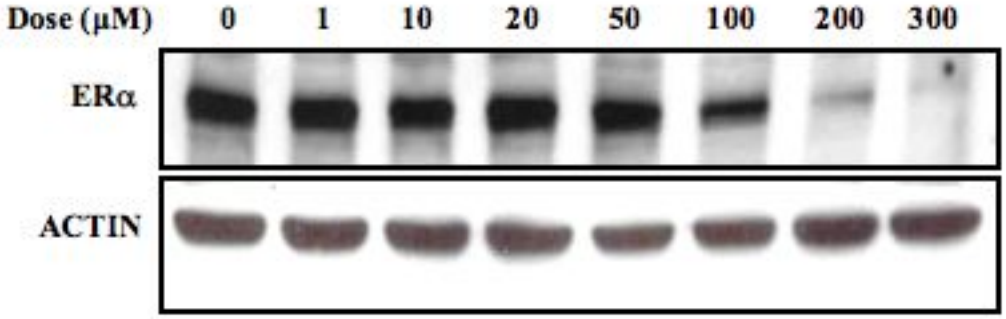

In order to test the efficacy of the derivatives on ERα protein downregulation, the chemically modified 1-Benzyl I3C was compared to its parent I3C compound for the ability to induce protein downregulation over a range of concentrations. As shown in figure 10, the effective range for ERα protein downregulation was ten fold lower with 1-Benzyl-I3C as compared to chemically unmodified I3C. This demonstrates the increased efficacy of N-benzyl on the disruption of ERα expression.

I3C-induced degradation of ERα protein causes the downregulation of GATA3 transcription factor gene expression

The temporal delay between I3C-induced ablation of ERα protein and loss of ERα transcripts suggests that either the indole-induced downregulation of ERα protein and transcripts result from independent I3C regulated pathways, or that the indole-mediated ERα protein degradation initiates a cellular cascade that directly accounts for the loss of ERα transcripts. One candidate transcription factor that may link the I3C downregulation of ERα protein and transcripts is GATA3, which is an ERα target gene (Tremblay and Viger, 2001) that has been shown to affect ERα promoter activity in a cross-regulatory feedback loop (Eeckhoute et al., 2007). To initially test whether I3C regulates GATA3 expression, MCF7 cells were treated with or without 200 μM I3C over a 72 hr time course and the levels of GATA3 and ERα gene products monitored by western blots and by RT-PCR. As shown in figure 11, I3C strongly down-regulates GATA3 protein and transcript levels in MCF7 cells as well as in T47D cells. This indole

Figure 11:

Effects of I3C on the expression of GATA3 protein and GATA3 transcripts. MCF-7 cells were treated with or without 200 μM I3C, and at the indicated times the level of GATA3 and ERα protein was monitored by western blot analysis (upper panels), and GATA3 and ERα transcript expression was determined by RT-PCR (lower panels). The PCR products were visualized on a 1 % agarose gel stained with ethidium bromide. HSP90 provided a loading control for the western blots and GAPDH provided a gel loading control for the RT-PCR. Densitometry numbers are the ratio of ERα or GATA3 to loading control, normalized to the DMSO ratio. T47D cells were treated with or without 200 μM I3C for 48 hr. Total cell lysates were electrophoretically fractionated and analyzed by Western blots for the levels of GATA3, ERα, and Actin (loading control) protein.

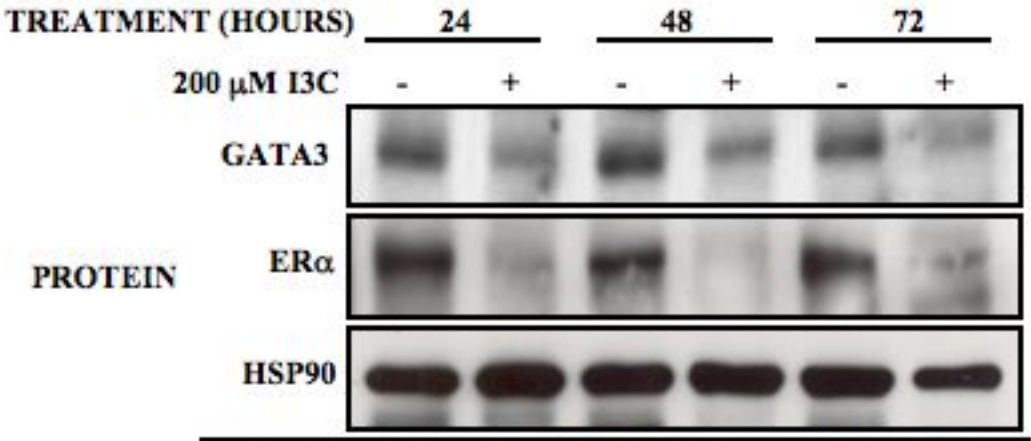

GATA3	1.00	0.48	1.30	0.47	0.89	0.26
ERα	1.00	0.06	1.35	0.03	1.46	0.08

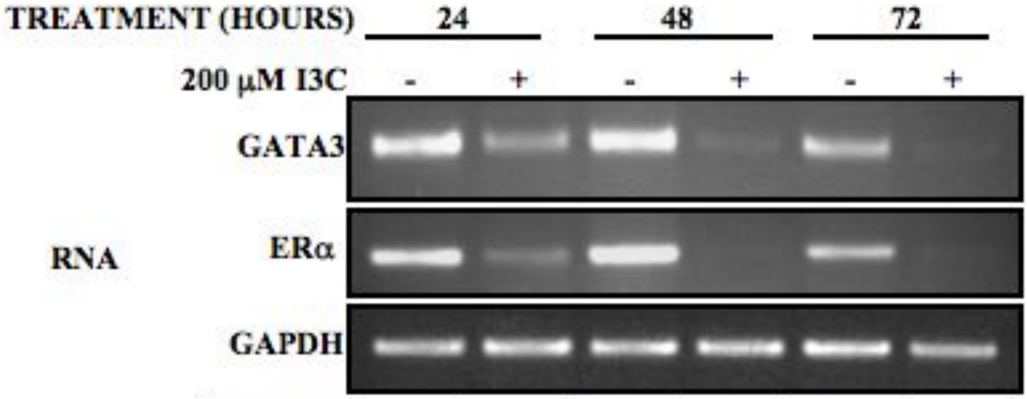

GATA3	1.00	0.38	1.09	0.05	0.67	0
ERα	1.00	0.25	1.18	0.04	0.77	0.01

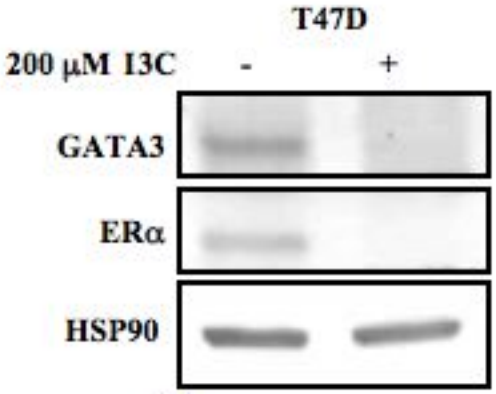

down-regulates GATA3 transcript levels before the protein levels are affected. Importantly, at the 24 hr time point when ERα protein is essentially ablated, *GATA3* gene products decrease in indole treated cells. The I3C-mediated downregulation of GATA3 protein and transcripts occurs with similar dose-response profiles as ERα, with an observed half-maximal down regulation at approximately 150 μM I3C (figure 12). Consistent with this was the disruption of ERα expression using a dominant-negative $GATA^{KRR}$, which blocks GATA3 transcriptional activity (figure 12). In addition, GATA3 expression was tied closely to ERα expression, with GATA3 expression only dtectable in hormone sensitive cell lines (MCF7, figure 13). There was no detectable expression in non-tumorigenic MCF10A and metastatic ERα negative MDA-MB-231 cells (figure 13). These results demonstrate that in MCF7 human breast cancer cells, GATA3 expression is strongly attenuated by I3C and that the kinetics of this response is consistent with GATA3 expression being regulated by ERα protein.

The 3' enhancer of the *GATA3* gene contains many estrogen-regulated elements that are responsible for increased ERα binding to *GATA3* cis-regulatory regions (Eeckhoute et al., 2007) (Fig 14, top panel). However, the consequences on *GATA3* gene transcription of ERα binding to cis-regulatory regions are unknown. Chromatin immunoprecipitation was used to determine whether the I3C downregulation of ERα protein in MCF7 cells affects the endogenous ERα interactions with the 3' enhancer of the *GATA3* gene. As shown in figure 14 (lower panel), in 24 hr I3C-treated cells, binding of ERα to a representative *GATA3* 3' enhancer element was significantly decreased in I3C treated cells compared to untreated cells. Thus, in MCF7 human breast cancer cells,

Figure 12:

The observed half-maximal downregulation of GATA3 is 150 μM I3C and involvement of GATA3 in ERα regulation. GATA3 and ERα protein was monitored by western blot analysis (upper panels), and GATA3 and ERα transcript expression was determined by RT-PCR (lower panels). The PCR products were visualized on a 1% agarose gel stained with ethidium bromide. HSP90 provided a loading control for the western blots and GAPDH provided a gel loading control for the RT-PCR. (Bottom Panel) T47D cells were transfected with empty vector control (neo), CMV-GATA3, or a dominant negative GATA3 construct ($GATA3^{KRR}$). Cells were harvested 72 hrs post transfection, and the levels of ERα, GATA3 and HSP90 (loading control) were measured by western blot. T47D cells were transfected with empty vector control (neo), CMV-GATA3, or a dominant negative GATA3 construct ($GATA3^{KRR}$).

PROTEIN

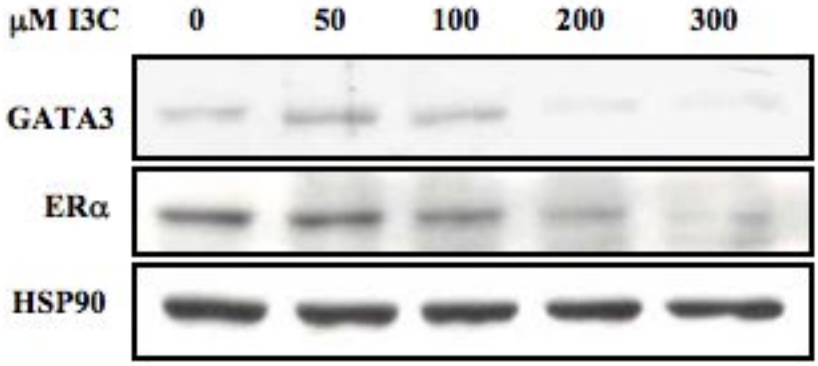
μM I3C
0
50
100
200
300
GATA3
ERα
HSP90

RNA

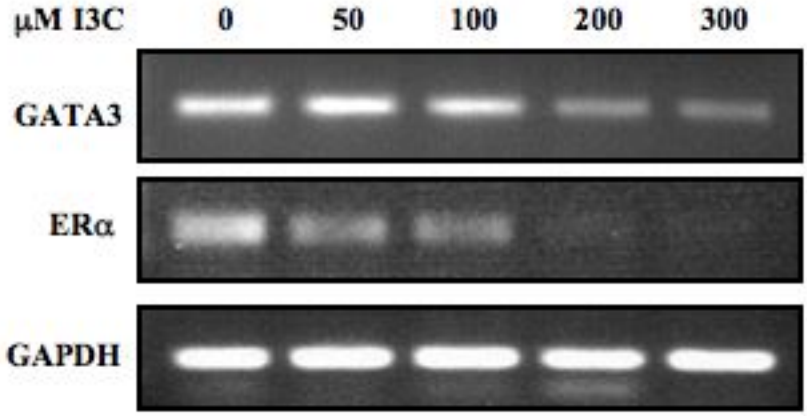
μM I3C
0
50
100
200
300
GATA3
ERα
GAPDH

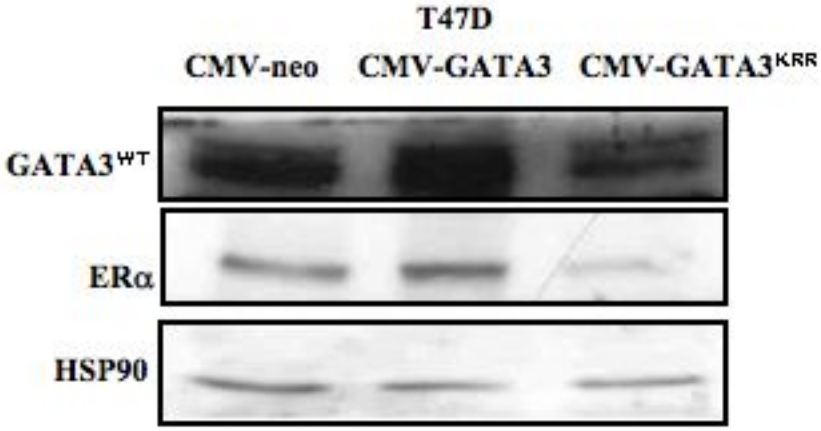
T47D
CMV-neo
CMV-GATA3
CMV-GATA3KRR
GATA3WT
ERα
HSP90

Figure 13:

GATA3 is expressed in hormone sensitive breast cancer cell lines and I3C disrupts this expression. MCF10A, MCF7, and MDA-MB-231 cells were treated with 200 μM I3C or DMSO vehicle control for 48 hr. Total Cell lysates were subjected to SDS-PAGE and the levels of GATA3 and HSP90 (loading control) protein was monitored by western blot analysis.

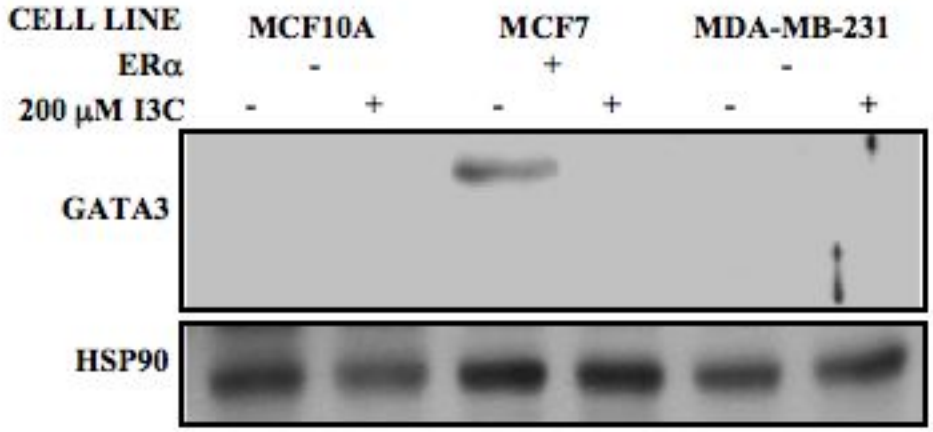
CELL LINE
MCF10A
MCF7
MDA-MB-231
ERα
-
+
-
200 μM I3C
-
+
-
+
-
+
GATA3
HSP90

Figure 14:

I3C disrupts ERα protein interaction with GATA3 regulatory regions. (Top panel) Genomic sequences of the GATA3 gene enhancer contain a consensus half-ERE site. Primers used to amplify ERE site for chromatin immunoprecipitation are underlined. Sequence and chromosomal location were obtained from the UCSC Genome Browser. (Bottom panel) Chromatin immunoprecipitation (ChIP) was employed to characterize endogenous ERα interactions with the ERE region of the GATA3 enhancer region. Chromatin was isolated from MCF-7 cells treated with or without 200 μM I3C for 24 hrs. ERα was immunoprecipitated from total cell extracts using Sepharose G bound to anti-ERα antibody and DNA released from ERα was amplified using the indicated oligonucleotide primers. Control primers directed at downstream site (distance = 1256 bp) showed no amplification in IP samples. Input samples represent total genomic DNA from each treatment (loading control).

ENHANCER ANALYSIS

chr10: 8,166,918-8,167,101

5'-
ACCAGCAAATAAATGCGTTTAAGATGTT

AGGGAGTGACCAAAGAGGAATATGTATG

CAGAGACCTGGAAAATATGAAACCAGTT

AAGAACTCAA**AGGTCA**TTTTGTTCAGGG
ERE

CAAAATTCTTGTGCATGGTGCTGACAGT

TTGCCCTCTGGGTGTTTTCAGAGCTTAA

AGGATCAAACTTGTCC-3'

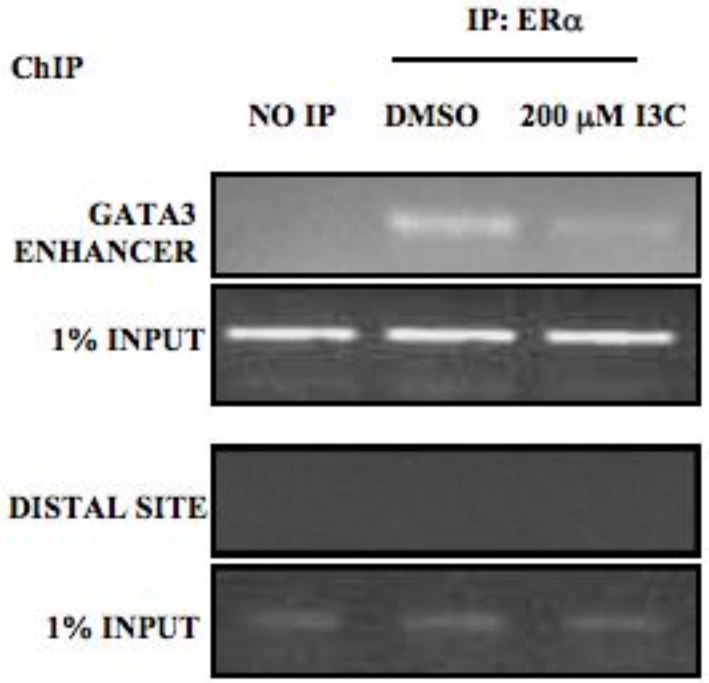

I3C down-regulates endogenous ERα interactions with the 3' enhancer region of the *GATA3* gene, which accounts for the indole-mediated loss of GATA3 transcripts.

A key prediction of ERα's direct role in mediating the I3C down regulation of GATA3 gene expression is that over-expression of exogenous ERα should prevent I3C inhibition of GATA3 protein and transcripts. MCF7 cells were stably transfected with either a CMV-ERα expression vector or with a CMV-neo empty vector control and examined for ERα gene expression in the presence or absence of I3C. As shown in figure 15, the over-expressed exogenous ERα protein is downregulated in I3C treated cells as predicted by the indole induced proteasomal degradation of ERα protein. However, enough exogenous ERα protein remains that the overall ERα levels in I3C treated cells are comparable to endogenous levels in control empty vector transfected cells treated with the vehicle control. In the presence of exogenous ERα protein, I3C-induced downregulation of endogenous GATA3 transcripts and protein is effectively blocked (Fig 15). Ectopic expression of ERα reversed the I3C downregulation in ERα and GATA3 transcripts, suggesting that the I3C-mediated degradation of ERα protein is a pivotal event that precedes and causes the loss of ERα and *GATA3* gene expression.

Downregulation of GATA3 expression is required for I3C inhibition of ERα transcription

Our results suggest that the I3C-induced ERα protein degradation triggers the loss of GATA3 expression, which then causes the downregulation of ERα transcription. A

Figure 15:

I3C down-regulation of GATA3 gene expression requires the I3C mediated loss of ERα protein. (A) MCF-7 cells were transfected with CMV-ERα or the CMV-Neo vector control and treated with or without 200 μM I3C for 48 hrs. Total Cell lysates were electrophoretically fractionated and analyzed by Western blots for the levels of GATA3, ERα, and Actin (loading control) protein. (HIGH) and (LOW) designations refer to film exposure times of the blot. Densitometry numbers are the ratio of GATA3 to loading control, normalized to the DMSO ratio. (B) Total RNA was collected from MCF-7 cells treated with or without 200 μM I3C 48 hrs, and RTPCR was used to detect GATA3 and ERα transcripts. GAPDH was used as total RNA loading control. PCR products were visualized on a 1% agarose gel stained with ethidium bromide.

PROTEIN

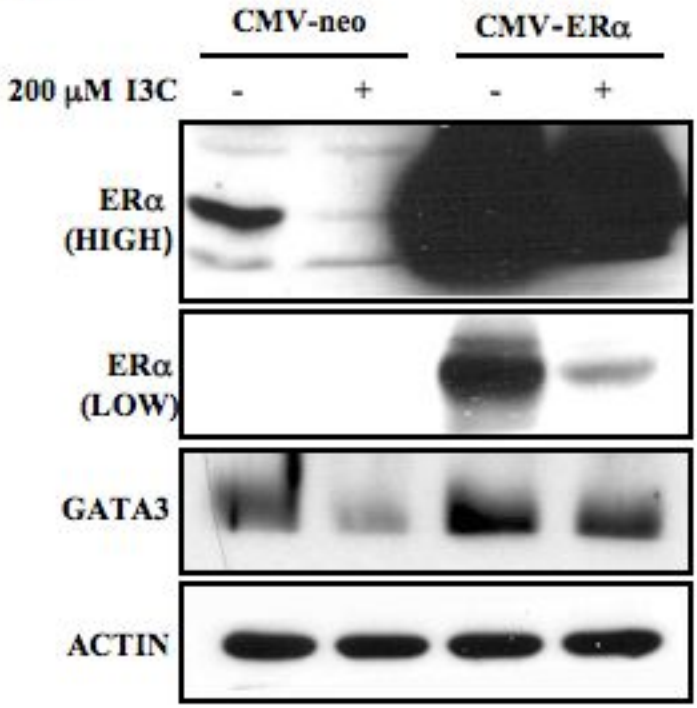
CMV-neo
CMV-ERα
200 μM I3C
-
+
-
+
ERα
(HIGH)
ERα
(LOW)
GATA3
ACTIN

RNA

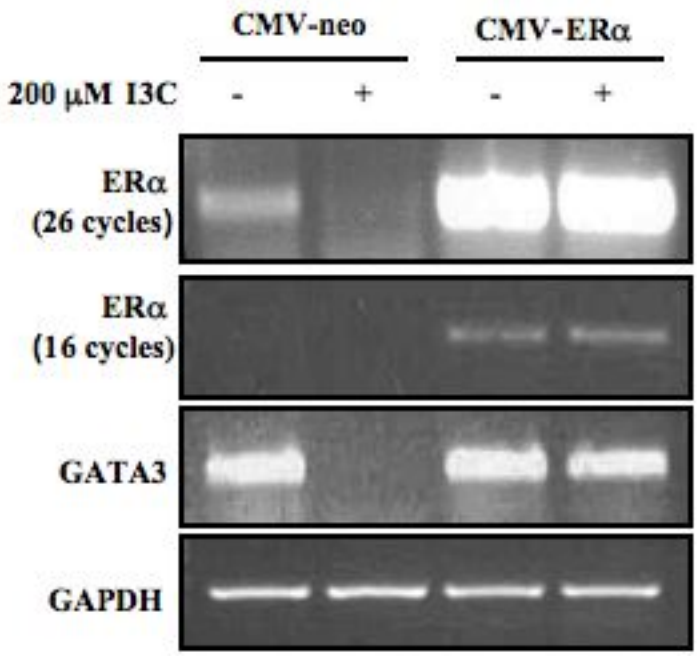
CMV-neo
CMV-ERα
200 μM I3C
-
+
-
+
ERα
(26 cycles)
ERα
(16 cycles)
GATA3
GAPDH

key test of this mechanism is that the ectopic expression of the GATA3 transcription factor from a constitutive expression vector should override the I3C downregulation of ERα transcripts, but have no effect on the I3C-induced degradation of ERα protein. MCF7 cells were transfected with either a CMV-GATA3 expression vector or with the CMV-neo empty vector and analyzed for ERα protein and transcripts in the presence or absence of I3C. As shown in Fig 16, expression of exogenous GATA3 prevented the I3C downregulation of endogenous ERα transcripts but failed to alter the I3C mediated loss of ERα protein levels. In empty vector-transfected cells, I3C downregulated both ERα protein and transcript levels.

We previously demonstrated that I3C inhibits ERα promoter activity (Sundar et al., 2006), which suggests that an indole-responsive transcription factor directly mediates this response. To assess the effects of ectopic GATA3 expression on the I3C inhibition of ERα promoter activity, MCF7 cells were co-transfected with an ERα promoter-luciferase reporter plasmid containing a 3561 bp fragment of the ERα promoter (pERα-3561-pgl2) along with either the CMV-GATA3 expression vector or the CMV-neo empty vector control. As shown in Figure 17, exogenous GATA3 was able to override the I3C-mediated downregulation of ERα promoter activity, demonstrating the central role of the GATA3 transcription factor in attenuation of ERα transcription by I3C. GATA3 was able to override I3C-mediated downregulation of ERα promoter in T47D cells as well (fig 17). Taken together, our results demonstrate that indole downregulation of GATA3 is a crucial intermediate step in the I3C regulated cascade that links I3C-induced ERα protein degradation to the loss of ERα transcripts and promoter activity.

Figure 16:

The I3C inhibition of ERα transcripts levels requires the down-regulation of GATA3 gene expression. MCF-7 cells were transfected with CMV-GATA3 or CMV-neo vector control and treated with or without 200 μM I3C for 48 hrs. Total Cell lysates were electrophoretically fractionated and analyzed by Western blots for the levels of GATA3, ERα, and Actin (loading control) protein (top panels). Total RNA was collected from MCF-7 cells treated with or without 200 μM I3C for 24 hrs and RTPCR was used to detect GATA3 and ERα transcripts (bottom panels). GAPDH was used as total RNA loading control. PCR products were visualized on a 1% agarose gel stained with ethidium bromide.

PROTEIN

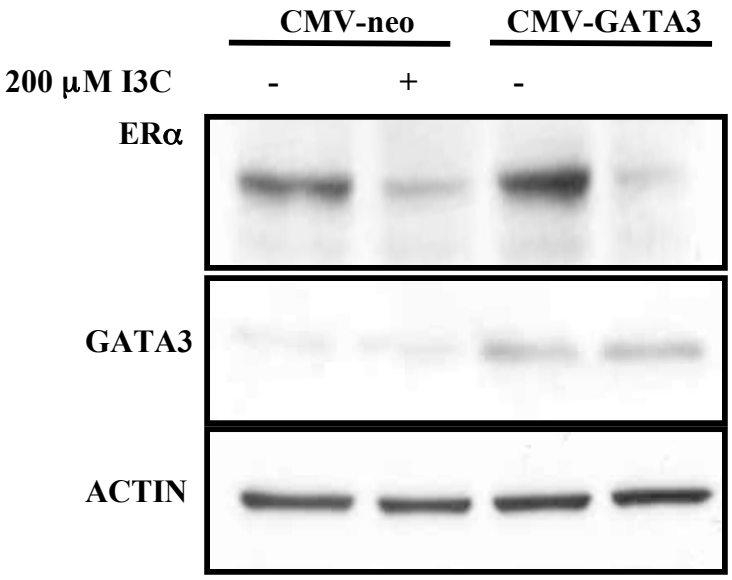
CMV-neo
CMV-GATA3
200 μM I3C
-
+
-
ERα
GATA3
ACTIN

RNA

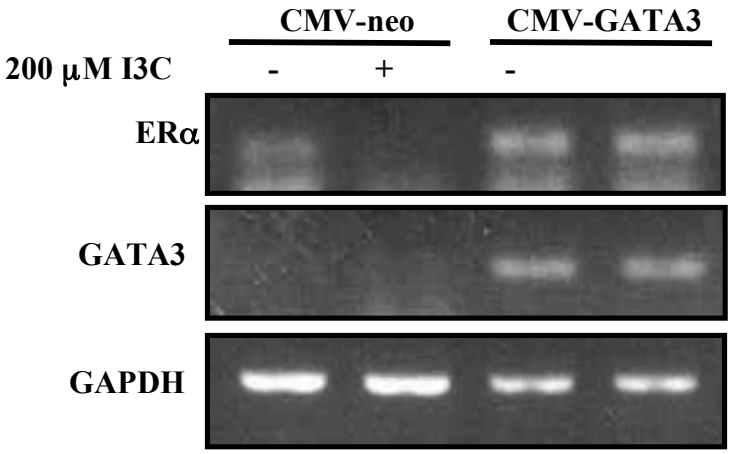
CMV-neo
CMV-GATA3
200 μM I3C
-
+
-
ERα
GATA3
GAPDH

Figure 17:

The I3C inhibition of ERα promoter activity requires the down-regulation of GATA3 gene expression. MCF-7 and T47D cells were cotransfected with the I3C-responsive -3561 bp fragment of the ERα promoter linked to a luciferase reporter plasmid along with either CMV-GATA3 or CMV-neo (vector control). At 24 hrs post-transfection, cells were treated with or without 200 μM I3C for 24 hrs, and the relative luciferase activity was evaluated in lysed cells using the Promega Luciferase Assay Kit. The reporter plasmid levels are normalized to the -3561 ERα promoter fragment treated with the DMSO vehicle control. Two additional controls (data not shown) included CMV-luciferase to validate transfection efficiency (positive control) and pgl2 to measure background fluorescence (negative control). Bar graphs indicate relative luciferase activity normalized to the protein input. Error bars were derived from the results of three independent experiments.

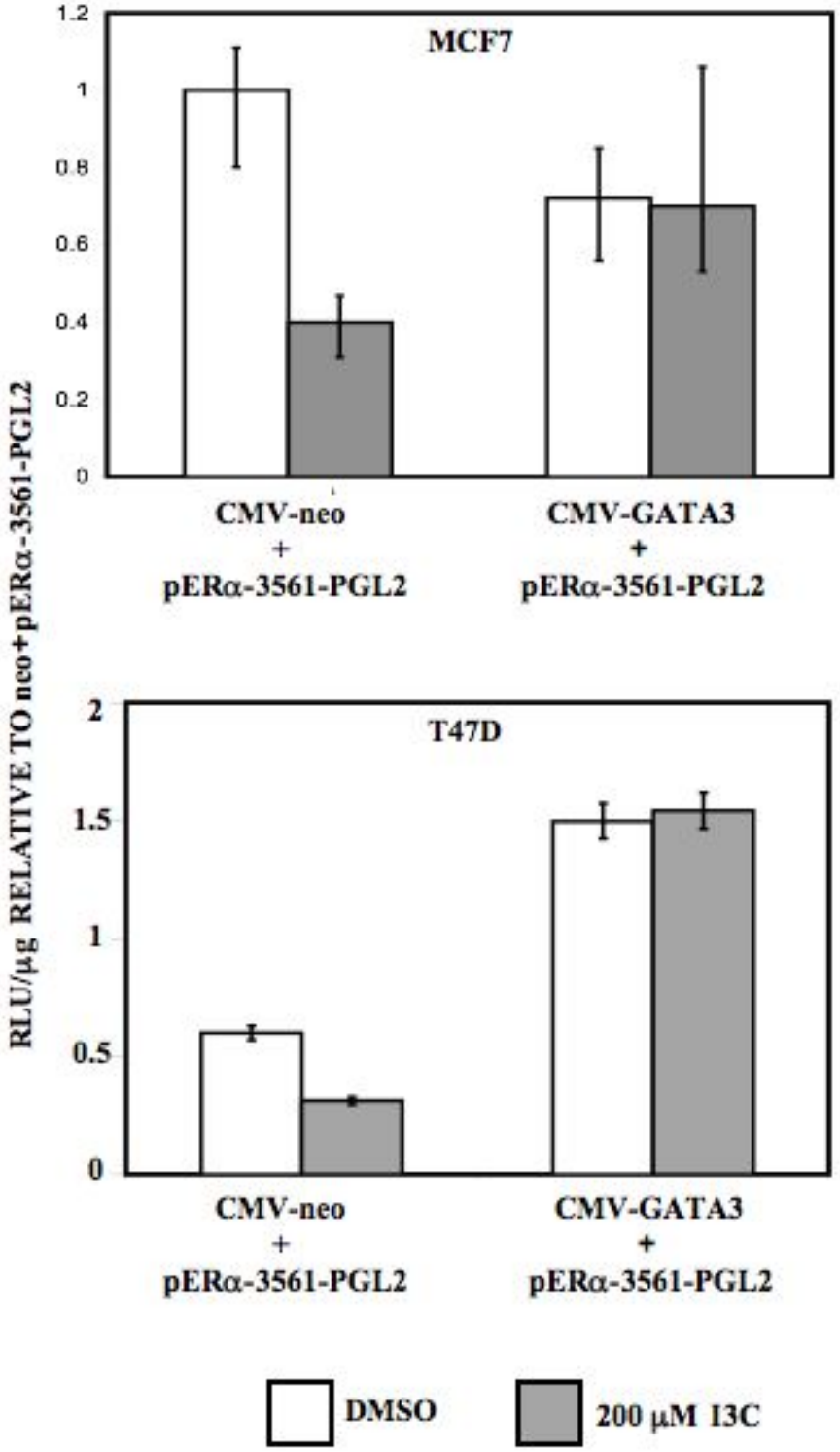
MCF7
1.2
1
0.8
0.6
0.4
0.2
0
CMV-neo
+
pERα-3561-PGL2
CMV-GATA3
+
pERα-3561-PGL2
RLU/μg RELATIVE TO neo+pERα-3561-PGL2
T47D
2
1.5
1
0.5
0
CMV-neo
+
pERα-3561-PGL2
CMV-GATA3
+
pERα-3561-PGL2
DMSO
200 μM I3C

Role of GATA3 in I3C-mediated inhibition of ERα promoter activity

Because the GATA3 transcription factor has many potential target genes, it was important to determine whether I3C treatment disrupts a direct interaction between GATA3 and the ERα promoter, or whether GATA3 mediates its effects through another intermediate transcriptional regulator. To define the I3C-responsive region in the ERα promoter, a series of 5' deletion mutants were generated and subcloned into luciferase reporter plasmids, and ERα promoter activity was assessed in transfected MCF7 cells treated with or without 200 μM I3C for 24 hr. As shown in Figure 18A, the -2294 promoter fragment was fully indole-responsive, whereas activities of the reporter plasmids linked to promoter fragments lacking the -2294 to -1892 bp region were not affected by I3C. This finding localizes the I3C responsive region between -2294 and -1892 bp upstream of the ERα transcription start site.

As diagrammed in Figure 18B, sequence analysis revealed that the I3C-responsive region of the ERα promoter contains predicted DNA binding sites for several families of transcription factors, including two putative binding sites for GATA3 at -2278 (GATA3-1) and at -2207 (GATA3-2). There are also consensus DNA binding sites for NFkB, Sp1, Ets, and Ap1 transcription factors, which have all been previously identified as regulated by indoles in several human cancer cell lines (Cram et al., 2001; Takada et al., 2005). In order to determine which elements are responsible for I3C-downregulation of ERα promoter activity in human breast cancer cells, select DNA sites within the -2294

Figure 18: **Identification of the I3C responsive region of the ERα promoter and the I3C responsive transcription factor**. **(**A) MCF-7 cells were transfected with the indicated ERα promoter 5' deletion constructs linked to a luciferase reporter gene, and 24 hr post-transfection cells were treated for 24 hr with either the DMSO vehicle control or with 200 μM I3C. Relative luciferase activity was evaluated in lysed cells using the Promega Luciferase Assay Kit and normalized to the reporter plasmid activity of the -3561 ERα promoter fragment in cells treated with DMSO. Two controls (data not shown) included CMV-luciferase to validate transfection efficiency (positive control) and pgl2 to measure background fluorescence (negative control). Bar graphs indicate relative luciferase activity normalized to the protein input and error bars were derived from the results of three independent experiments. (B) Transcription factor binding site analysis of the I3C responsive region was performed using TFSearch program, followed by manual curation of potential sites. Positions displayed are relative to the ERα promoter-A transcription start site. Bolded bases indicate consensus sequences of the indicated transcription factor sites within the ERα promoter. Underlined sequence indicates the positions of site-directed mutagenesis and the mutations that were introduced into the ERα promoter. (C) MCF-7 cells were transfected with luciferase reporter plasmids driven by either the wild type ERα promoter fragment starting at -2294 upstream of the RNA site start, or with ERα promoter fragments with the designated mutations in the consensus GATA3-1, GATA3-2 or Ap1 transcription factor binding sites. 24 hr transfected cells were treated for an additional 24 hrs with either DMSO or 200 μM I3C. Relative luciferase activity was evaluated in lysed cells as above. Bar graphs indicate relative luciferase activity normalized to the protein input.

A

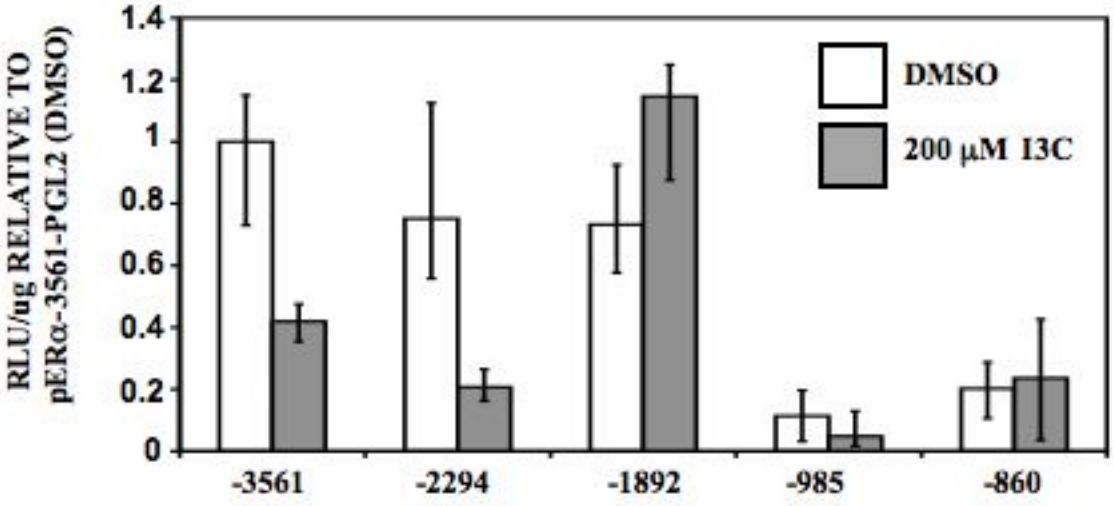

B

FACTOR	GATA3-1	GATA3-2	Ap1
LOCATION	-2278	-2207	-2159
ERα SEQUENCE	TATCCCAGA	GATATCCA	ATGATTCACAGC
MUTAGENESIS	GCGCCCAGA	GGCGCCCA	ATTGATCACAGC

C

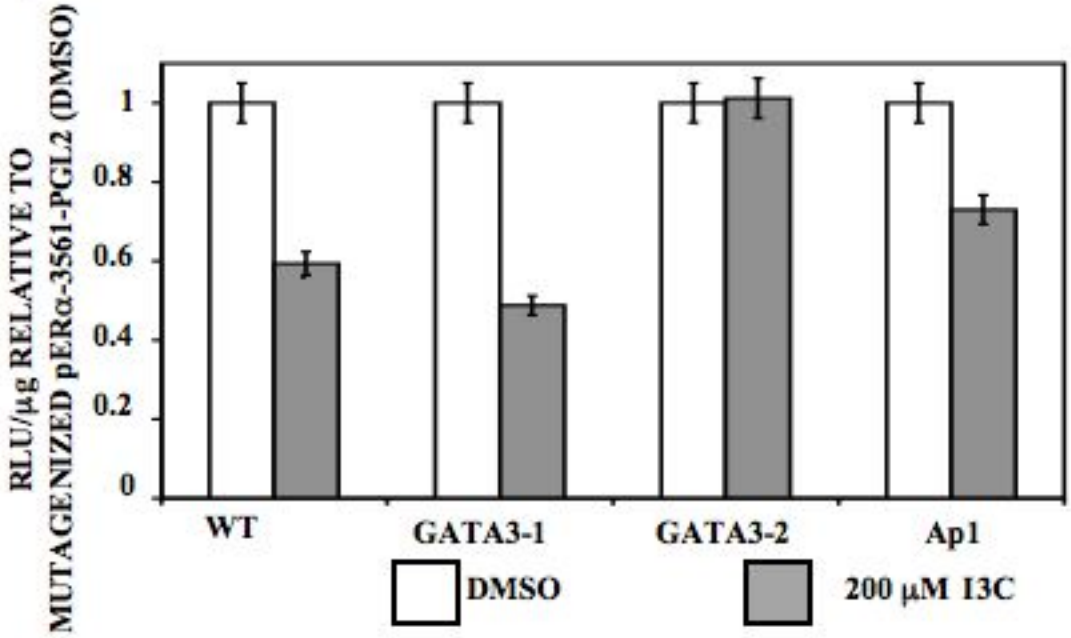

ERα promoter fragment were mutagenized and the entire promoter fragments inserted into luciferase reporter plasmids. These constructs were then transfected into MCF7 cells, and effects of I3C on wild type (WT) and mutated (GATA3-1, GATA3-2 and Ap1) promoter activities were analyzed. As shown in figure 18C, mutation of the GATA3-2 site at -2207, but not mutation of any other site, prevented I3C downregulation of ERα promoter activity.

Chromatin immunoprecipitation (ChIP) was used to determine whether I3C could affect endogenous GATA3 recruitment to the native ERα promoter. Cells were treated with or without 200 μM I3C for 24 hr, DNA derived from chromatin immunoprecipitated with anti-human GATA3 antibody was PCR amplified with primers specific to the GATA3 DNA binding sites contained within the ERα promoter. As shown in Figure 19, GATA3 is bound to ERα promoter in untreated MCF7 cells at the predicted consensus sequence, and I3C treatment strongly downregulated GATA3 binding to this promoter region. Taken together, our results show that GATA3 directly interacts with the ERα promoter and mediates I3C control of ERα promoter activity.

Figure 19:

GATA3 endogenous binding to the ERα promoter decreases with I3C. The left panel shows the ERα genomic sequence containing both predicted GATA3 binding sites (bolded) within the I3C-responsive region of ERα promoter. Primers used to amplify GATA3 sites for Chromatin Immunoprecipitation are underlined. Chromatin was isolated from MCF-7 cells treated with or without 200 μM I3C for 24 hrs. GATA3 was immunoprecipitated from total cell extracts using Sepharose G bound to anti-ERα antibody. DNA released from ERα was amplified using indicated primers. Control primers directed at upstream site (-3812 bp) showed no amplification in IP samples. Input samples represent total genomic DNA from each treatment (loading control).

PROMOTER ANALYSIS

chr6: 152,168,042-152,168,226

5'-AATGCCTCTGTTCAGAGACTGGGGGCTA

GGGCCAGTAAGGCATTTGATCCACATG**TATC**CCA
gata3-1

GAAGGCTTTTATTGTTAAATTATATTCTTTCGGAA

AAACCACCCATGTCCTATTTTGTAAACTT**GATATC**
gata3-2

CATACACTTTTGACTGGCATTCTATTTTAGCCGTA

AGACTATGATTCACAGCAA-3'

ChIP

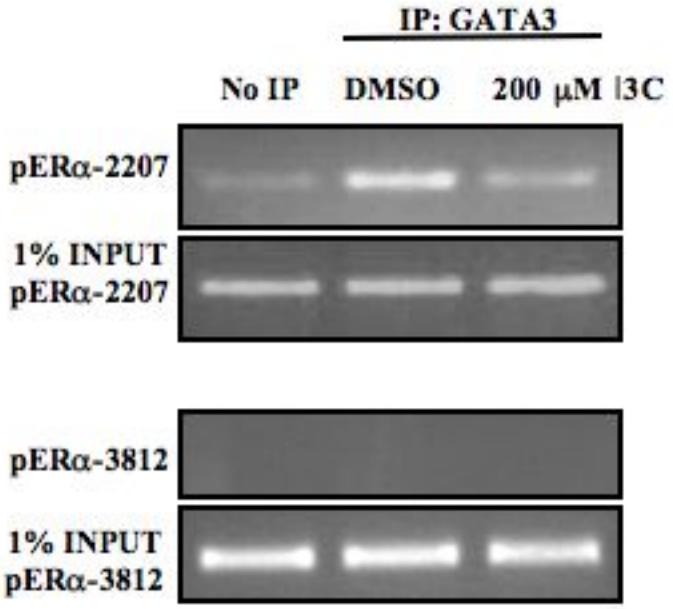

DISCUSSION

We have established the cellular mechanism by which I3C, a promising anti-cancer phytochemical from Bassica genius vegetables, ablates ERα expression and estrogen-dependent proliferation of estrogen responsive human breast cancer cells, and have uncovered a critical role for the GATA3 transcription factor in this indole-regulated cellular cascade. As summarized in figure 20, our results demonstrate that I3C triggers the ubiquitin 26S proteasome mediated degradation of ERα protein in a process that requires the aryl hydrocarbon receptor (AhR) and the E3 ubiquitin ligase ring box-1 (Rbx1). The I3C-mediated degradation of ERα protein directly down-regulates expression of GATA3, which then disrupts the GATA3/ ERα cross-regulatory loop because of the loss of GATA3 stimulated *ESR1* promoter activity. The cellular consequences of the I3C triggered transcriptional cascade are the inhibition of ERα expression and consequent loss of ERα responsive proliferation.

Ablation of either AhR or Rbx1 expression prevented the I3C induced degradation of ERα protein, demonstrating the necessity of both cellular components in this process. We propose that the I3C activation and nuclear import of the AhR helps to tether the Rbx1 E3 ubiquitin ligase to ERα for its ubiquitination and targeting for destruction. I3C has only a weak affinity for AhR (Chen et al., 1996; Ociepa-Zawal et al., 2007), and in combination with the small fraction of I3C that actually enters a cell (Staub et al., 2002), explains the relatively high concentration (200 μM) of I3C that is needed to observe the maximal degradation of ERα protein. AhR-induced degradation of

Figure 20:

Proposed Model for the I3C disruption of a cross-regulatory positive feedback loop involving expression of GATA3 and ERα by stimulating the degradation of ERα protein. In the absence of I3C, ERα and the GATA3 transcription factor maintain a cross-regulatory positive feedback loop that results in a high level of ERα expression. ERα stimulates GATA3 transcription by interacting with an enhancer region in the GATA3 gene, while GATA3 stimulates ERα promoter activity by interacting its corresponding binding sites in the ERα promoter. I3C disrupts this feedback loop by inducing the ubiquitination and proteasome mediated degradation of ERα protein. The I3C induced degradative pathway requires the Rbx1 E3 ubiquitin ligase and the I3C activation and nuclear localization of AhR. We propose that I3C-activated AhR tethers Rbx1 to its ERα protein substrate for ubiquitination and subsequent destruction.

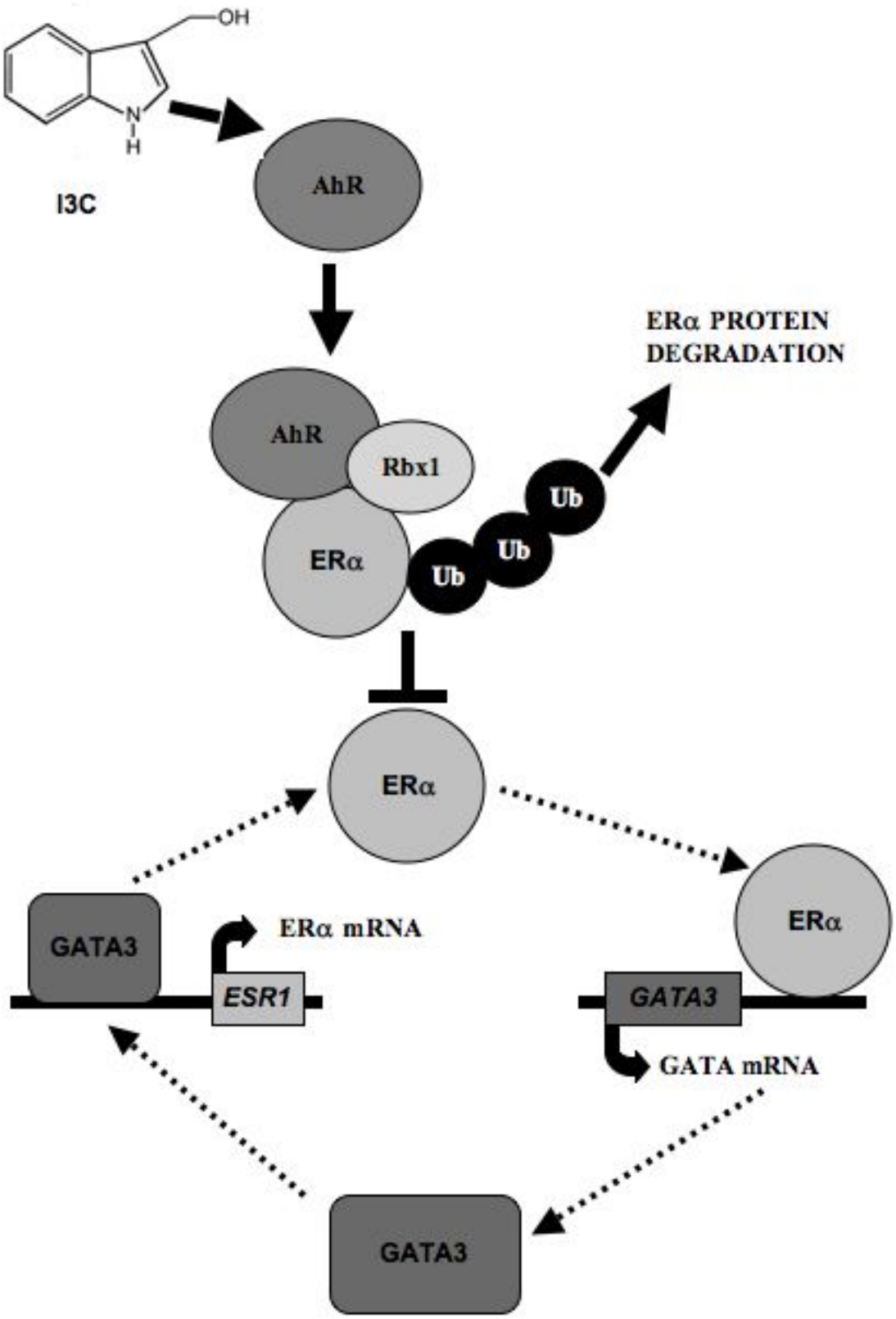
OH
N
H
I3C
AhR
ERα PROTEIN
DEGRADATION
AhR
Rbx1
ERα
Ub
Ub
Ub
ERα
GATA3
ERα mRNA
ESR1
ERα
GATA3
GATA mRNA
GATA3

ERα has been observed previously (Wormke *et al.*, 2003; Ohtake *et al.*, 2007), but with high-affinity ligands such as TCDD that is associated with reproductive defects in a variety of animal species (Antkiewicz et al., 2005). However, I3C is a natural dietary component, and unlike anthropogenic high-affinity AhR ligands, is reported to be beneficial to human health in epidemiological studies (Higdon et al., 2007). A critical intermediate step within the I3C triggered transcriptional cascade is the downregulated expression of the GATA3 transcription factor, which disrupts the maintenance of a positive cross-regulatory between GATA3 and ERα (Eeckhoute et al., 2007). Expression of GATA3 is stimulated by ERα (see figure 20), and the time required for the maximal downregulation of GATA3 gene products in I3C treated cells accounts for the kinetic differences between the rapid I3C induced degradation of ERα protein and the longer duration observed for the loss of ERα transcripts. Ecoptic expression of GATA3 reversed the I3C-mediated decrease in ERα promoter activity, but had no effect on the indole-induced degradation of ERα protein, suggesting that loss of ERα protein precedes the loss of GATA3 expression. Several recent studies have linked the cellular actions of ERα and GATA3 in mammary epithelial cell proliferation in both human breast cancer cells and in rodent model systems (Asselin-Labat et al., 2008; Kouros-Mehr et al., 2008b). GATA3 controls expression of many genes involved in the differentiation and proliferation of mammary luminal epithelial cells and is a strong predictor of tumor differentiation and estrogen receptor status of breast cancer (Kouros-Mehr et al., 2008a). Consistent with this concept, GATA3 and ERα are co-expressed in human breast cancer, and GATA3 is associated with maintaining estrogen responsive proliferation (Fang et al., 2008). Furthermore, expression of ERα has been shown to be critical in the development

of the normal breast epithelium, and GATA3 -/- mice display mammary glands that are strikingly similar to ERα -/- mammary glands (Kouros-Mehr *et al.*, 2006; Asselin-Labat, 2007). Thus, we propose that I3C will be most effective in disrupting the estrogen dependent growth of human cancer cells, such as breast cancer, that co-express ERα, GATA3 and AhR.

ERα is an important target of therapeutic strategies to control the proliferation of hormone dependent breast cancers, although, the preferred clinical options have significant adverse side effects and can lead to resistance to the treatments due to the persistence of active estrogen receptors. Aromatase inhibitors can reduce estrogen production at the cancer site, however, extended treatment can lead to bone loss as well as arthralgia due to estrogen requirements in the heart (Safi *et al.*, 2005; Ewer and Gluck, 2009). The adverse side effects of Selective Estrogen Receptor Modulators (or SERMs), such as tamoxifen, are associated with the ligand-independent activation of ERα. Because I3C functions as a potent Selective Estrogen Receptor Downregulator (or SERD) of ERα expression, this indole can diminish both ligand-dependent and -independent ERα activation in breast cancer cells, and consequently disrupt expression of the ERα target genes involved in cell proliferation.

One of the SERDs that is currently in clinical use, fluvestrant, causes the degradation of ERα in breast cancer cells (Osborne et al., 2004), however, this degradative process also occurs in many other tissues and can lead to pulmonar emboli, deep vein thromobosis, ostoepenia, oseoporosis and artharlgia. We propose that I3C will

be most effective in disrupting the estrogen dependent growth of human cancer cells, such as breast cancer, that co-express ERα, GATA3 and AhR, and therefore will have a significantly reduced systemic side effects in tissues such as heart and bone that express and are developmentally regulated by alternate GATA family members (Charron *et al.*, 1999; Garimella *et al.*, 2007; Afouda *et al.*, 2008). Furthermore, in addition to the I3C-dependent ablation of ERα gene expression, this indole also activates ERβ (Sundar et al., 2006), which would allow many beneficial estrogen responses to be maintained in I3C treated cells, including anti-proliferative signaling by this ER subtype. The novel properties of I3C, and its strong SERD function, implicate this indole has a highly tissue specific therapeutic potential for estrogen responsive cancers with the promise to improve the overall clinical outcome of patients.

ACKNOWLEDGEMENTS:

The authors thank A. J. Maxwell for generation of the -2294 ERα promoter construct and feedback. We greatly appreciate the comments and suggest by the entire Firestone laboratory during the course of our work. This study was supported by National Institutes of Health Public Service grant CA102360 awarded from the National Cancer Institute. S.N. Sundar was supported by a postdoctoral fellowship from the Susan G. Komen Breast Cancer Fund, and C. N. Marconett was supported by a dissertation fellowship from the California Breast Cancer Research Program (#13GB-1801).

Chapter II-A

Indole-3-Carbinol mediated disruption of Insulin-like Growth Factor signaling pathway in estrogen-dependent human breast cancer cells.

ABSTRACT

Indole-3-Carbinol (I3C) is a dietary phytochemical that arrests the proliferation of estrogen-dependent human breast cancer cells. Estrogen signaling stimulates growth and proliferation of these cells by activation of key downstream targets, such as Insulin-like Growth Factor Receptor-1 (IGF1R) and Insulin Receptor Substrate-1 (IRS1) of the Insulin-like Growth Factor (IGF1) signaling pathway. Using the estrogen sensitive MCF7 breast cancer cell line, we show that I3C downregulates both IGF1R and IRS1 RNA and protein expression. We established that this decrease in expression was contingent upon Estrogen Receptor-α (ERα) ablation by I3C. Therefore, I3C is able to inhibit IGF signaling in hormone sensitive breast cancer cells by blocking expression of critical intracellular signaling pathway components that are required not only for proliferation but also for progression toward a more advanced, hormone insensitive stage of human breast cancer.

INTRODUCTION

Insulin-like Growth Factor Receptor (IGF1R), a transmembrane receptor tyrosine kinase, undergoes autophosphorylation upon binding to its ligand, Insulin-like Growth Factor (IGF1), which leads to phosphorylation and activation of key intracellular proteins, chiefly Insulin Receptor Substrate-1 (IRS1). Once activated, IRS-1 recruits a wide array of downstream signaling pathways known to cause proliferation of hormone sensitive breast cancer cells (Chitnis *et al.*, 2008). Aside from being a requisite for normal growth and development, the IGF1R signaling pathway is also well-associated with the genesis of breast cancer (Jones *et al.*, 2007; Jones *et al.*, 2009). High levels of serum IGF1 can increase breast cancer risk by up to 7-fold in pre-menopausal women, and are therefore, often used as a prognostic in these women. Additionally, elevated IGF1R and IRS protein levels correlate extremely well with increased tumorigenicity, metastases, and invasion (Nagle *et al.*, 2004). Moreover, IGF1R expression increases by up to seven fold in estrogen sensitive breast cancer cells compared to normal epithelial cells (Happerfield *et al.*, 1997).

The dependence of estrogen sensitive breast cancer cell proliferation on IGF1R and IRS1 expression has been demonstrated through enhanced MAPK signaling, and improved responsiveness to estradiol (E_2) (Clarke *et al.*, 1997). The pro-proliferative activities of estradiol are mediated by Estrogen Receptor-alpha (ERα), which is activated upon E_2 binding and subsequent dimerization. This dimer associates with other key proteins to form a transcription factor complex that binds to DNA recognition motifs

termed Estrogen Response Elements (*EREs*), and activates target genes' transcription. Addition of E_2 to estrogen sensitive breast cancer cells induces the expression of IGF1R and IRS1 (Stewart *et al.*, 1990; Mauro *et al.*, 2001). Conversely, ERα negative breast cancer cell lines express comparatively low levels of IGF1R and IRS1 (Surmacz and Bartucci, 2004).

Elucidation of the important roles that IGF1, IGF1R, and IRS1 play in maintenance and proliferation of breast cancer has sparked pharmaceutical interest, and therefore, influenced the development of several therapeutics that target this specific pathway. One approach has been to disrupt IGF1 binding to IGF1R, either by employing neutralizing monoclonal antibodies directed against IGF1, or by increasing levels of IGF Binding Proteins (IGFBP), which naturally bind and sequester IGF1(Van den Berg *et al.*, 1997; Goya *et al.*, 2004). In addition, monoclonal antibodies can be directed toward IGF1R to induce receptor-mediated endocytosis, followed by proteolytic degradation (Lee *et al.*, 2003; Sachdev *et al.*, 2003; Wang *et al.*, 2005). However, problem with such an approach is that antibody binding can also induce partial activation of the receptor in some cases (Li *et al.*, 2000).

An alternative, therefore, is to modulate IGF1R activity through chemical disruption by using small molecular inhibitors that block IGF1R's autophosphorylation capability (Carboni *et al.*, 2005; Wittman *et al.*, 2005; Garcia-Echeverria, 2006). While effective at blocking phosphorylation, and thus activation, the lack of specificity, owing to the homology between receptor tyrosine kinases, makes this strategy less promising

because of the high probability of off-target effects. Since IGF1R and IRS1 are expressed in the majority of normal tissues, along with playing essential roles such as neuronal development, maintenance of cardiac function, and signaling of pancreatic beta cells, disruption of these activities can lead to dire consequences (Da Silva Xavier *et al.*, 2004; Liu *et al.*, 2009). Considering the drawbacks of aforementioned approaches, it becomes exceedingly important that alternate therapies targeting the IGF signaling axis be created which are more effective, and have reduced side-effects.

Epidemiological and physiological studies have suggested that phytochemicals from vegetables and fruits represent intriguing natural sources that can be exploited for creating new classes of potential anti-cancer molecules with minimal adverse side-effects (Manson *et al.*, 2005). One such phytochemical is Indole-3-Carbinol (I3C), a natural compound derived by hydrolysis from *glucobrassicin* produced in *Brassica* cruciferous vegetables such as cabbage, broccoli, and Brussels sprouts. There is compelling evidence in estrogen-sensitive human breast cancer cell lines, such as MCF7 and T47D, that I3C treatment disrupts estrogen responsive gene expression (Auborn et al., 2003; Cover et al., 1998; Wang et al., 2006), and inhibits estrogen-dependent proliferation. We now demonstrate that I3C blocks expression of both IGF1R and IRS1 mRNA and protein levels in estrogen responsive human breast cancer cells through targeted disruption of ERα expression. This specific downregulation of IGF1R and IRS1 expression contributes directly to I3C-mediated inhibition of estrogen-dependent proliferation.

MATERIALS & METHODS

Reagents

ERα and HSP90 antibodies were purchased from Santa Cruz Biotechnology (Santa Cruz, CA). IGF1R and IRS1 antibodies were purchased from Cell Signaling Technology (Danvers, MA). Indole-3-Carbinol (I3C), 17β-Estradiol (E_2), and Dimethylsulfoxide (DMSO) were obtained from Sigma Chemical Company (St. Louis, MO). Propyl pyrazole triol (PPT) was obtained from LC Laboratories (Woburn, MA). All other chemicals were of the highest quality available.

Cell Culture

MCF7 human breast cancer cells were obtained from American Type Culture Collection (Manassas, VA). Cells were grown in Dulbecco's Modified Eagles Medium (DMEM) from BioWhittaker (Walkersville, MD), supplemented with 10% fetal bovine serum from Mediatech (Manassas, VA), 10μg/ml insulin, 50 U/ml penicillin, 50 U/ml streptomycin, and 2 mM L-glutamine from Sigma (St. Louis, MO). Cells were grown to subconfluency in a humidified chamber at 37°C containing 5% CO_2. A 200 mM stock solution of I3C was dissolved in DMSO. A 100 μM stock of PPT and 10 μM stock of E_2 were made by dissolving each in DMSO. I3C, PPT, or E_2 was then diluted 1:1000 in media prior to culture plate application. Phenol red-free media supplemented with dextran charcoal-stripped media from Gemini Bio-Products (Sacramento, CA) was employed for all estrogen sensitivity assays.

Western Blotting

After the indicated treatments, western blots were performed as previously indicated (Sundar et al., 2006). Mouse anti-ERα (sc-8005), rabbit anti-IRS1 (CS-2382), and rabbit anti-IGF1R (CS-3027) were diluted 1:200 in TBST. Hsp90 (#610419 BD Transduction laboratories, Franklin Lakes, NJ), hsp60 (XXX), and actin (#AAN01 Cytoskeleton, Inc. Denver, CO) were used as loading controls, and antibodies for these were diluted 1:2000 and 1:1000 respectively, in TBST. Immunoreactive proteins were detected after incubation with horseradish peroxidase-conjugated secondary antibodies diluted $3x10^{-4}$ in 1% NFDM in TBST. Blots were then treated with enhanced chemiluminescence reagents (Eastman Kodak, Rochester NY) visualization on film.

Expression Plasmid Transfection

Cells were grown and indicated treatments performed on 10 cm tissue culture plates from Nunc (Fisher Scientific, Rochester, NY). Human CMV-IRS1 expression plasmid was obtained from Addgene, “Addgene plasmid 11238” (Cambridge, MA). Human pBABE-IGFIR plasmid was obtained from Addgene "Addgene plasmid 11212" (Cambridge, MA). Human CMV-ERα was a kind gift from Dr. Benita Katzenellenbogen, University of Illinois at Urbana-Champagne. Transfection of expression vectors was performed using Polyfect transfection reagent from Qiagen (Valencia, California) per manufacturers’ recommended protocol.

RT-PCR

Total RNA from MCF7 cells treated with indicated compounds was isolated with TRI Reagent according to manufacturer's protocol from Sigma (St. Louis, MO). Total RNA (4 μg) was used to synthesize cDNA using Moloney murine leukemia virus-reverse transcriptase from Promega Corp (Madison, WI) with random hexamers as primers. The cDNA reaction product (400 ng) was amplified with primers of the following sequences:

ERα Forward: 5'-AGCACCCAGTGAAGCTACT-3',

ERα Reverse: 5'-TGAGGCACACAAACTCCT-3';

IGF1R Forward: 5'-TGAGGATCAGCGAGAATGTG -3',

IGF1R Reverse 5'-GACCCATTCCCAGAGAGAGA -3';

PR Forward: 5'-CGAAAACCTGGCAATGATTTAGAC -3',

PR Reverse 5'-GAACCAGATGTGATCTATGCAGGA -3';

IRS1 Forward: 5'- CAGAGGACCGTCAGTAGCTCAA-3',

IRS1 Reverse 5'- GGAAGATATGAGGTCCTAGTTGTGAAT-3';

GAPDH Forward 5'-TGAAGGTCGGAGTCAACGGATTTG-3',

GAPDH Reverse: 5'- CATGTGGGCCATGAGGTCCACCAC-3'.

PCR products were analyzed on 1.2 % agarose gel along with 1-kb Plus DNA ladder from Invitrogen (Carlsbad, CA) and the products were visualized with GelRed from Biotium (Hayward, CA).

Chromatin Immunoprecipitation (ChIP) Assays

MCF7 cells were grown to subconfluency and treated for 48 hr with 200 μM I3C or DMSO vehicle control. ChIP was performed as previously described (Sundar et al, 2008). Primers for ChIP experiments were as follows:

pIRS1 Forward: 5'- ACACCCATTGAACCACCCTA-3',

pIRS1 Reverse: 5'-CGTTTGTTTGTGGGGAGACT-3';

pIGF1R Forward: 5'-GGAGCCGCTCATTCATTTTGAC-3',

pIGF1R Reverse: 5'-CTAGGCGAGGAAAAACAAGC-3'.

Products were visualized on a 1.5 % agarose gel buffered with TBE.

RESULTS

I3C downregulates IGF1R and IRS1 expression in MCF7 human breast cancer cells

I3C is able to block growth and proliferation of breast cancer cells (Cover *et al.*, 1998). The Insulin-like Growth Factor pathway plays a critical role in cell growth and tumor progression (Werner and Bruchim, 2009). Therefore, we tested the effects of I3C on the expression of IGF pathway members in the hormone sensitive breast cancer cell line MCF7.

Cells were exposed to increasing concentrations of I3C for 48 hours to determine the half maximal effect on IGF1R and IRS1 downregulation. Total protein levels for each dose were determined by Western Blot analysis of electrophoretically fractionated cell extracts, and the corresponding transcript levels were analyzed by RT-PCR quantification of isolated total RNA. As shown in figure 21, I3C exposure to MCF7 cells elicited downregulation of IGF1R and IRS1 protein and RNA levels in a dose-dependent manner.

The half-maximal response was observed at approximately 150 μM I3C, which interestingly corresponded with I3C-dependent downregulation of ERα, with total ablation occurring at 200 μM I3C. This concentration of I3C was previously shown to cause the maximal inhibition of estrogen dependent proliferation without any apoptotic

Figure 21:

The observed half-maximal downregulation of IGF1R and IRS1 is 150 μM I3C. MCF7 cells were treated with increasing concentrations of I3C for 48 hr. IGF1R, IRS1 and ERα protein was monitored by western blot analysis (upper panels), and IGF1R, IRS1 and ERα transcript expression was determined by RT-PCR (lower panels). The PCR products were visualized on a 1% agarose gel stained with ethidium bromide. HSP90 provided a loading control for the western blots and GAPDH provided a gel loading control for the RT-PCR.

PROTEIN

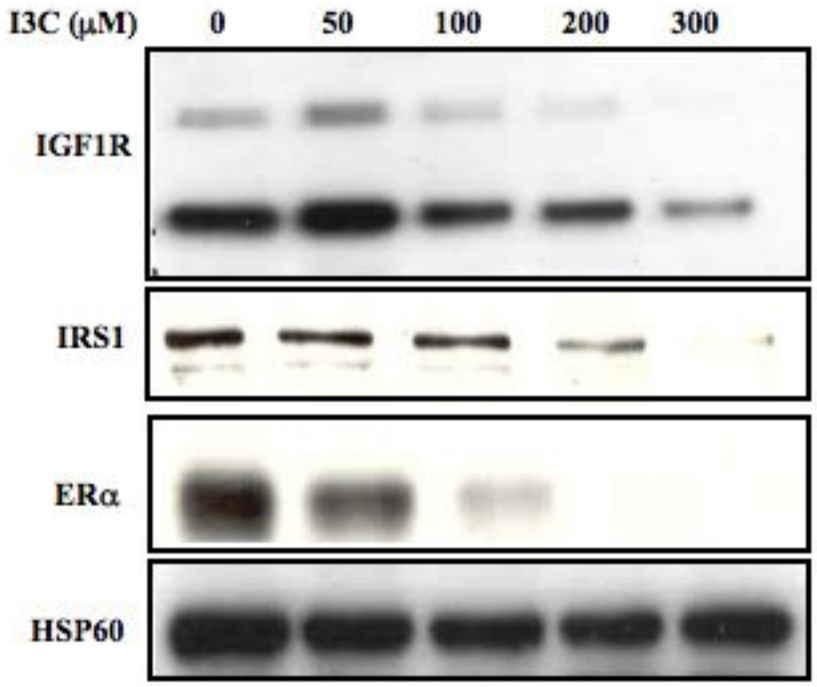
I3C (μM)
0
50
100
200
300
IGF1R
IRS1
ERα
HSP60

RNA

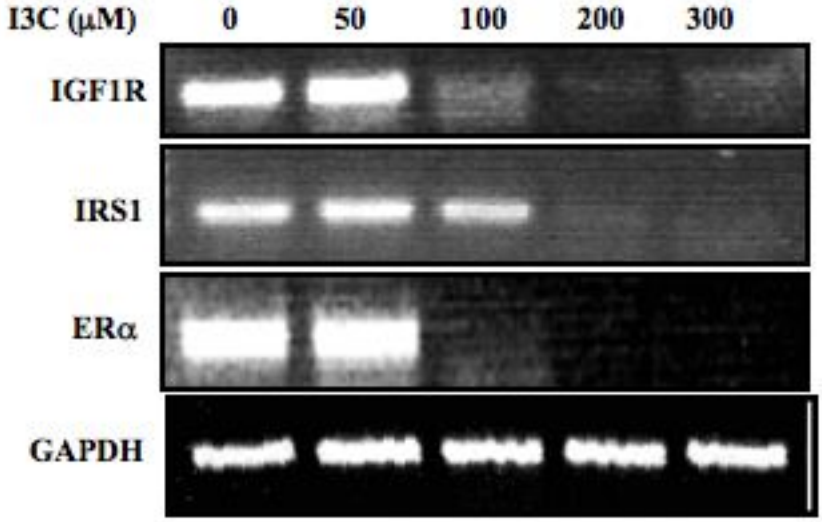
I3C (μM)
0
50
100
200
300
IGF1R
IRS1
ERα
GAPDH

Figure 22:

Effects of I3C on the expression of IGF1R and IRS1 protein and transcripts. MCF-7 cells were treated with or without 200 μM I3C, and at the indicated times the level of IGF1R, IRS1 and ERα protein was monitored by western blot analysis (upper panels), and IGF1R, IRS1 and ERα transcript expression was determined by RT-PCR (lower panels). The PCR products were visualized on a 1% agarose gel stained with ethidium bromide. HSP90 provided a loading control for the western blots and GAPDH provided a gel loading control for the RT-PCR.

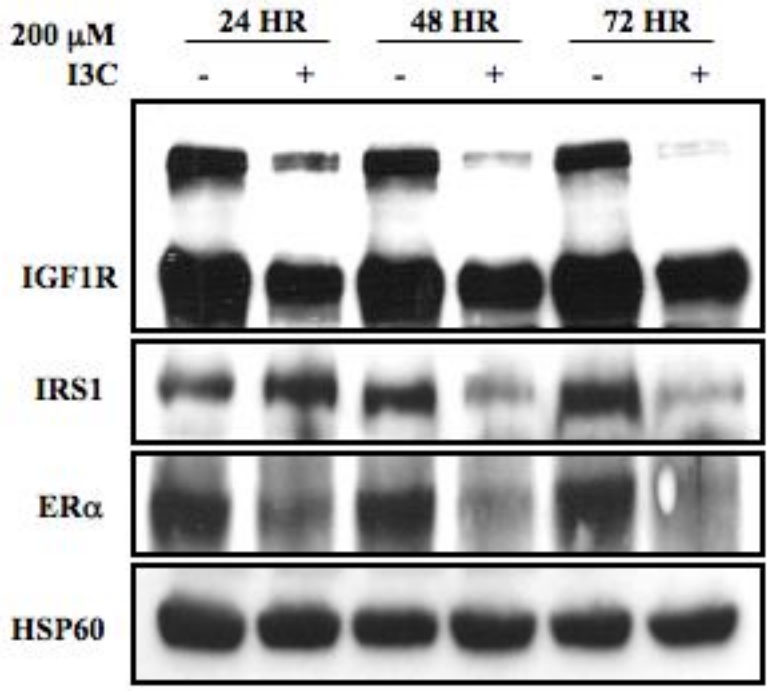
200 μM
I3C
24 HR
48 HR
72 HR
- + - + - +
IGF1R
IRS1
ERα
HSP60

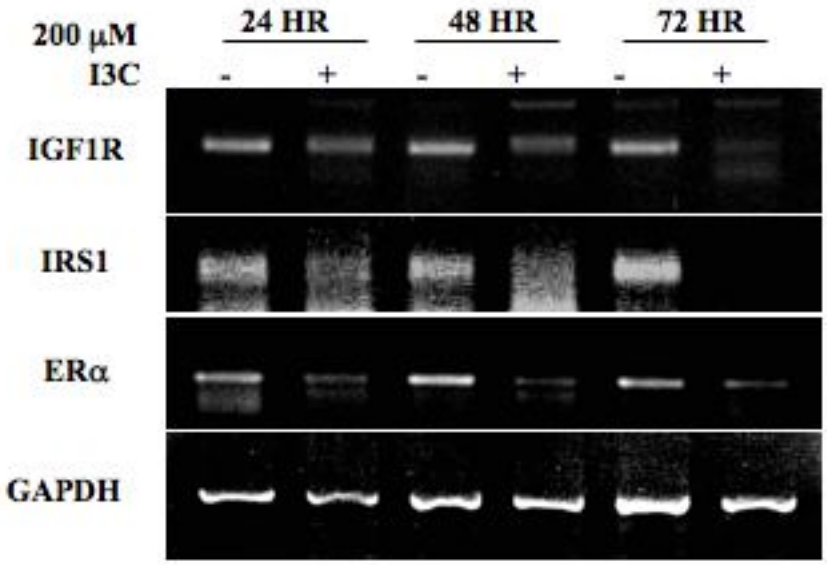
200 μM
I3C
24 HR
48 HR
72 HR
- + - + - +
IGF1R
IRS1
ERα
GAPDH

effects (Sundar *et al.*, 2006). Therefore, 200 μM I3C was used throughout the duration of the rest of the study. IGF1R and IRS1 downregulation was maintained over a 72 hr time course with 200 μM I3C, as shown in figure 22. No changes were observed for gel loading control genes hsp60 (protein) or GAPDH (mRNA) throughout the dose response or time course. Therefore, I3C decreases expression of IGF1R and IRS1 in the hormone sensitive MCF7 human breast cancer cell line.

I3C mediated decline in IGF1R and IRS-1 levels is only observed in ERα positive cell lines

To determine the types of breast cancer this downregulation occurs in, the effect of I3C on IGF1R and IRS1 in multiple breast cancer cell lines with varying ERα status was studied. MCF10T, MCF7, and T47D were used to represent ERα positive cell lines, MCF10A and MB-MDA-231 represented ERα negative status (Shekhar *et al.*, 1998; Zhou *et al.*, 2007). Each cell line was exposed to 200 μM I3C for 48 hours. Interestingly, IGF1R and IRS1 protein and RNA downregulation was observed only in ERα positive cell lines, further indicating a correlation between the IGF1R signaling pathway and ERα (figure 23).

The correlation between hormone status and downregulation of IGF1R and IRS1 suggested that ERα may play a critical role in the observed I3C effect. I3C is known to block ERα activity though ablation of ERα expression by a process that is highly specific to the chemical structure of I3C, as the acid condensation dimmer of I3C,

Figure 23:

IGF1R and IRS1 are expressed in hormone sensitive breast cancer cell lines and I3C disrupts this expression. MCF10A, MCF7, and MDA-MB-231 cells were treated with 200 μM I3C or DMSO vehicle control for 48 hr. Total Cell lysates were subjected to SDS-PAGE and the levels of IGF1R, IRS1 and HSP90 (loading control) protein was monitored by western blot analysis.

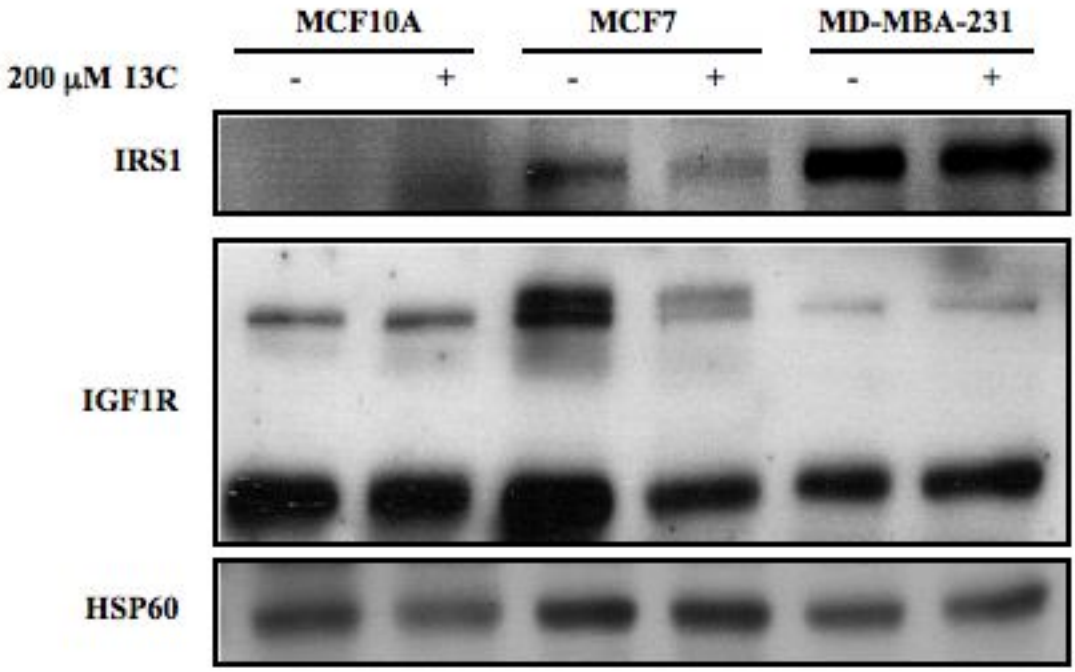
MCF10A
MCF7
MD-MBA-231
200 μM I3C
-
+
-
+
-
+
IRS1
IGF1R
HSP60

3,3'diindoylylmethane (DIM) is able to induce a similar G1 cell cycle arrest but fails to ablate ERα expression. In order to test if the I3C mediated downregulation of IGF1R and IRS1 was consistent with the known mechanism of action MCF7 cells were treated with DMSO vehicle control, 200 μM I3C, 30 uM DIM, or 200 uM Tryptophol, an indole with similar structure to I3C but with no observable affect on proliferation for 48 hours. Total protein and RNA was harvested and subjected to western blotting and RTPCR, respectively. As shown in figure 24, I3C was able to selectively block IGF1R and IRS1 transcript expression. DIM and tryptohol failed to do so, suggesting that IGF1R and IRS1 downregulation are specific to the mechanism of I3C action, and not a generalized effect of overall growth inhibition or nonspecific indole addition.

I3C disrupts IGF1R signaling via ERα in an estrogen dependent manner.

ERα, once activated upon binding to its ligand estrogen, acts as a transcription factor to induce expression of a variety of genes. Addition of estrogen can induce IGF1R promoter activity (Maor *et al.*, 2006). Furthermore, ligand-activated ERα can bind to regulatory regions of the IRS1 promoter and subsequently increase IRS1 transcription in mice (Mauro *et al.*, 2001).

I3C is known to downregulate ERα expression (Wang *et al.*, 2006). Therefore, we postulated that ERα ablation by I3C causes attenuation of IGF1R and IRS1 transcription, and consequently leads to low IGF1R and IRS1 protein levels. In order to probe this hypothesis, MCF7 cells were grown in steroid deficient media in the presence or absence

Figure 24:

DIM and Tryptophol fail to induce the downregulation of IGF1R and IRS1 seen with I3C (A) MCF-7 cells were treated with the indicated concentrations of indoles for 48 hrs, and IGF1R and IRS1 transcript expression was determined by RT-PCR (top panels) and IGF1R protein expression was monitored by western blot analysis (lower panels). The PCR products were visualized on a 1% agarose gel stained with ethidium bromide. Actin provided a loading control for the western blots and GAPDH provided a gel loading control for the RT-PCR.. Representative blot of three independent experiments shown.

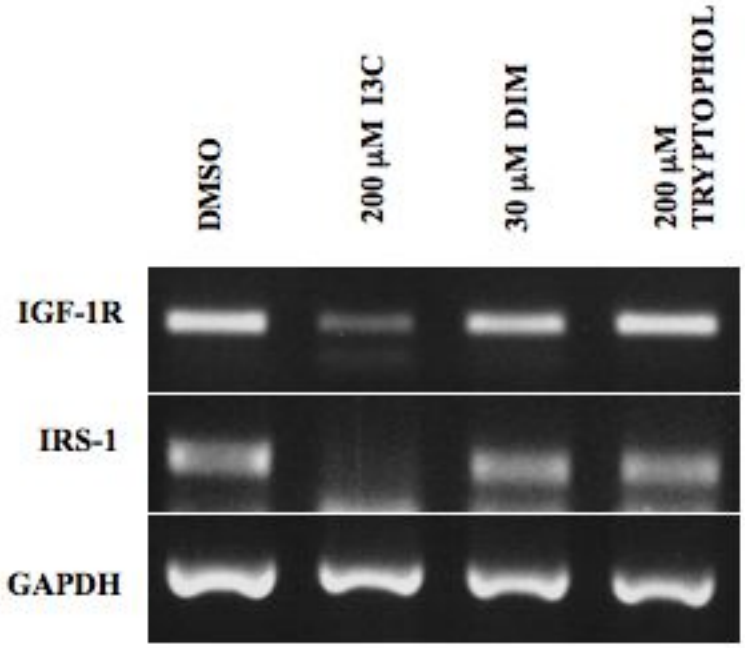
DMSO
200 μM I3C
30 μM DIM
200 μM TRYPTOPHOL
IGF-1R
IRS-1
GAPDH

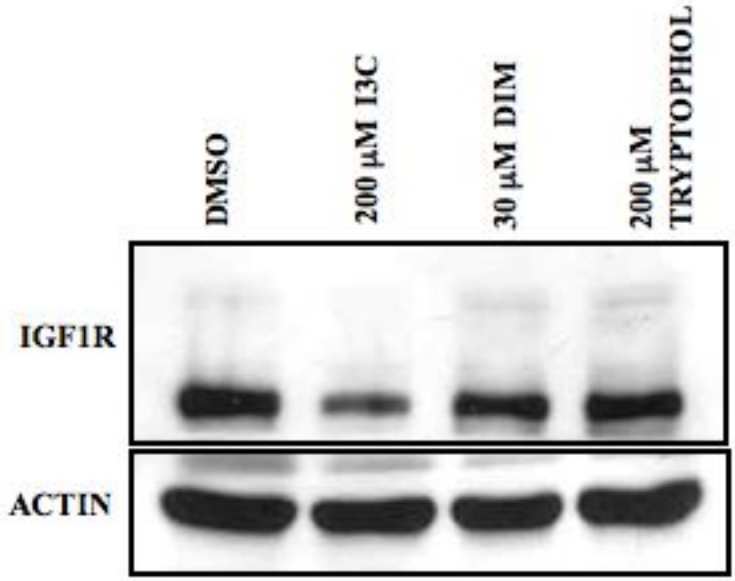
DMSO
200 μM I3C
30 μM DIM
200 μM TRYPTOPHOL
IGF1R
ACTIN

Figure 25:

I3C blocks estrogen dependent expression of IGF1R and IRS1 protein and transcript expression. MCF7 cells were grown in steroid deficient media for 24 hrs, then treated with the indicated combinations of 200 μM I3C, 10 nM E2 and 100 nM PPT. IGF1R, IRS1 and ERα protein expression was monitored by western blot analysis (top panels). Actin provided a loading control for the western blots. Representative blot of three independent experiments is shown. IGF1R, IRS1 and ERα transcript expression was determined by RT-PCR (lower panels). Transcript levels were normalized to GAPDH loading controls and the fold change in transcript expression relative to DMSO is shown.

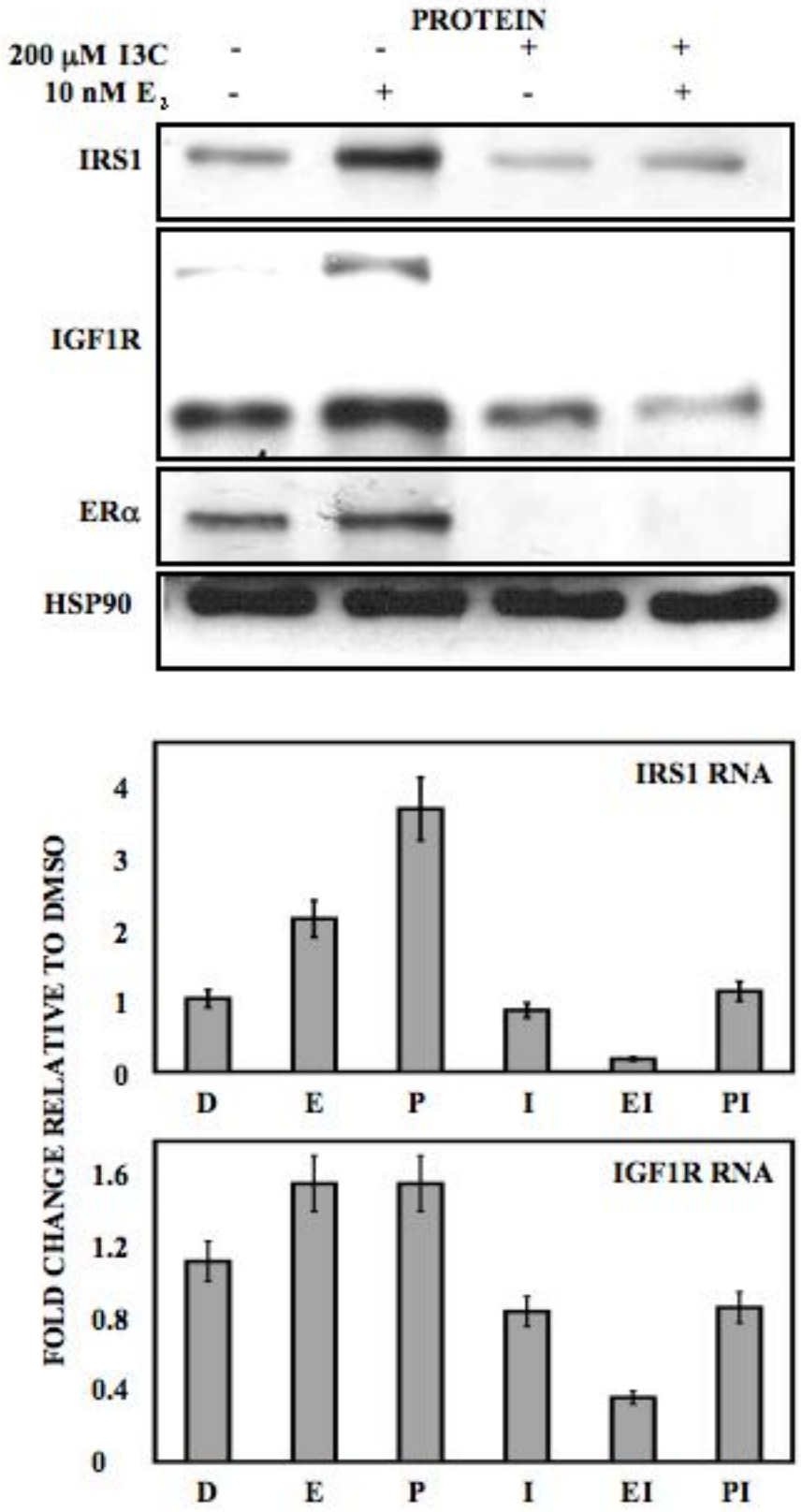
PROTEIN
200 μM I3C - - + +
10 nM E2 - + - +
IRS1
IGF1R
ERα
HSP90
IRS1 RNA
IGF1R RNA
FOLD CHANGE RELATIVE TO DMSO
0
1
2
3
4
0.4
0.8
1.2
1.6
D
E
P
I
EI
PI

of 200 μM I3C or10 nM 17-β-estradiol (E_2). Figure 25 clearly shows that IGF1R and IRS1 mRNAs are elevated in the presence of estradiol, whereas they are markedly reduced in the presence of I3C; the result is mirrored by protein levels, as evident in figure 25.

In order to determine which of the estrogen receptor subtypes was responsible for this induction, and thus affected by I3C, we treated MCF7 cells with 10 nM propyl pyrazole triol (PPT), and ERα specific agonist, alone or in combination with 200 μM I3C. As shown in figure 25, PPT significantly increased IRS1 and IGF1R RNA, and I3C ablated this increase. Taken together, this indicates that I3C blocks ERα dependent stimulation of IRS1 and IGF1R transcription in MCF7 hormone sensitive breast cancer cells.

I3C disrupts ERα association with both IGF-1R and IRS-1 promoters

The ability of I3C to disrupt estrogen stimulation of IGF1R and IRS1 suggests that the effects are mediated through ERα. ERα is able to bind directly to DNA, and recruit activating transcription factors through its two trans-activation domains, and as such is likely to be essential for enhanced expression of IGF1R and IRS1 in hormone sensitive breast cancer cells. Therefore, endogenous association of ERα with the promoter regions of IGF1R and IRS1 was examined. An ERα-Sp1 composite element within the IGF1R promoter (between -458 to +53) has been shown to be important in estrogen dependent upregulation of IGF1R expression (Maor *et al.*, 2006), however this

511 bp region contained several transcription factor binding sites, including two EREs. Similarly, IRS1 expression increases with endogenous binding of ERα to the IRS1 promoter in mice. However, the sequence of the IRS1 promoter regulatory region diverges at this identified site between mice and humans (figure 26). Therefore, we determined potential sites of ERα binding within the IRS1 promoters based on the ERα consensus binding site sequence, or estrogen response element (ERE).

Two unique ERα binding sites for IGF1R were identified within the estrogen responsive region upstream of the transcription start site; one located 222 bases upstream (-222 IGF1R) and the other 426 bases upstream (-426 IGF1R) of the transcription start site. One site at -1975, within 2 kB of the transcription start site, was identified for IRS1. Interestingly, -426 IGF1R and the IRS1 site and are half-ERE elements located in close proximity to predicted Sp1 binding sites (Figure 26). Because Sp1 is a transcription factor involved in target gene activation whose activity can also be altered with I3C (Cram *et al.*, 2001), we used chromatin immunoprecipitation to test endogenous association of ERα and Sp1 with IGF1R and IRS1 promoters.

We observed that the ERα and Sp1 complex binds to both the -426 IGF1R and IRS1 sites, but not on the predicted -222 IGF1R site (Figure 26). Additionally, Sp1 recruitment to both IGF1R and IRS1 remained unaltered in the presence of I3C. Nevertheless, endogenous binding of ERα was markedly reduced, which renders the whole complex inactive, thereby proving that loss of ERα by I3C leads to reduced transcription of both IGF1R and IRS1.

Figure26:

I3C disrupts ERα protein interaction with IGF1R and IRS1 regulatory regions. Alignment of human and mouse genomic sequence revealed sequence divergence at the previously identified ERE site within the mouse Sp1 promoter. Human genomic sequence is on top, mouse genomic sequence is on the bottom. Matching bases denoted by vertical line. Genomic sequences of the IGF1R and IRS1 promoter contain a composite half-ERE site-Sp1 site (middle panels). Primers used to amplify ERE site for chromatin immunoprecipitation are underlined. Sequence and chromosomal location were obtained from the UCSC Genome Browser. (Bottom panels) Chromatin immunoprecipitation (ChIP) was employed to characterize endogenous ERα interactions with the ERE region of the IGF1R and IRS1 promter regions. Chromatin was isolated from MCF-7 cells treated with or without 200 μM I3C for 24 hrs. ERα was immunoprecipitated from total cell extracts using Sepharose G bound to anti-ERα antibody and DNA released from ERα was amplified using the indicated oligonucleotide primers. Control primers directed at an alternate site in the IGF1R promoter (-426) showed no amplification in IP samples. Input samples represent total genomic DNA from each treatment (loading control).

Side by Side Alignment*

```
227373130 ggaggccgggggggaggcgggggcgccggagctgggc 227373165
>>>>>>>>> || |||   |||| || |||| ||| || |    || >>>>>>>>>
082288542 gggggcgctggggcggaggggacgcgggtgacctgc 082288577
```

mSp1 **mERE**

human IRS1 promoter-chr2:227,373,725-227,373,914

5'-ACACCCATTGAACCACCCTATAAGTTTTTAACCT**TGACC**ACAAGGA

ERE

TAACAGGGAGAAAACAAGGATGGTGCCAGCTCAACTGTACAGGAAAA

TGGTTACTTCATGAGTGGACCAGATCAGCAGCCTGGGTCTACTTGAA

GCGCCCCTTTCAG**GGTCA**CCTTGCGGTATCAGTCTCCCCACAAACA

Sp1 *ERE*

AACG-3'

human IGF1R promoter-chr15:97,009,802-97,009,969

5'-GGAGCCGCTCATTCATTTTGACTCCGCGTTTCTGCCCCTCGCCGG

CCTCGCCTGT**TGACC**CGGACT**TCGGGGCG**ATCTTGCGAACTGCGTC

ERE ***Sp1***

GCGCCCTC**CCGCGGCGG**AAGCTCGGGCGT**CCGGCCGCC**TC**CCGC**

Sp1 ***Sp1***

GCGGCCAGGGCCGGGCTTGTTTTTCCTCGCCTAG-3'

Sp1

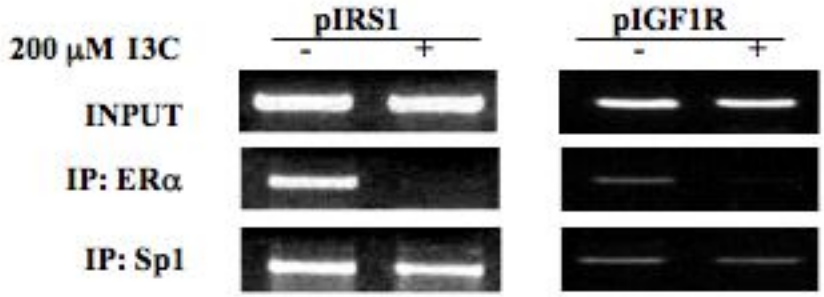

Over-expression of ERα overcomes the effect of I3C on IGF-1R and IRS-1 transcript and protein levels.

I3C is able to modulate the expression of ERα. In order to determine if I3C dependent downregulation of ERα is sufficient for loss of IGF1R and IRS1 expression, MCF7 cells were transfected with a plasmid containing human ERα gene, followed by analysis of IGF1R and IRS1 expression in the presence or absence of I3C. As shown in figure 27, exogenous expression of ERα was sufficient to rescue IGF1R and IRS1 RNA levels.

Figure 27:

I3C down-regulation of IGF1R and IRS1 gene expression requires the I3C mediated loss of ERα protein. Total RNA was collected from MCF-7 cells treated with or without 200 μM I3C 48 hrs, and RTPCR was used to detect IGF1R, IRS1 and ERα transcripts. GAPDH was used as total RNA loading control. PCR products were visualized on a 1% agarose gel stained with ethidium bromide.

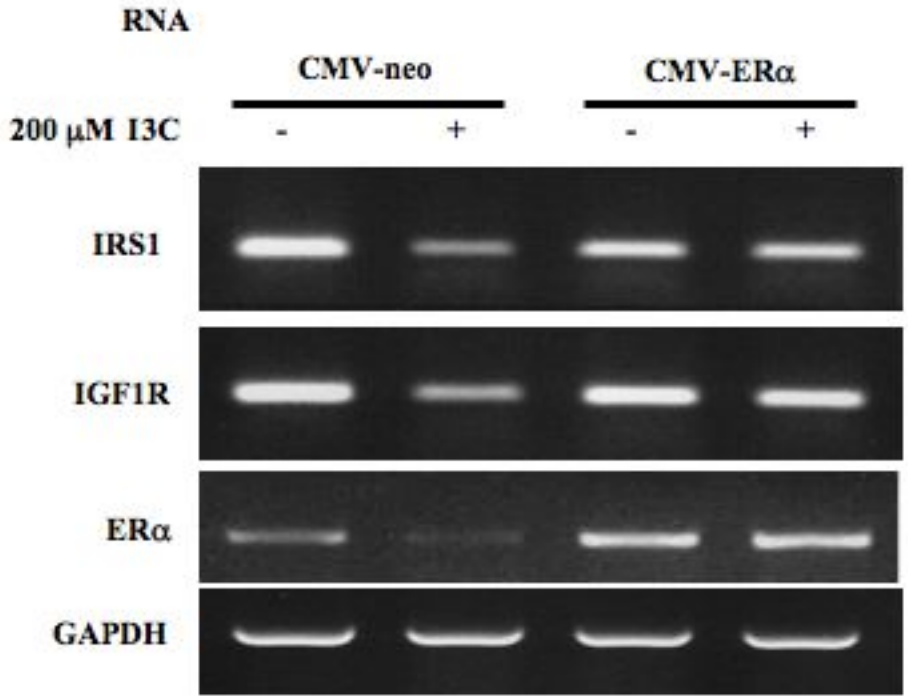
RNA
CMV-neo
CMV-ERα
200 μM I3C
-
+
-
+
IRS1
IGF1R
ERα
GAPDH

DISCUSSION

We have established the precise molecular mechanism involved in the I3C-dependent inhibition of the IGF stimulatory pathway. Our results demonstrate that I3C-dependent downregulation of ERα ablates the transcriptional activation of downstream target genes IGF1R and IRS1. The connection between ERα expression and proliferation in breast cancer has been well documented (Santen *et al.*, 2009). IGF1 activation of the intracellular phosphorylation of IGF1R and IRS1 increasing their kinase activity can lead to phosphorylation and ligand independent activation of ERα (Strissel *et al.*, 2008). Additionally, activation of IRS1 can induce its nuclear translocation and activate or modulate ERα transcriptional activity (Sisci *et al.*, 2007).

Our data suggest that I3C exploits an alternate mechanism to disrupt signaling between these pathways, namely by disrupting ERα expression and shutting off IGF1R and IRS1 transcript stimulation by ERα. In mice, transcriptional activation of IRS1 by ERα has been documented (Mauro *et al.*, 2001). Additionally, IGF1R transcript stimulation by the addition of E2 has been demonstrated (Maor *et al.*, 2006).

Current therapies targeting IGF signaling in breast cancer directly inhibit receptor tyrosine kinase activation through the use of small molecule inhibitors, antibodies, or modulation of the growth hormone-IGF axis. However, these disruptions are not specific to breast cancer and can disrupt the vital functioning of IGF signaling in off-target tissues, such as pancreatic islet function. However, blocking the production of IGF1R

and IRS1 in a mechanism specific to the abberant expression of IGF1R and IRS1 in hormone sensitive breast cancer represents a targeted approach to confer specificity of this therapy.

ACKNOWLEDGEMENTS

The authors thank C. Ronald Kahn for generation of the CMV-IRS1 expression plasmid and Dr. Eva Surmacz for the pBABE-IGF1R plasmid.

Chapter II-B

Indole-3-carbinol exerts anti-estrogenic effects on transcription of hTERT, the catalytic subunit of human telomerase in breast cancer cells.

ABSTRACT

Telomerase, a ribonucleoprotein complex composed of both protein (hTERT) and RNA (hTERC) components is capable of extending cellular lifespan through the addition of telomeric repeats to the end of chromosomes has been implicated in breast carcinogenesis. Indole-3-carbinol (I3C), a dietary phytochemical found in cruciferous vegetables has demonstrated antiproliferative effects in human breast cancer cells, including the hormone sensitive MCF7 breast cancer cell line. We have characterized the effect I3C has on hTERT expression in hormone sensitive breast cancer cells. I3C is able to block hTERT expression through a loss of transcriptional activation. I3C mediated loss of hTERT expression was attributed to disrupted endogenous binding to a composite ERα -Sp1 site. The block in hTERT expression disrupted telomerase activity, and ectopic expression of hTERT was able to restore telomerase activity. Therefore we have uncovered a critical role I3C employs to block the proproliferative activities of telomerase in hormone sensitive breast cancer cells.

INTRODUCTION

Telomerase is a key enzyme involved in the complex regulation of cellular life span. It is well known that elevated levels of telomerase leads to increased capacity for cellular proliferation. The critical role of telomerase in the biology of many cancers is also strengthened by clinical observations of elevated telomerase expression levels in the majority of human cancers (Shay and Bacchetti, 1997). In breast cancer, increase in telomerase expression is observed as an early carcinogenic event (Jong *et al.*, 1999), and this event correlates causally with genomic instability (Baird, 2008). Given the ability of telomerase to increase cell division and its elevated expression in early breast cancer lesions, it is reasonable to conclude that telomerase plays an important role in promotion of breast cancer. Increased telomerase activity has been strongly implicated in mediated immortalization of primary breast epithelial cells (Li *et al.*, 2002), and this also adds strength to the idea that elevated activity of telomerase is a fairly early event.

Cellular telomerase levels are known to be regulated primarily at the transcriptional level. The promoter of hTERT gene contains many transcription factor binding sites such as ERE, Sp1, myc, Ets, and HIF1 and studies have shown that the ERE and Sp1 sites are critical to the basal expression of hTERT (Kyo *et al.*, 1999). Estrogenic regulation of telomerase by direct (ERE) and indirect (estrogen induction of c-Myc) mechanisms has also been well established by previous studies (Takakura *et al.*, 1999).

Transcriptional ablation of ERα can thus heavily disrupt expression of hTERT gene. This is known to be achieved by exposure to selective estrogen receptor downregulators or SERDs. We report here that the selective downregulation of ERα by

phytochemical derived from cruciferous vegetables, Indole-3-Carbinol (I3C) leads to repression of hTERT expression in estrogen responsive MCF7 human breast cancer cells. Our results taken together present yet another facet of the myriad of cellular effects that I3C elicits in cancer cells.

MATERIALS AND METHODS

Materials

I3C and 17β estradiol were purchased from Sigma-Aldrich (St. Louis, MO). pBABE-hTERT plasmid was a kind gift from Dr. Martha Stampfer at LBNL. I3C, PPT and E_2 were dissolved in dimethyl sulfoxide (DMSO) (Sigma-Aldrich, St. Louis, MO) to a concentration 1000X higher. All media components were purchased from Lonza (Allendale, NJ) and plates from NUNC-Fischer (Pittsburgh, PA). All other materials were purchased from the specified sources.

Cell Culture

MCF7 human breast cancer cells were obtained from American Type Culture Collection (Manassas, VA). Cells were grown in Dulbecco's Modified Eagles Medium (DMEM) from BioWhittaker (Walkersville, MD), supplemented with 10 % fetal bovine serum from Mediatech (Manassas, VA), 10 μg/ml insulin, 50 U/ml penicillin, 50 U/ml streptomycin, and 2 mM L-glutamine from Sigma (St. Louis, MO). Cells were grown to subconfluency in a humidified chamber at 37°C containing 5% CO_2. A 200 mM stock solution of I3C was dissolved in DMSO. I3C was then diluted 1:1000 in media prior to culture plate application.

Western Blotting

After the indicated treatments, western blots were performed as previously indicated (Sundar et al., 2006). Rabbit anti-Sp1 (sc-59) and rabbit anti-phospho threonine (sc-5267) were diluted 1:200 in TBST. Rabbit anti-actin (#AAN01 Cytoskeleton, Inc. Denver, CO) was used as a loading control, diluted 1:1000 in TBST. Immunoreactive proteins were detected after incubation with horseradish peroxidase-conjugated secondary antibodies diluted $3x10^{-4}$ in 1% NFDM in TBST. Blots were then treated with enhanced chemiluminescence reagents (Eastman Kodak, Rochester NY) for visualization on film.

Reverse Transcriptase-Polymerase Chain Reactions (RT-PCR)

Cells were treated with mentioned compounds and harvested in 1 ml of Tri-reagent (Sigma, St.Louis, MO). RNA was extracted and 1 μg was subjected to RT using random hexamers, followed by PCR with the following primers:

hTERT Forward: 5'-CGG AAG AGT GTC TGG AGC AA-3'

hTERT Reverse: 5'-GGATGAAGCGGAGTCTGGA-3'

ERα Forward: 5'-AGCACCCAGTGAAGCTACT-3',

ERα Reverse: 5'-TGAGGCACACAAACTCCT-3';

Sp1 Forward: 5'- CAC CAC AGC TGT CAT TTC ATC CAT-3',

Sp1 Reverse 5'-CCA TGG ATG AAA TGA CAG CTG TGG TG-3';

GAPDH Forward 5'-TGAAGGTCGGAGTCAACGGATTTG-3',

GAPDH Reverse: 5'-CATGTGGGCCATGAGGTCCACCAC-3'. PCR products were analyzed on 1.2% agarose gel along with 1-kb Plus DNA ladder from Invitrogen (Carlsbad, CA) and the products were visualized with GelRed from Biotium (Hayward, CA).

Transfections

MCF7 cells were transfected with appropriate plasmids (1 μg) using Polyfect transfection reagent (Qiagen, Valencia CA) as per manufacturer's instructions in full serum and antibiotic supplemented media. 24 hrs post transfection cells were exposed to media containing 600 μg/ml G418 sulfate (Gibco, Carlsbad CA) for selection of stable pools of cells. Empty pBABE-neo plasmid was utilized for the selection controls.

Telomere Repeat Amplification Protocol (TRAP Assay)

MCF7 cell pellets were subjected to lysis in 300 μL of CHAPS lysis buffer and protein standardization performed with the BioRad Protein Assay reagent. For each sample 1.5 μg of cell extract was added to the TRAPeze Telomerase Detection Kit assay (Millipore, Billerica MA). Telomerase activity was detected by Alexa488 probe binding to specific telomeric sequence, loading was measured by internal sulforophane probe directed to nonspecific DNA sequence.

RESULTS

Aberrant expression of the telomerase ribonucleoprotein complex occurs within hormone sensitive breast cancer cells. Estrogen has the demonstrated ability to increase expression of hTERT, the protein catalytic subunit of the telomerase enzyme (Ito *et al.*, 1998; Kanaya *et al.*, 1998). I3C is able to selectively ablate ERα expression in hormone sensitive breast cancers. Therefore, the effect of I3C on estrogen dependent stimulation of hTERT expression was examined in hormone sensitive MCF7 human breast cancer cells. As shown in Figure 28, exogenous addition of 10 nM E_2 to MCF7 cells grown in steroid deficient media stimulated RNA levels of hTERT. The addition of 200 μM I3C concomitantly with E_2 administration resulted in abrogation of E_2 dependent stimulation of hTERT expression. Therefore, I3C was able to block estrogen dependent stimulation of hTERT gene expression.

Previous studies have identified a composite ERα-Sp1 site as critical to the basal expression of hTERT in hormone sensitive breast cancer cells. Because hTERT expression is disrupted by I3C, determination of I3C dependent alterations in Sp1 activity was critical to understanding hTERT promoter regulation by I3C. I3C does not alter Sp1 expression or localization (Cram *et al.*, 2001), therefore determination of protein modification status to Sp1 protein was performed by immunoprecipitating Sp1 from I3C treated cells and accessing phosphorylation status. I3C failed to alter phospho-serine or phospho-tyrosine levels of Sp1 (data not shown), but did induce increased phosphorylation of Sp1 at threonine residues (figure 28).

Figure 28:

I3C is able to disrupt estrogen dependent stimulation of hTERT expression and increase Sp1 phosphorylation. (Upper panel) MCF7 cells were grown in steroid deficient media for 24 hrs, then treated with the indicated combinations of 200 μM I3C and 10 nM E_2. hTERT transcript expression was determined by RT-PCR. The PCR products were visualized on a 1% agarose gel stained with ethidium bromide. GAPDH provided a gel loading control for the RT-PCR. Representative gel of two independent experiments is shown. (Lower panel) MCF-7 cells were treated with the 200 μM I3C or DMSO vehicle control. Total cell extracts were immunoprecipitated with mouse anti-Sp1 antibody and electrophoretically fractionated samples blotted with either rabbit-anti-Sp1 or rabbit-anti-phospho-threonine antibodies (Sp1-THR^P). Result was repeated two times, representative blot shown.

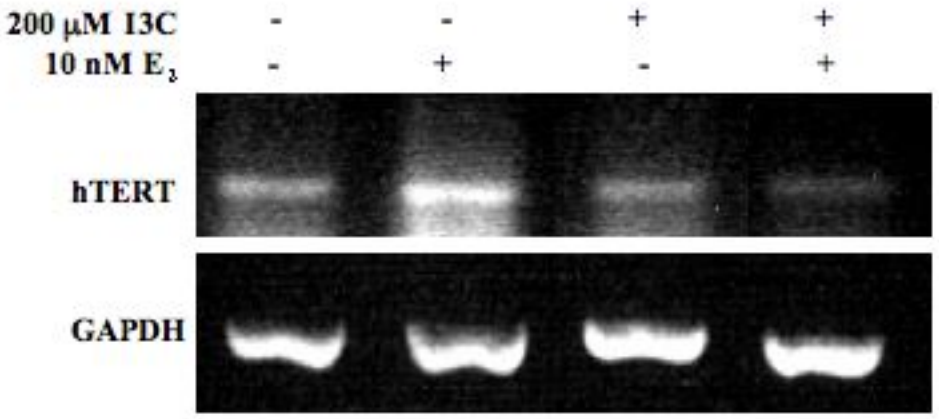
200 μM I3C - - + +
10 nM E2 - + - +
hTERT
GAPDH

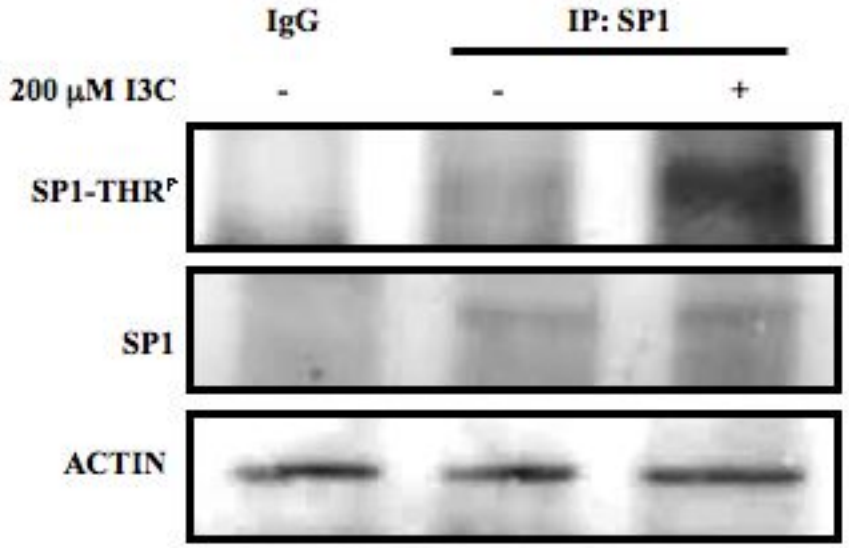
IgG
IP: SP1
200 μM I3C - - +
SP1-THRP
SP1
ACTIN

In order to determine if disruption of either ERα, Sp1, or both was critical to the I3C dependent ablation of hTERT expression, ectopic expression of ERα, Sp1, or their combination was performed by transient transfection into MCF7 cells, with CMV-neo serving as a transfection control. After 48 hr treatment with 200 μM I3C or DMSO vehicle control total RNA levels were measured by RT-PCR. As shown in figure 29, ectopic expression of either ERα or Sp1 alone was unable to restore hTERT expression in the presence of I3C. However, co-expression of both ERα and Sp1 together resulted in restoration of hTERT RNA levels. Therefore, the I3C dependent downregulation of ERα and disruption of Sp1 activity was critical to hTERT downregulation.

Upon steroid activation ERα is able to heterodimerize with Sp1 and bind to composite ERα-Sp1 DNA cis regulatory regions to modulate gene transcription. In order to determine if the requirement for ERα and Sp1 was due to physical DNA binding endogenously to an identified ERE-Sp1 element along the telomerase promoter chromatin immunoprecipitation to the site was performed. MCF7 cells were treated with 200 μM I3C for 48 hrs and subjected to immunoprecipitation with anti-ERα and anti-Sp1 antibodies. Primers specific to the hTERT promoter revealed that I3C was able to disrupt endogenous binding of both ERα and Sp1 to the ERE-Sp1 composite element (figure 29). This disruption of ERα-Sp1 binding can therefore account for the loss of basal hTERT expression seen with I3C treatment of MCF7 human breast cancer cells.

Figure 29:

I3C disrupts endogenous binding of ERα and Sp1 at critical regulatory site within the hTERT promoter. (Upper panels) MCF-7 cells were transfected with CMV-ERα, CMV-Sp1, the combination of CMV-ERα and CMV-Sp1, or the CMV-Neo vector control and treated with or without 200 μM I3C for 48 hrs. Total RNA was collected and RTPCR was used to detect ERα, Sp1, and hTERT transcripts. GAPDH was used as total RNA loading control. PCR products were visualized on a 1% agarose gel stained with ethidium bromide. (Lower panels) Chromatin immunoprecipitation (ChIP) was employed to characterize endogenous ERα interactions with the ERE-Sp1 composite element within the hTERT promoter. Chromatin was isolated from MCF-7 cells treated with or without 200 μM I3C for 48 hrs. ERα was immunoprecipitated from total cell extracts using Sepharose G bound to anti-ERα antibody or anti-Sp1 antibody and DNA was amplified using the indicated oligonucleotide primers. Input samples represent total genomic DNA from each treatment (loading control).

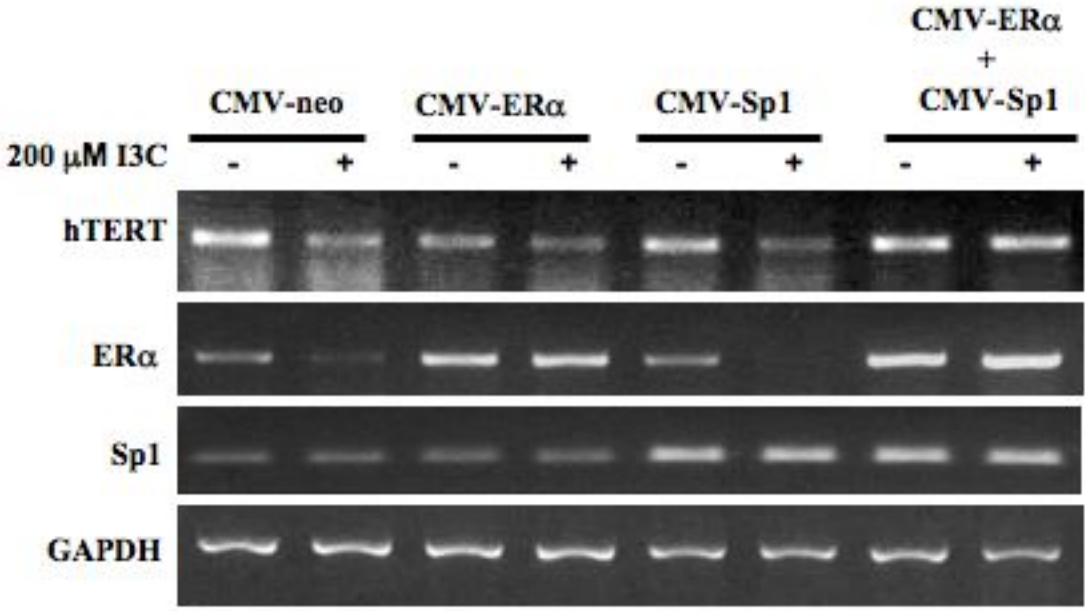
CMV-neo
CMV-ERα
CMV-Sp1
CMV-ERα
+
CMV-Sp1
200 μM I3C
-
+
-
+
-
+
-
+
hTERT
ERα
Sp1
GAPDH

ChIP

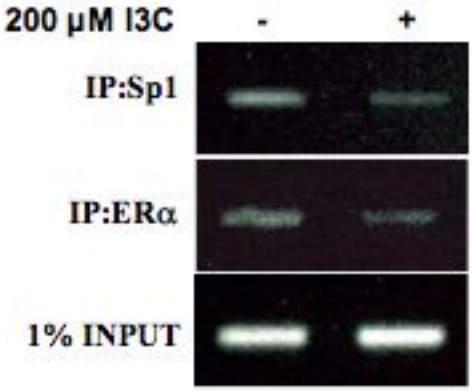
200 μM I3C
-
+
IP:Sp1
IP:ERα
1% INPUT

The telomerase ribonucleoprotein comlex is ascribed a variety of functions, including the repair of DNA damage, blocking cellular scenescence, and extention of telomeric repeats to chromosome ends (Blasco *et al.*, 1996; Buchkovich and Greider, 1996; Smith *et al.*, 2003). In order to functionally characterize the I3C dependent loss of hTERT RNA accessment of functional telomerase was performed. MCF7 cells stably transfected with either pBABE-neo or pBABE-hTERT were subjected to 200 μM I3C treatment of DMSO vehicle control for 48 hr and their level of telomerase activity accessed using the telomeric repeat amplification protocol (TRAP assay). As shown in figure 30, I3C was able to decrease telomerase activity in vector transfected control MCF7 cells. However, the disruption of hTERT expression by I3C was reversed by ectopic expression of hTERT, suggesting that transcript ablation is the sole mechanism I3C employs to modulate hTERT levels and therefore telomerase activity.

Figure 30:

I3C dependent inhibition of telomerase activity is overcome by exogenous expression of hTERT. MCF7 cells were stably transfected with pBABE-hTERT or pBABE-neo vehicle control. Cells were treated with 200 uM I3C or DMSO vehicle control for 48hr, then subjected to cellular lysis using CHAPS lysis buffer. Telomeric repeat DNA extention from template DNA was measured using fluorescent probes (telomere extension = increased fluorescence) as indicated in Millipore TRAP assay kit. Internal sulforophane probe to nonspecific DNA sequence served as loading control.

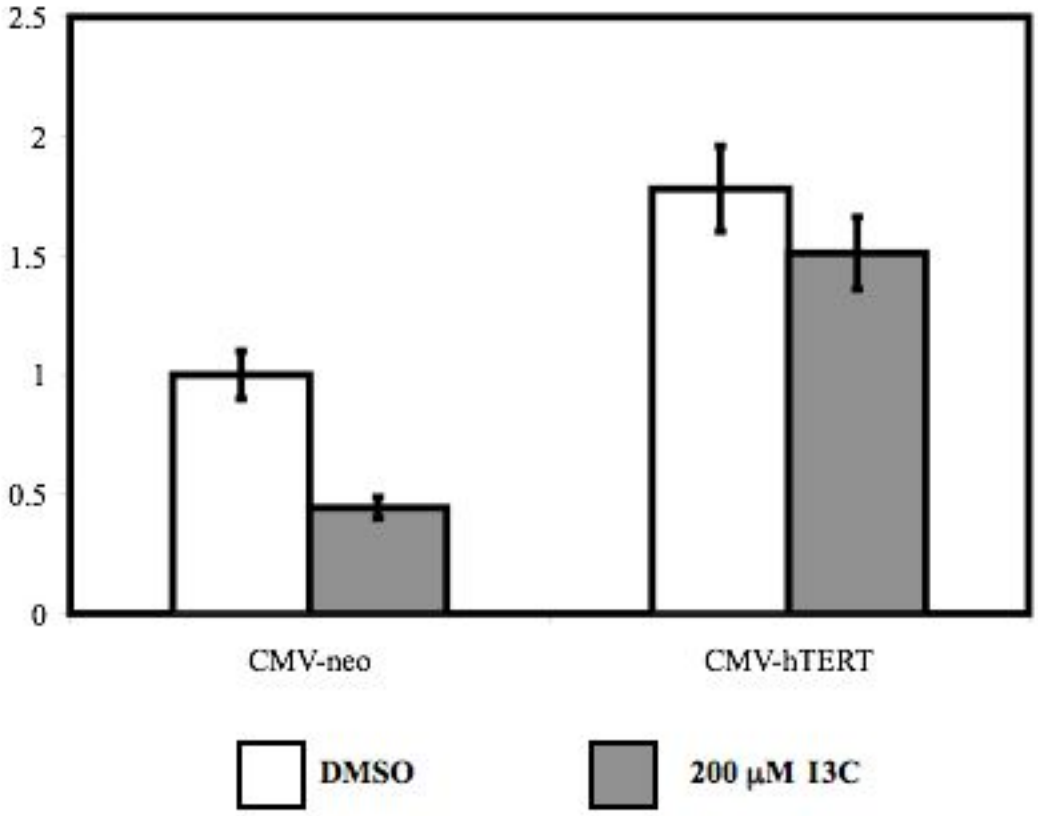
2.5
2
1.5
1
0.5
0
CMV-neo
CMV-hTERT
DMSO
200 μM I3C

DISCUSSION

We have identified I3C as a phytochemical processing the ability to ablate hTERT expression and therefore disrupt telomerase enzymatic activity. I3C accomplishes this through targeted disruption of transcription factors, which are necessary for basal transcription of hTERT in hormone sensitive breast cancer cells. I3C disruption of ERα expression has been attributed to numerous other downstream target effects in breast cancer cells. Telomerase activity can now be counted among the genes whose disruption by I3C occurs in an estrogen dependent manner.

Our results demonstrated that Sp1 plays a critical role in the I3C dependent abrogation of hTERT expression. Sp1 phosphorylation at Thr 579 has been previously demonstrated as a critical regulatory mechanism of Sp1 inactivation, as Thr 579 is located within the DNA binding domain and phosphorylation on this reside is able to disrupt DNA binding (Armstrong *et al.*, 1997). Therefore, increased phosphorylation of Sp1 at threonine residues may be responsible for the disruption of Sp1 binding to the ERE-Sp1 composite element within the ERα promoter. The combination of I3C mediated ERα ablation and abrogation of Sp1 activity constitutes a complete loss of transcriptional stimulation within the cis regulatory regions of the hTERT promoter, resulting in a loss of hTERT expression and telomerase enzymatic activity.

Telomerase enzymatic activity is critical to the maintenance of proliferative potential in hormone sensitive human reproductive cancers. Therapeutics which disrupt

telomerase activity have been the target of recent pharmaceutical research, with the development of A2-5 antisense from Atlantic pharmaceuticals, which selectively targets the hTERC RNA forming double stranded RNA, which is degraded (Kushner *et al.*, 2000; Paranjape *et al.*, 2006). Another avenue being explored is viral introduction of dominant negative forms of hTERT protein, to complex with the available hTERC RNA and prevent the ribonucleoprotein complex activity (Zhang *et al.*, 1999a; Zhang *et al.*, 1999b). Alternatively the development of small molecule inhibitors is underway, the most promising of which is 3'-azido-3'deoxythymidine to inhibit RNA-DNA complex formation (Gomez *et al.*, 1998), however each of these methods has drawback relating to delivery mode, off target effects, and nonspecific cytotoxic effects, respectively. The development of chemotherapeutics with reliable activity, target tissue specificity, and reduced side effects is critical to the advancement of therapeutic options targeting this key component of disregulation in cancer.

I3C, as a naturally occurring component of the diet, fulfils these requirements. Abrogation of hTERT expression through the targeted disruption of key transcriptional regulators blocks endogenous activation of hTERT and therefore represents a new method of targeted therapeutics, one which implies tissue specificity due to the lack of telomerase expression in adult tissues.

Chapter III

BZL101, an aqueous extract from the *Scutellaria barbata* plant, induces arrest and apoptosis of multiple breast and prostate cancer cell lines through distinct mechanisms regardless of hormonal status

ABSTRACT

BZL101 is an aqueous extract from the *Scutellaria barbata* plant shown to have anticancer properties in a variety of human cancers. In order to determine its efficacy on human reproductive cancers, we assessed the response of two representative breast cancer cell lines, the hormone sensitive MCF7 and the hormone insensitive MDA-MB-231, and two representative prostate cancer cell lines. We determined that BZL inhibits reproductive cancer growth in all cell lines tested, corresponding to distinct changes in expression levels of key cell cycle components. Specifically, BZL101 induced a G1 cell cycle arrest and corresponding ablation of Cyclin D, CDK2, and CDK4 expression in MCF7 cells. MDA-MB-231 and PC3 cells arrested in S phase with corresponding ablations in Cyclin A2 and CDK2. LNCaP cells arrested in G2/M phase upon exposure to BZL101 with a corresponding decrease in expression of Cyclin B1 and CDK1. Our results indicate that BZL101 exerts cell type specific molecular changes that lead to arrest of reproductive cancer proliferation.

INTRODUCTION

Reproductive cancer is the second leading cause of cancer death and affects 219,000 people in the United States each year, with 27,000 succumbing to the disease (Jemal *et al.*, 2007). Reproductive cancers are classified by their ability to proliferate in response to steroid hormones; estrogens in the case of breast cancer and androgens in the case of prostate cancer (Mohla *et al.*, 2009). Steroid binding to its cognate receptor induces the active conformation of steroid receptors, allowing them to bind consensus DNA sequences and activate downstream target gene transcription (Adeyemo *et al.*, 1993; Kallio *et al.*, 1994). Over two-thirds of all breast cancers are estrogen sensitive at time of initial diagnosis and 80 % of prostate cancers are androgen sensitive at time of diagnosis. However, both breast and prostate cancers can evolve beyond their initial hormone dependent state to a more advanced "hormone insensitive" state, (Bosland, 2000; Aneja *et al.*, 2006). This change can be due to selective pressures against hormone receptor growth dependence, such as the administration of endocrine disruptors to halt cancer progression (Cui *et al.*, 2006; Traish and Morgentaler, 2009).

Several therapies currently exist for selectively targeting hormone-dependent growth of both breast and prostate cancers. Aromatase inhibitors (AIs) are the preferred clinical option, which act by inhibiting estrogen synthesis, thereby decreasing the amount of ligand available for binding to estrogen receptors (ERs). Selective estrogen receptor modulators (SERMs) and selective estrogen receptor downregulators (SERDs) are implemented as an alternative treatment with AI proves ineffective. SERMS act as

antagoinists to ER activity, while SERDs ablate estrogen receptor expression. The primary treatment for patients with prostate cancer is anti-androgen, or, chemical castration (Lynch *et al.*, 2001), aimed at reducing the levels of circulating androgens in the body.

However, these treatments are only effective until the cancer evolves beyond hormone sensitivity, which occurs in 80% of prostate cancers within 3 years of diagnosis (Gregory *et al.*, 2001) and 20 % of breast cancers within 5 years of diagnosis (Reddel *et al.*, 1988; Howell *et al.*, 2005). Therapies targeting these hormone-insensitive forms of reproductive cancer include radiation and chemotherapy, aimed at inducing enough DNA damage to halt replication of actively dividing cells, including cancer cells. Unfortunately, the off-target effects of radiation and chemotherapy induce harsh and sometimes fatal side effects. Therefore, there exists an obvious need for alternative therapies, which could ideally target both hormone sensitive and insensitive reproductive cancers with minimal side effects.

Phytochemicals are a natural source of pharmaceuticals with a long histories of human interaction in traditional medicines, which has led to over 60 % of anticancer drugs developed in the last 20 years being derived from natural products (Newman and Cragg, 2007). One such herb, *Scutellaria barbata*, known colloquially as Ban Zhi Lian (BZL), has demonstrated anticancer properties in hepatocarcinoma and leukemia, specifically able to induce G1 cell cycle arrest followed by apoptosis of these cancers (Kim *et al.*, 2007; Dai *et al.*, 2008) with effective concentrations of 2 mg/mL and 1

mg/mL, respectively. Aqueous extracts of BZL (BZL101) contain active anticancer compounds (Liu *et al.*, 2008), which are able to block glycolysis and disrupt cancer progression in a number of cell lines (Fong *et al.*, 2008). Determination of the effects BZL101 can exert on a variety of hormone sensitive and insensitive reproductive cancers could therefore be beneficial in the development of BZL101 as an alternative treatment of reproductive cancers with increased efficacy and reduced side effects.

MATERIALS & METHODS

Reagents

BZL101 dried powder (Bionovo, Emeryville, CA) was diluted in nano-H_2O to 1.5, 2, or 3mg/mL dependent on cell line. Stock concentrations were then added to media and the mixture sterile filtered through a 0.45 μM filter prior to administration on cells. All other reagents were purchased from Sigma (St. Louis, MO) and were of the highest quality available.

Cell Culture

MCF7 and MDA-MB-231 human breast cancer cells were obtained from American Type Culture Collection (Manassas, VA). Cells were grown in Dulbecco's Modified Eagles Medium (DMEM) from BioWhittaker (Walkersville, MD), supplemented with 10 % fetal bovine serum (FBS) from Mediatech (Manassas, VA), 10 μg/ml insulin, 50 U/ml penicillin, 50 U/ml streptomycin, and 2 mM L-glutamine from Sigma (St. Louis, MO). MDA-MB-231 cells were grown in Isacoves Modified Eagles Medium (IMDM) from Lonza (Basel, Switzerland), supplemented with 10 % FBS from Mediatech, 50 U/ml penicillin, 50 U/ml streptomycin, and 2 mM L-glutamine from Sigma (St. Louis, MO). LNCaP and PC3 human prostate cancer cells were obtained from American Type Culture Collection (Manassas, VA). Cells were grown in DMEM supplemented with HEPES buffer solution 1 M, and 2 mM L-glutamine. All cells were grown to subconfluency in a humidified chamber at 37°C containing 5 % CO_2 prior to treatment.

Flow Cytometry

Cells were plated onto Corning six-well tissue culture dishes (Corning, NY) and were treated with the indicated concentrations of BZL or sterile-filtered nH_2O. The medium was changed every 24 h. Cells were hypotonically lysed in 500 µl of DNA staining solution [0.5 mg/ml propidium iodide (PI), 0.1 % sodium citrate, 0.05 % Triton X-100 (Sigma)]. Lysates were filtered using 60 µm Nitex flow mesh (Sefar America, Kansas City, MO) to remove cell membrane and debris. PI-stained nuclei were detected using a PL-2 detector with a 575 nm band pass filter on a Beckman-Coulter (Fullerton, CA) fluorescence-activated cell sorter analyzer with laser output adjusted to deliver 15 MW at 488 nm. Nuclei (10000 per sample) were analyzed from each sample at a rate of 300–500 nuclei/s. The percentages of cells within the G1, S and G2/M phases of the cell cycle were determined by analyzing the histographic output with the multicycle computer program MPLUS, provided by Phoenix Flow Systems (San Diego, CA), in the Cancer Research Laboratory Microchemical Facility at the University of California at Berkeley.

Western Blotting

After the indicated treatments, MCF7 cells were washed with PBS and harvested in 1 ml PBS and pelleted by centrifugation at 2000 rpm for 10 min. PBS was aspirated and the

pellet was resuspended in radio immunoprecipitation buffer (150 mM sodium chloride, 0.5 % deoxycholate, 0.1 % NP-40, 0.1 % SDS, and 50 mM tris) containing protease inhibitors (50 μg/ml phenylmethylsulfonyl fluoride, 10 μg/ml aprotinin, 5 μg/ml leupeptin, 0.1 μg/ml NaF, and 10 μg/ml β-glycerophosphate). These extracts were then quantified using the Lowry method from Bio-Rad laboratories (Hercules, CA). Normalized amounts of protein were mixed with Gel Loading Buffer (GLB) composed of 25 % glycerol, 0.075 % SDS, 1.25 ml B-mercaptoethanol, 10 % bromophenol blue, 3.13 % 0.5M SDS and 0.4 % SDS at pH 6.8, and fractionated on 10 % polyacrylamide/ 0.1 % SDS resolving gels using electrophoresis. Prestained Rainbow Protein ladder (Amersham, Arlington Heights, IL) was used as a reference for size. Proteins were transferred to nitrocellulose membranes where equal loading was verified by Ponceau S staining. Blots were blocked with 5 % Nonfat Dry Milk (NFDM) dissolved in TBST (10 mM Tris-HCl at pH 8, 150 mM NaCl, and 0.05 % Tween 20) at room temperature. The blots were then rinsed briefly with TBST and incubated overnight at 4°C in antibodies diluted in TBST. Antibodies were diluted in TBST as follows: CDK1 (sc-53, 1:500), CDK2 (sc-163, 1:1000), CDK4 (sc-749, 1:500), CDK6 (sc-7180, 1:200), Cyclin E (sc-20684, 1:200), Cyclin A (sc-596, 1:500), Cyclin B (sc-752, 1:500) were all obtained from Santa Cruz Biotechnology (Santa Cruz, CA). Cyclin D1 (#CC11) from Calbiochem (San Diego, CA) was diluted 1:200 in TBST. AR (ab47570) from Abcam (Cambridge, UK) was diluted 1:200 in TBST. PARP (44-698G) from Zymed was diluted 1:200 in TBST with 3% BSA. Hsp90 and actin were used as loading controls. Hsp90 from BD Transduction laboratories #610419 (Franklin Lakes, NJ) was diluted 1:2000 in TBST. Actin from Cytoskeleton, Incorporated #AAN01 (Denver, CO) was diluted 1:1000 in

TBST. Immunoreactive proteins were detected after incubation with horseradish peroxidase-conjugated secondary antibodies diluted $3x10^{-4}$ in 1% NFDM in TBST. Blots were then treated with enhanced chemiluminescence reagents (Eastman Kodak, Rochester NY).

RT-PCR

Total RNA from MCF7 cells treated with indicated treatment was isolated with TRI Reagent according to manufacturer's protocol from Sigma (St. Louis, MO). Total RNA (4µg) was used to synthesize cDNA using Moloney murine leukemia virus-reverse transcriptase (Promega Corp., Madison, WI) with random hexamers as primers. The cDNA reaction product (200ng) was used with 10 µM primers. Promers were as follows: CDK1 Forward: 5'- AAG CCG GGA TCT ACC ATA CCC-3'; CDK1 Reverse: 5'- CCT GGA ATC CTG CAT AAG CAC-3'; CDK2 Forward: 5'- CCA GTA CTG CCA TCC GAG AG-3'; CDK2 Reverse: 5'-CGG CGA GTC ACC ATC TCA GC-3'; CDK4 Forward: 5'- CTG AGA ATG GCT ACC TCT CGA-3'; CDK4 Reverse: 5'- AGA GTG TAA CAA CCA CGG GTG-3'; CDK6 Forward: 5'- CTT TGC CTA GTT CAT CGA TAT C-3'; CDK6 Reverse: 5'- CCG AGT AGT GCA TCG CGA TCT-3'; Cyclin A1 Forward: 5'-TTC CCG CAA TCA TGT ACC CTG-3'; Cyclin A1 Reverse: 5'-TAG CCA GCA CAA CTC CAC TCT T-3'; Cyclin A2 Forward: 5'-TCC ATG TCA GTG CTG AGA GGC-3'; Cyclin A2 Reverse: 5'-GAA GGT CCA TGA GAC AAG GC-3'; Cyclin D Forward: 5'-TCC TCC TCT TCC TCC TCC TC-3'; Cyclin D Reverse: 5'-TCA AGT GTG ACC CAG ACT GC-3'; Cyclin B1 Forward: 5'-AGG AAG AGC AAG CAG TCA

GAC-3'; Cyclin B1 Reverse: 5'-GCA GCA TCT TCT TGG GCA CAC-3'; AR FORWARD: 5'- CCT GAT CTG TGG AGA TGA AGC TTC-3'; AR REVERSE: 5'-TGT CGT GTC CAG CAC ACA CTA CAC-3'; ERα FORWARD: 5'-AGC ACC CAG TGA AGC TAC-3'; ERα REVERSE: 5'-TGA GGC ACA CAA ACT CCT-3'; GAPDH Forward: 5'-TGA AGG TCG GAG TCA ACG GAT TTG-3'; GAPDH Reverse: 5'- CAT GTG GGC CAT GAG GTC CAC CAC-3'. PCR products were analyzed on 1.2% agarose along with 1-kb Plus DNA ladder from Invitrogen (Carlsbad, CA) and the products visualized with GelRed from Biotium (Hayward, CA).

Luciferase Assays

MCF7 cells grown to 70% confluency in six-well Nunc plates and were transfected with 2μg/well of the indicated plasmid construct. Transfections were performed in serum free media using Superfect (Qiagen) transfection reagent as per manufacturers instructions. Cells were treated 24 hr post transfection with DMSO or 2mg/mL BZL for 24 hr. Cells were then lysed and relative luciferase activity was evaluated using the Promega Luciferase Assay kit (Promega Corp., Madison, WI). Relative luciferase activities were normalized to the protein input and pCDK2-2313 or pCDK4-1767 construct with standard error. Experiments were performed in triplicate to verify accuracy.

Immunofluorescence

Cells were grown and indicated treatments performed on 2 well chamber slides from Nunc (Fisher Scientific, Rochester, NY). The cells were fixed with 3.75 % formaldehyde in PBS for 15 min at room temperature. After three additional washes with PBS, the plasma membrane was permeabilized with 0.1% Triton-X-100; 10 mM Tris-HCl at pH 7.5, 120 mM sodium chloride; 25 mM potassium chloride, 2 mM EGTA; and 2 mM EDTA) for 10 min at room temperature. Slides were incubated with 3% BSA (Sigma) before incubation with antibody. Texas Red-conjugated phalloidin were used at a 1:400 dilution. Stained cells were mounted with Vectashield Mounting medium containing DAPI (Vector Laboratories, Burlingame, CA). Stained and mounted cells were then processed with a Zeiss Axioplan epiflourescence microscope (Carl Zeiss, Thornwood, NY).

RESULTS

BZL101 adversely affects proliferation of multiple cancers

To determine whether BZL101 affects the proliferation of a variety of reproductive cancers, we treated two breast cancer cell lines, which differ in their hormone responsiveness, with and without BZL101. Initially, we measured their proliferation over time using a hemocytometer to make manual observations. As shown in Figure 31, MCF7 hormone sensitive breast cancer cells treated with BZL101 showed a marked decrease in proliferation. MB-MDA-231 hormone insensitive breast cancer cells (Figure 31) showed not only a cessation of proliferation but a decrease in total population in a time-dependent manner, suggesting cell death. To determine if BZL101 exerted this effect in other reproductive cancers, we examined proliferation in several prostate cancer cell lines with and without BZL101, again using a hemocytometer. As shown in Figure 31, hormone sensitive LNCaP cells exhibited a marked decrease in cell number in a time-dependent manner, again suggesting exacerbated cell death. The hormone insensitive cell line PC3 also exhibited a decrease in proliferation in a time-dependent manner; however, cell death was not as prominent in PC3 as in LNCaP. Therefore, we were able to establish that BZL101 inhibits the proliferation of several reproductive cancer cell lines.

Optimal concentrations of BZL101 vary between cell lines

The optimal dose of BZL101 for each cell line was determined by testing a series

Figure 31:

BZL101 inhibits proliferation of human breast and prostate cancer cells. MCF7, MDA-MB-231, LNCaP, and PC3 human reproductive cancer cells were treated with BZL101 or nH_20 vehicle control over a 72 hr time course. Cells were stained with Trypan blue and cell number accessed with a hemocytometer. Results shown are representative of 3 independent experiments.

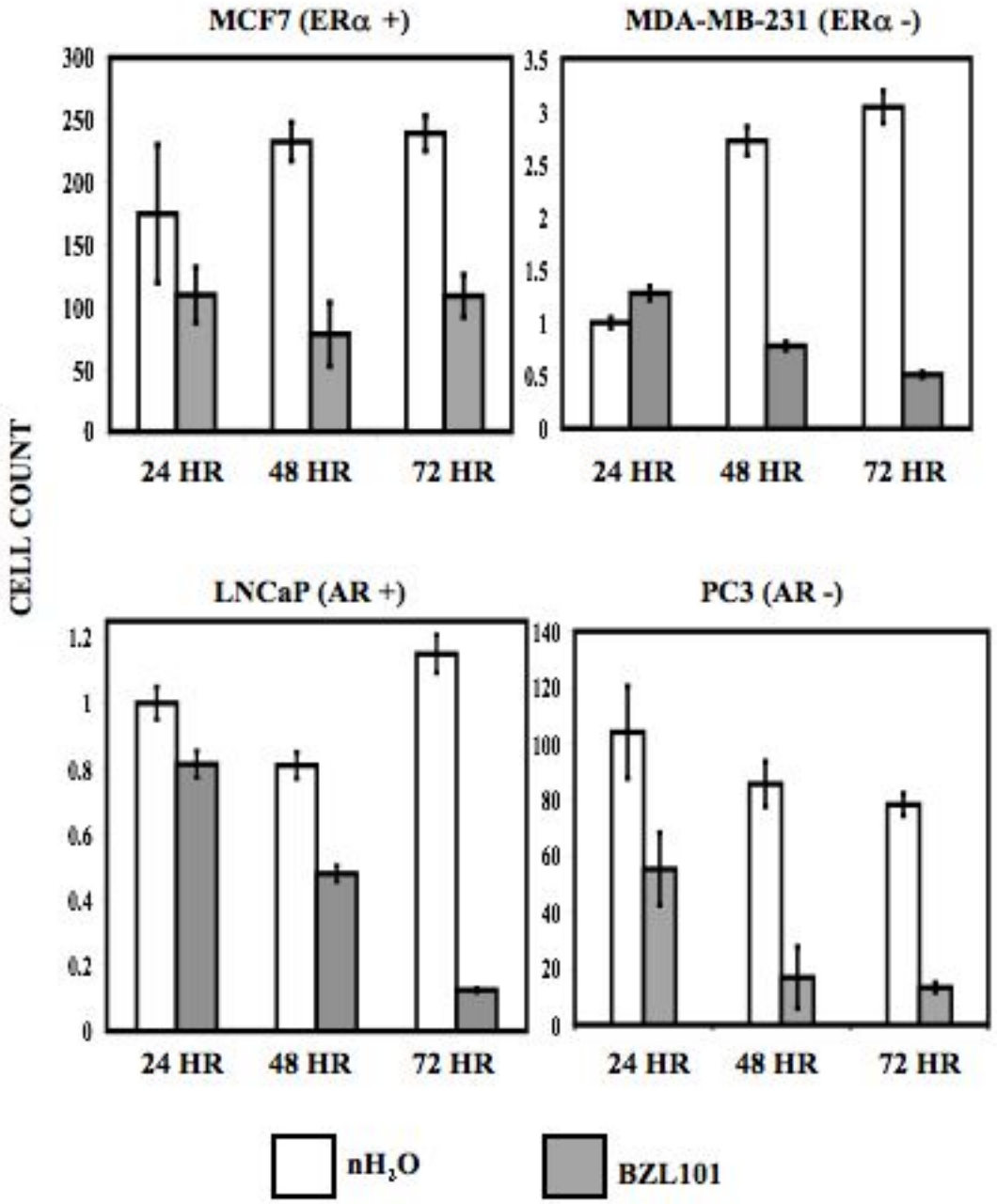
MCF7 (ERα +)
MDA-MB-231 (ERα -)
LNCaP (AR +)
PC3 (AR -)
CELL COUNT
24 HR
48 HR
72 HR
nH2O
BZL101

of concentrations of BZL101 and measuring the percentage of cells in the sub-G1 peak, indicating DNA fragmentation and a general increase in cellular debris. Measurements of DNA fragmentation were made using propidium iodide staining of DNA and measured by flow cytometry. Figure 32 shows the response of PC3 hormone insensitive prostate cancer cells to increasing concentrations of BZL101 for a 48 hr time period. The observed correlation between increasing BZL101 doses and increases in percentage of cells in the sub-G1 phase was found in all four cell lines (data not shown). Each cell line exhibited greater cell death, as measured by the sub-G1 peak, in both a dose and time-dependent manner upon treatment with BZL101.

Figure 33 displays all cell lines studied with a marked increase in the sub-G1 fraction of cellular staining. This is consistent with cell death. Shown in Figure 33 is the response of hormone sensitive and insensitive breast cancers MCF7 and MD-MBA-231, respectively, to no treatment and treatment with BZL101. An increase in the sub-G1 peaks of both cell lines were observed at their optimal doses: 2.0 mg/mL BZL101 for MCF7 and 3.0 mg/mL BZL101 for 231. Similarly, hormone sensitive and insensitive prostate cancers LNCaP and PC3, respectively, were treated with BZL101 to determine their optimal doses. LNCaP cells had a maximum sub-G1 peak at a concentration of 1.5 mg/mL BZL101, and at 3.0 mg/mL BZL101 for PC3. Each cell line is shown at its optimal dose of BZL101 to demonstrate the level of DNA fragmentation, which correlated to the required dose for optimal cell cycle arrest.

Figure 32:

Dependence of BZL101 concentration on increased Cellular Debris. (Top panels) PC3 cells were treated with or without BZL101 for 48 hr, hypotonically lysed and stained with propidium iodide. Cells were processed with coulter cell counter and relative PI staining per cell is shown (n=10,000). (Bottom graph) Fold increase in the amount of cellular debris generated by increasing doses of BZL101, relative to n$H_2$0 control.

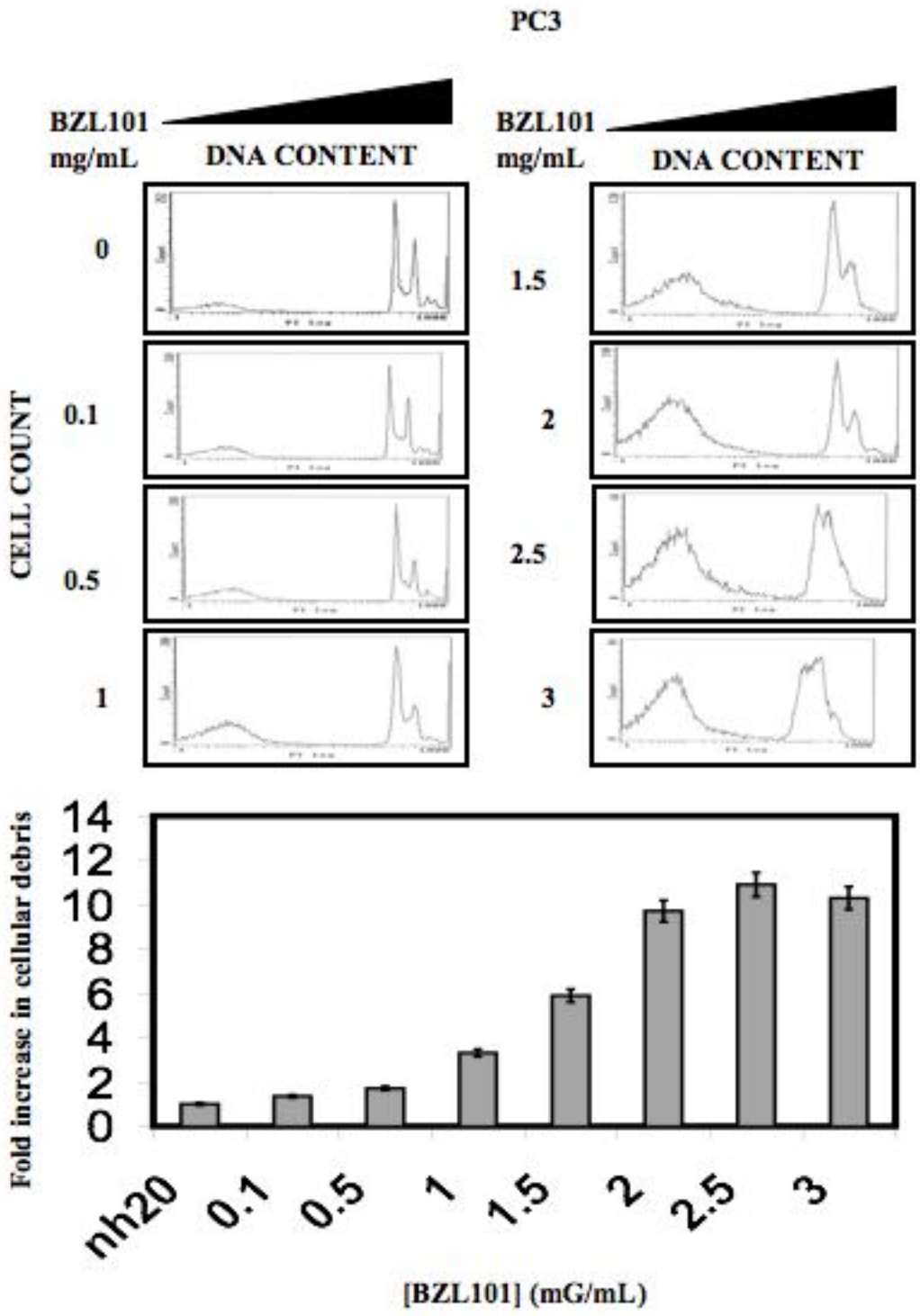
PC3
BZL101
mg/mL
DNA CONTENT
BZL101
mg/mL
DNA CONTENT
0
0.1
0.5
1
1.5
2
2.5
3
CELL COUNT
Fold increase in cellular debris
14
12
10
8
6
4
2
0
nh20
0.1
0.5
1
1.5
2
2.5
3
[BZL101] (mG/mL)

Figure 33:

BZL101 increases the amount of cellular debris in hormone dependent and independent breast and prostate cancer cell lines. BZL101 or nH_20 vehicle control was applied to cancer cell lines: MCF7 (2 mg/mL), MDA-MB-231 (3 mg/mL), LNCaP (1.5 mg/mL), and PC3 (3 mg/mL) for 48 hr. Cells were hypotonically lysed and stained with propidium iodide prior to analysis by coulter cell counter. Cell count versus PI staining is displayed (n=10,000) per treatment. All analysis was performed in triplicate.

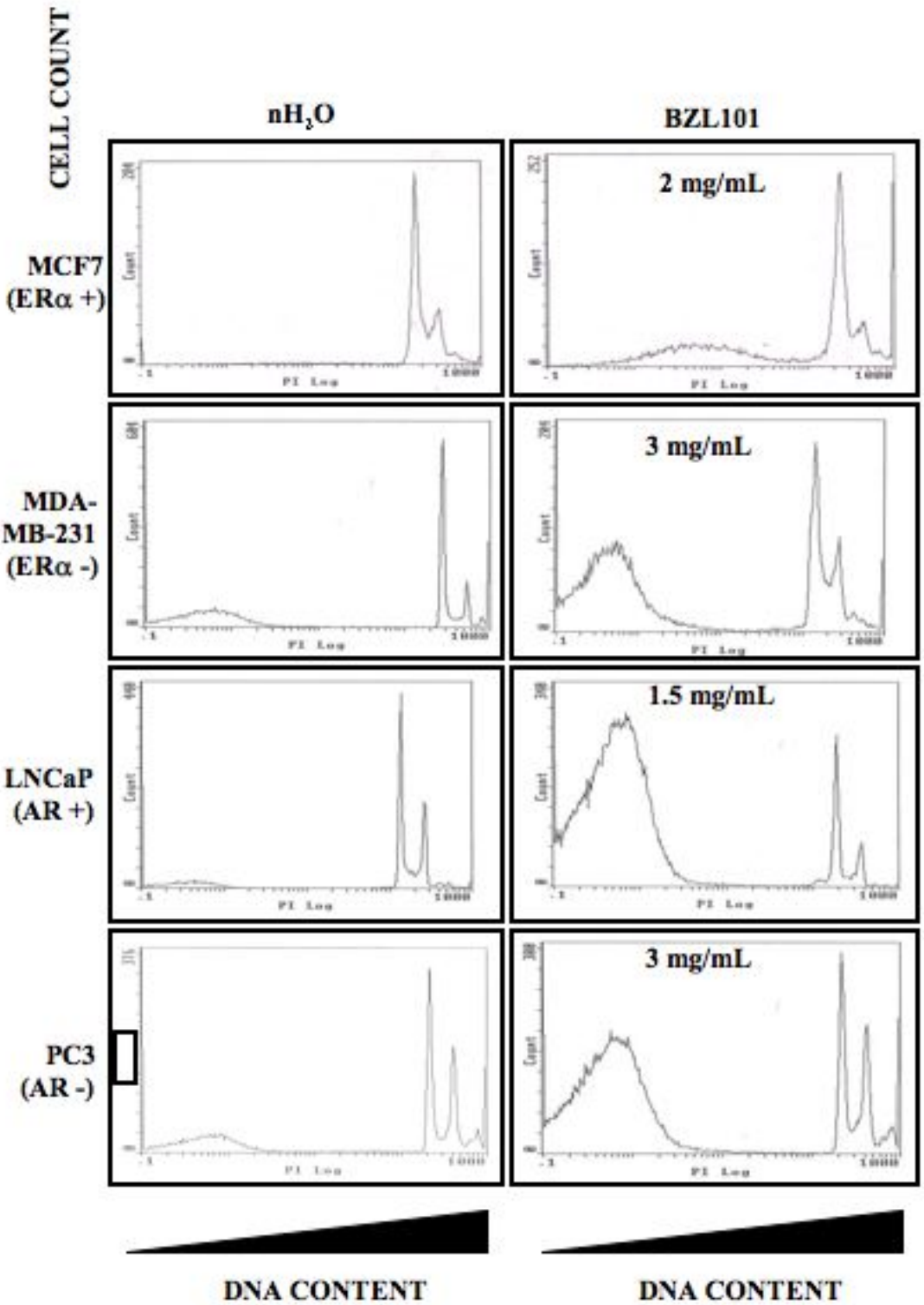
CELL COUNT
nH2O
BZL101
MCF7
(ERα +)
2 mg/mL
MDA-
MB-231
(ERα -)
3 mg/mL
LNCaP
(AR +)
1.5 mg/mL
PC3
(AR -)
3 mg/mL
DNA CONTENT
DNA CONTENT

Different cell lines exhibit different cell cycle arrests upon treatment of BZL101

Although the minimum dose of BZL101 required to observe cellular arrest and cell death differed slightly between cell lines, in each cell line the same dose caused both arrest within the cell cycle and an increase in the sub-G1 peak. Figure 34 shows that the concentration of BZL101 required to induce maximal S-phase cell cycle arrest in 231 cells is the same concentration required to increase the percentage of cells within the sub-G1 peak. If arrest within the cell cycle was a nonspecific event brought about by nonspecific cellular death, we would expect each cell line to undergo the same S-phase increase as observed in 231 cells. However, this is not the case. As shown in Figure 35, cell cycle arrest occurred in different phases for each of the four cell lines treated with BZL101. The farther progressed and hormone insensitive cell lines 231 and PC3 showed an S-phase arrest (both cell lines exhibiting a 15% increase in percentage of cells in S-phase). The hormone sensitive cell lines MCF-7 and LNCaP showed a G1 (15% increase) and G2/M arrest (9%), respectively. It is important to note that the molecular makeup of BZL101 has been studied, and many anti-cancerous molecules such as apigenin, luteolin, and resveratrol identified as components (Liu *et al.*, 2008). Therefore, we would hypothesize that individual cell lines react with differing sensitivity to individual components of BZL101, leading to an overall decrease in proliferation and increased cellular death.

Figure 34:

Comparison of BZL101 induced cellular debris to cell cycle arrest in MDA-MB-231 cells. MDA-MB-231 cells were treated with increasing concentrations of BZL101 and nH_20 vehicle control for 48 hr. Cells were hypotonically lysed and subjected to PI staining, the intensity of which determined cellular DNA content. Cellular debris generates by BZL101 (left panels) was compared to the amount of cell cycle arrest (right panels). Image shown is representative of data performed in triplicate. (Lower panel) Graph depicting the cell cycle phase distribution for each concentration of BZL101 with Standard Error (SE).

MDA-MB-231

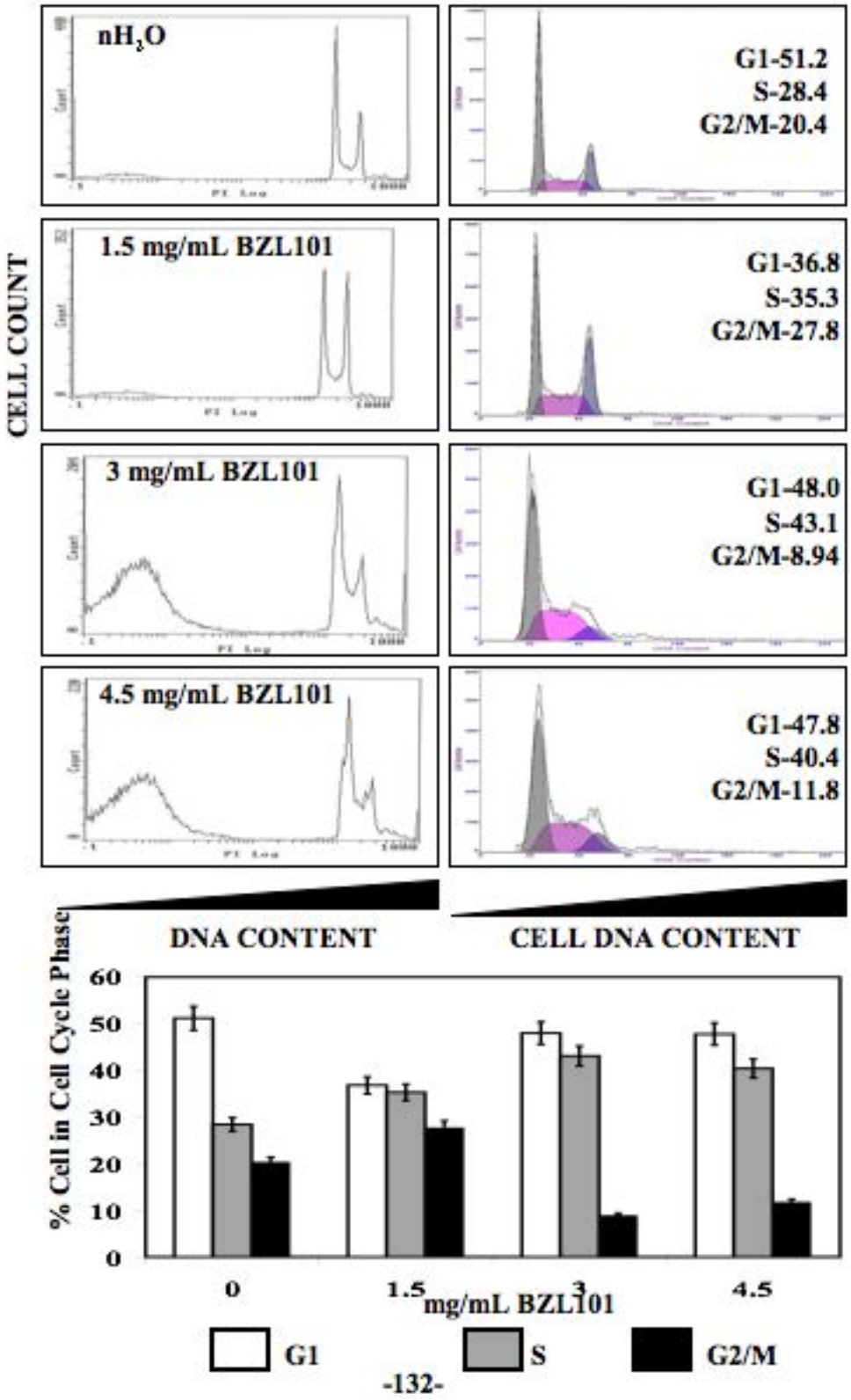
nH2O
G1-51.2
S-28.4
G2/M-20.4
1.5 mg/mL BZL101
G1-36.8
S-35.3
G2/M-27.8
3 mg/mL BZL101
G1-48.0
S-43.1
G2/M-8.94
4.5 mg/mL BZL101
G1-47.8
S-40.4
G2/M-11.8
CELL COUNT
DNA CONTENT
CELL DNA CONTENT
% Cell in Cell Cycle Phase
60
50
40
30
20
10
0
0
1.5
3
4.5
mg/mL BZL101
G1
S
G2/M

Figure 35:

BZL101 induction of cell cycle arrest in hormone sensitive and insensitive breast and prostate cancer cell lines. BZL101 or nH_20 vehicle control was applied to cancer cell lines: MCF7 (2 mg/mL), MDA-MB-231 (3 mg/mL), LNCaP (1.5 mg/mL), and PC3 (3 mg/mL) for 48 hr. Cells were hypotonically lysed and stained with propidium iodide prior to analysis by coulter cell counter. Cell count versus PI staining is displayed (n=10,000) per treatment. Cell cycle phase analyzed using Win-MultiCycle software. All analysis was performed in triplicate.

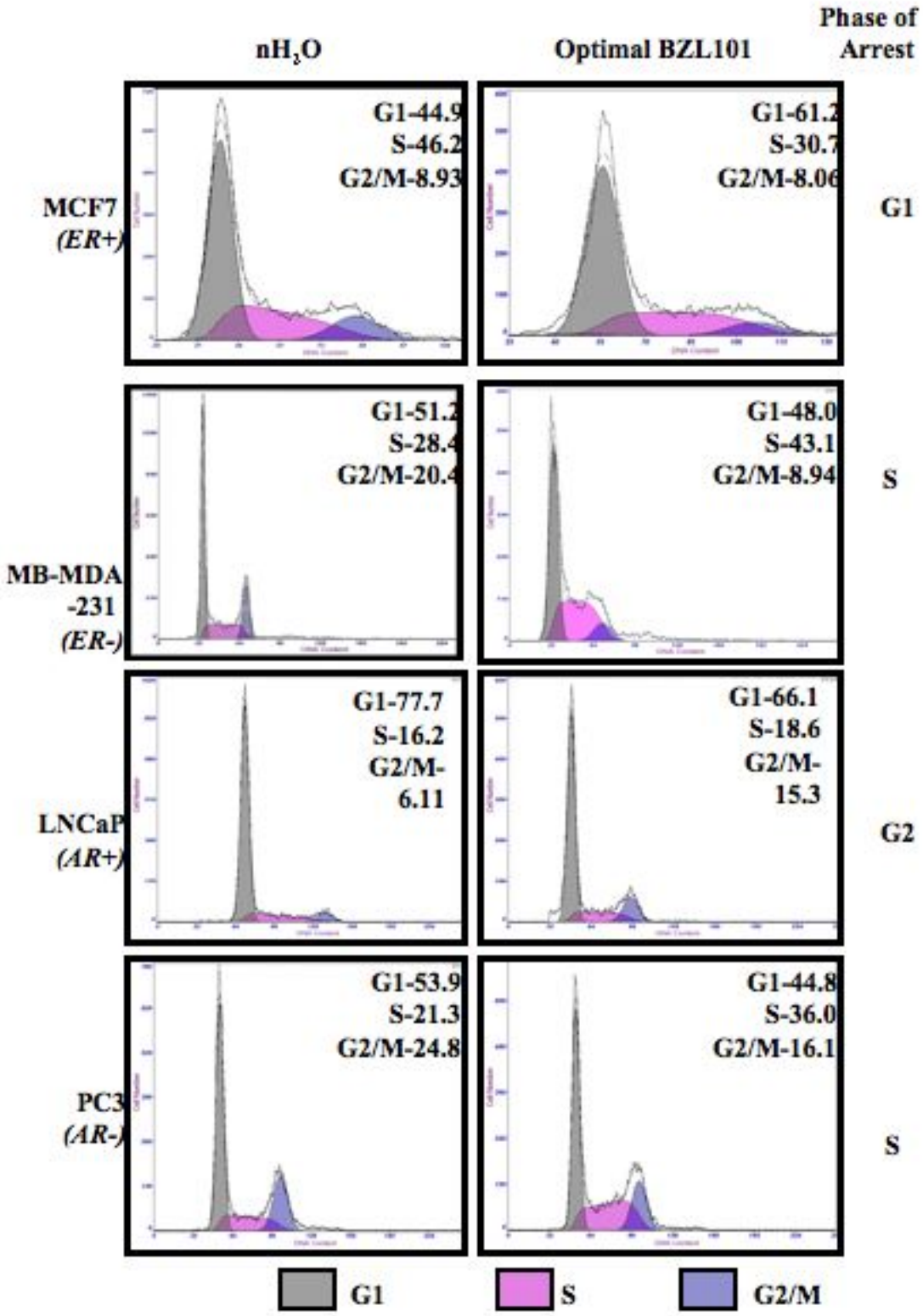
nH2O
Optimal BZL101
Phase of Arrest
MCF7 (ER+)
G1-44.9
S-46.2
G2/M-8.93
G1-61.2
S-30.7
G2/M-8.06
G1
MB-MDA -231 (ER-)
G1-51.2
S-28.4
G2/M-20.4
G1-48.0
S-43.1
G2/M-8.94
S
LNCaP (AR+)
G1-77.7
S-16.2
G2/M-6.11
G1-66.1
S-18.6
G2/M-15.3
G2
PC3 (AR-)
G1-53.9
S-21.3
G2/M-24.8
G1-44.8
S-36.0
G2/M-16.1
S
G1
S
G2/M

Protein levels of cell cycle regulators exhibit down regulation with BZL101

To further investigate the molecular basis of the observed cell cycle arrests, cells were treated with BZL101 for 48 hours and levels of cell cycle proteins were determined by Western Blot analysis. Tubulin was used as a loading control. Shown in Figure 36 are the levels of critical cell cycle regulatory proteins that were examined in all four cell lines tested. In MCF-7 cells, a down regulation of cyclin dependent kinases (CDKs) 1, 2, and 4 was observed as well as a decrease in cyclin D1 and cyclin A. Interestingly, cyclin B protein levels increased upon treatment with BZL101. One could correlate the G1 arrest previously observed with the decrease in cyclin D1, CDK2 and CDK4, all of which are intergral to the G1-S transition of the cell cycle. However, no decrease was seen in CDK6 levels, another cell cycle protein that facilitates the G1 transition, indicating the specificity of the mechanism involved. Interestingly, ERα levels decrease in response to BZL101 treatment, suggesting BZL101 may be able to disrupt hormonal signaling in hormone sensitive breast cancer cells.

Figure 36 also displays the protein levels of the cyclin and cdk proteins in 231 cells after a 48 hr treatment with BZL101. A decrease in the levels of CDK2 and cyclin E are reflected in the S phase cell cycle arrest previously demonstrated. Upon close examination, it appears that an increase in the higher molecular weight (50 kDa) inactive isoform of cyclin E is induced with treatment, decreasing cyclin E-CDK2 activity. Levels of CDK1 and cyclins A, B and D1 were found to decrease with treatment as well. The levels of CDK4 and CDK6, which play a role in the G1 phase, were unchanged with

Figure 36:

Protein levels of cell cycle proteins exhibit down regulation with BZL101 treatment. BZL101 or nH_20 vehicle control was applied to cancer cell lines: MCF7 (2 mg/mL), MDA-MB-231 (3 mg/mL), LNCaP (1.5 mg/mL), and PC3 (3 mg/mL) for 48 hr. Total cell lysates were subjected to SDS-PAGE and the levels of cell cycle regulators and HSP90 (loading control) protein was monitored by western blot analysis.

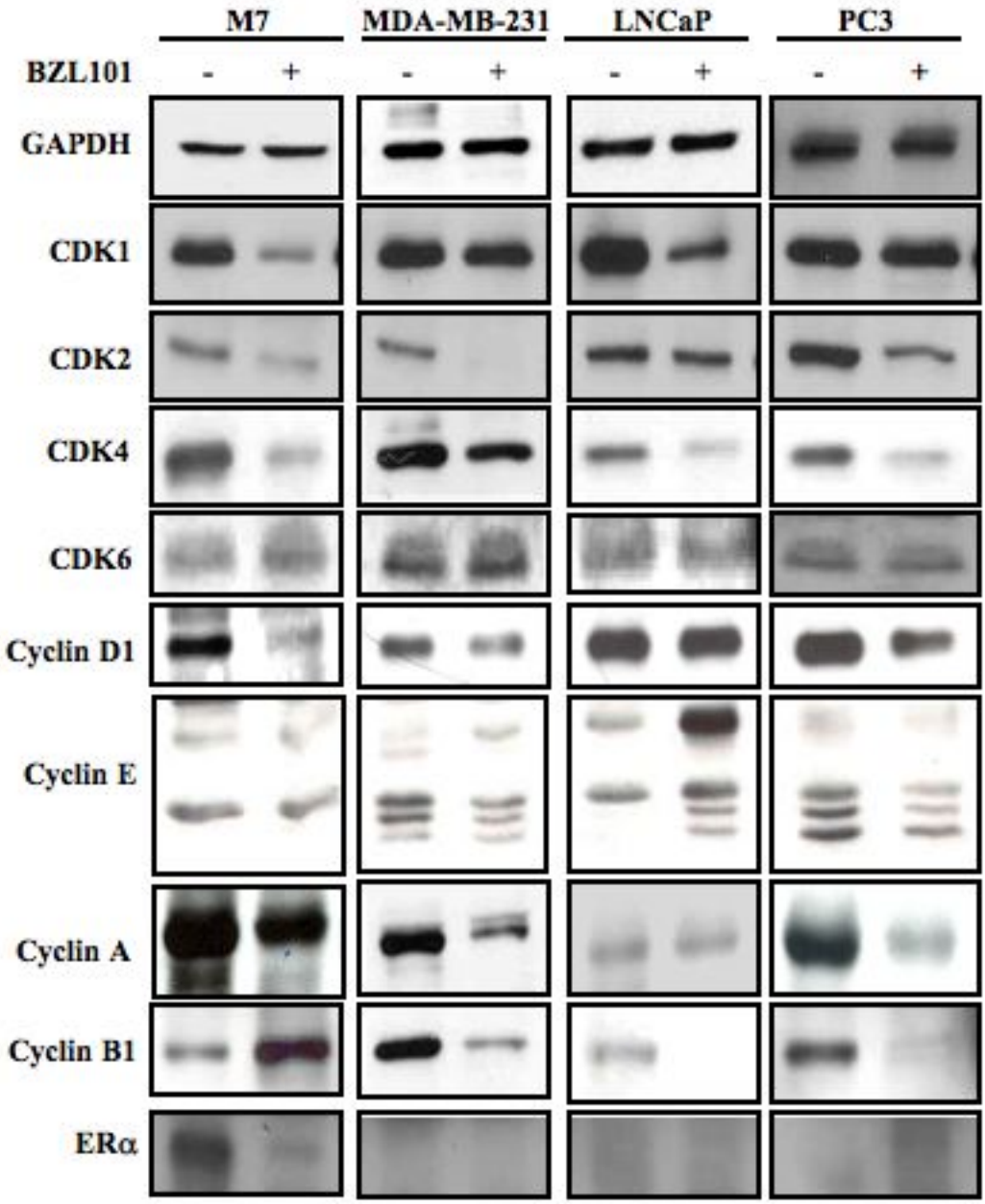
M7
MDA-MB-231
LNCaP
PC3
BZL101
- + - + - + - +
GAPDH
CDK1
CDK2
CDK4
CDK6
Cyclin D1
Cyclin E
Cyclin A
Cyclin B1
ERα

treatment of BZL101. Western analysis of LNCaP cells is also shown in Figure 36. The G2/M cell cycle arrest observed is further supported by the precipitous drop in cyclin B levels, as well as its cognate protein partner CDK1. Decreases in protein levels were also seen in CDK2 and CDK4. A slight increase is also seen in cyclin E, most of this increase is the non-tumorigenic 50kDa isoform, signifying an increase of cytoplasmically localized cyclin E-CDK2 complex.

Lastly, in Figure 36 is the protein data obtained from PC3 cells. CDK1, CDK2, and CDK4 along with cyclins A, B, D, and E all exhibit lower levels of protein with treatement of BZL101. CDK6 levels were unchanged, and PC3 lacked expression of either hormone receptor as previously reported.

BZL101 disrupts RNA levels of key cell cycle regulatory components and steroid receptors

The disruption of key cell cycle component protein expression by BZL101 could be accompolished by several cellular mechanisms. In order to determine if the decrease in protein expression was dependent on ablation of transcript levels, hormone sensitive MCF7 and LNCaP as well as hormone insensitive MDA-MB-231 and PC3 breast and prostate cancer cells were subjected to 48 hr treatment with their optimal dose of BZL101, total RNA was isolated and RTPCR preformed. As shown in figure 37, BZL101 ablated RNA levels of CDK1, CDK2, and CDK4, as well as cyclin D1, E, and A2. Cyclin D1 is transcriptional targets for ERα, and BZL101 was able to disrupt ERα

transcript expression as well, further suggesting that estrogen dependent signaling was ablated in MCF7 cells. Cyclin A1 is a known target for chemotoxic stress. Interestingly, cyclin A1 levels are not disrupted by BZL101, suggesting that the cells are not responding to nonspecific chemotoxic shock but rather to discrete molecular events happening within the cell. In addition, the protein downregulation of cyclin A seen in MCF7 cells can be attributed to cyclin A2 downregulation.

Specific and distinct molecular changes occur to RNA expression within MDA-MB-231 cells as well. BZL101 was able to ablate CDK1, CDK2, and CDK4 RNA levels, as well as cyclin D1, A2, and B1 (figure 37). Interestingly, cyclin E RNA levels increased slightly with BZL101 treatment suggesting the increase in the 50kDa isoform and decrease in 35 and 33kDa forms is due to BZL101 specific effects on protein regulation.

Hormone sensitive LNCaP prostate cancer cells responded to BZL101 by downregulation of CDK1, CDK4, Cyclin A2 and Cyclin B1 (figure 37). Interestingly, CDK2 RNA levels were unaffected, which corresponded to the lack of protein downregulation seen. Cyclin E and cyclin D1 levels were unaffected by BZL101 as well, consistent with the lack of G1 cell cycle arrest in LNCaP cells. Strikingly, AR transcript levels decreased with treatment, suggesting BZL101 may be able to disrupt hormone signaling in human prostate cancer cells.

Figure 37:

BZL101 disrupts RNA levels of key cell cycle regulatory components and steroid receptors. BZL101 or nH_20 vehicle control was applied to cancer cell lines: MCF7 (2 mg/mL), MDA-MB-231 (3 mg/mL), LNCaP (1.5 mg/mL), and PC3 (3 mg/mL) for 48 hr. RNA levels of cell cycle regulatory components were determined by RT-PCR. The PCR products were visualized on a 1.2 % agarose gel stained with ethidium bromide. GAPDH provided a gel loading control for the RT-PCR. Representative gels of three independent experiments are shown.

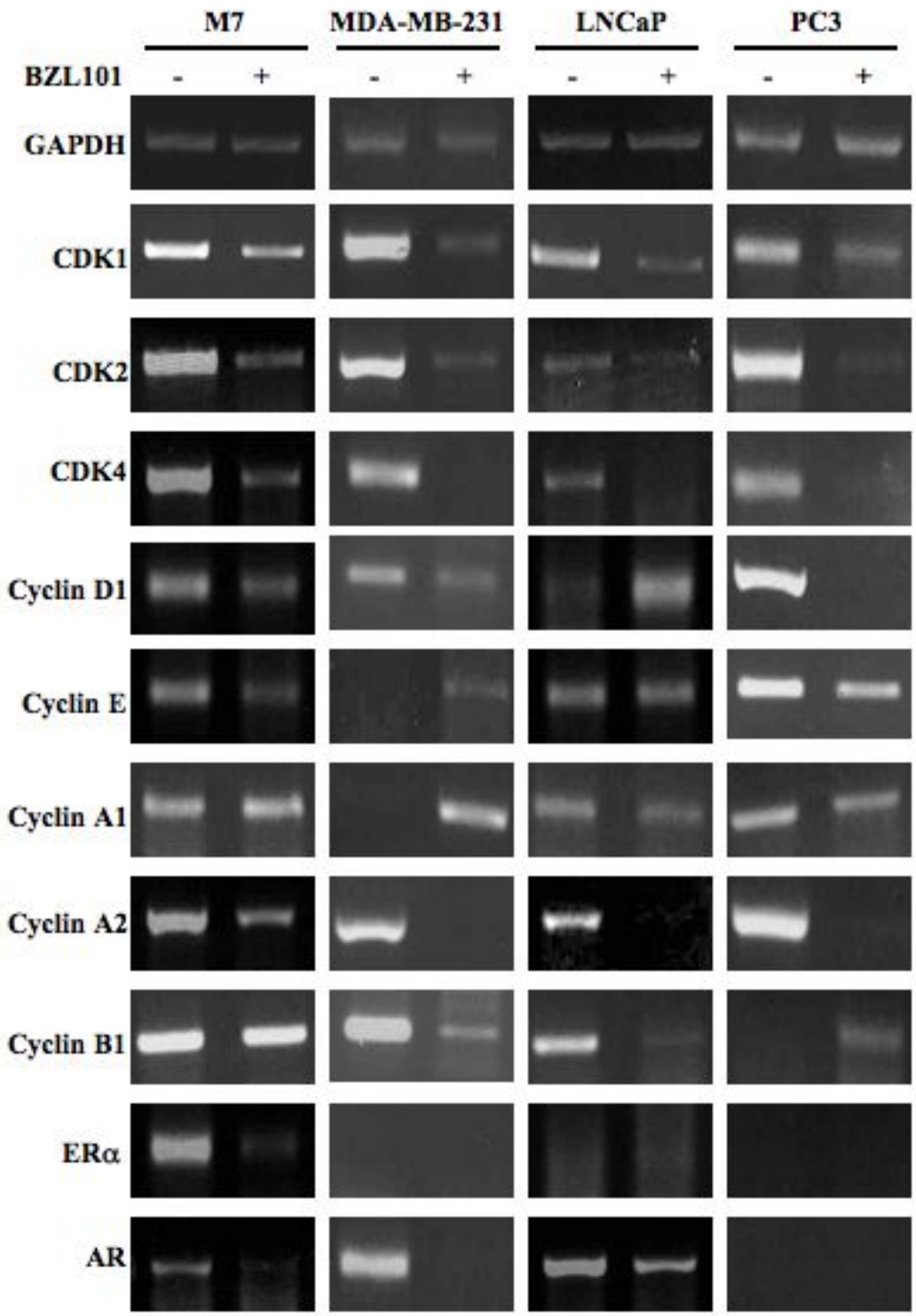
M7
MDA-MB-231
LNCaP
PC3
BZL101
- + - + - + - +
GAPDH
CDK1
CDK2
CDK4
Cyclin D1
Cyclin E
Cyclin A1
Cyclin A2
Cyclin B1
ERα
AR

Hormone insensitive PC3 prostate cancer cells, in which BZL101 induced an S phase arrest, had a marked decrease in RNA levels of CDK2, CDK4, and cyclins D1, and A2, which corresponded to decreases in protein. Cyclin E RNA levels decreased moderately, which is consistent with the moderate decrease in all isoforms of cyclin E protein.

BZL101 sustained loss of cell cycle component expression over time

The specific ablation of late stage cell cyclins in indicative of a block in cell cycle progression. Sustaining this proliferation inhibition is critical to overall antiproliferative activity of BZL101. Therefore, effects on cell cycle progression and late stage cyclin expression were studied in MDA-MB-231 cells over a 48 hr time course. As shown in figure 38, 3 mg/ml BZL101 was able to induce an S phase arrest by 12 hr post treatment. Increased exposure time to the same concentration of BZL101 increased the amount of cells trapped in S phase. Interestingly, S phase arrest occurs relatively early (12 hr), with concomitant changes in late stage cell cycle regulators cyclin A and B. Changes in cell cycle machinery with ascribed function in other cell cycle phases have altered expression after prolonged exposure to BZL101. An example of this is CDK4 downregulation in MDA-MB-231 cells, which occurs only after 48 hours of exposure and 36 hours after the initiation of cell cycle arrest, making this proteins downregulation a secondary effect and not the initial mechanism BZL101 utilizes to halt cell cycle proliferation.

Figure 38:

BZL101 sustained loss of cell cycle component expression over time. MDA-MB-231 cells were treated with 3mg/mL of BZL101 over a 48 hr time course. (Top graph) Cells were hypotonically lysed and stained with propidium iodide prior to analysis by coulter cell counter. Cell count versus PI staining is displayed (n=10,000) per treatment. Cell cycle phase analyzed using Win-MultiCycle software. All analysis was performed in triplicate. (Bottom panels) Total cell lysates were subjected to SDS-PAGE and the levels of cyclin A, cyclin B, CDK4 and HSP90 (loading control) protein was monitored by western blot analysis.

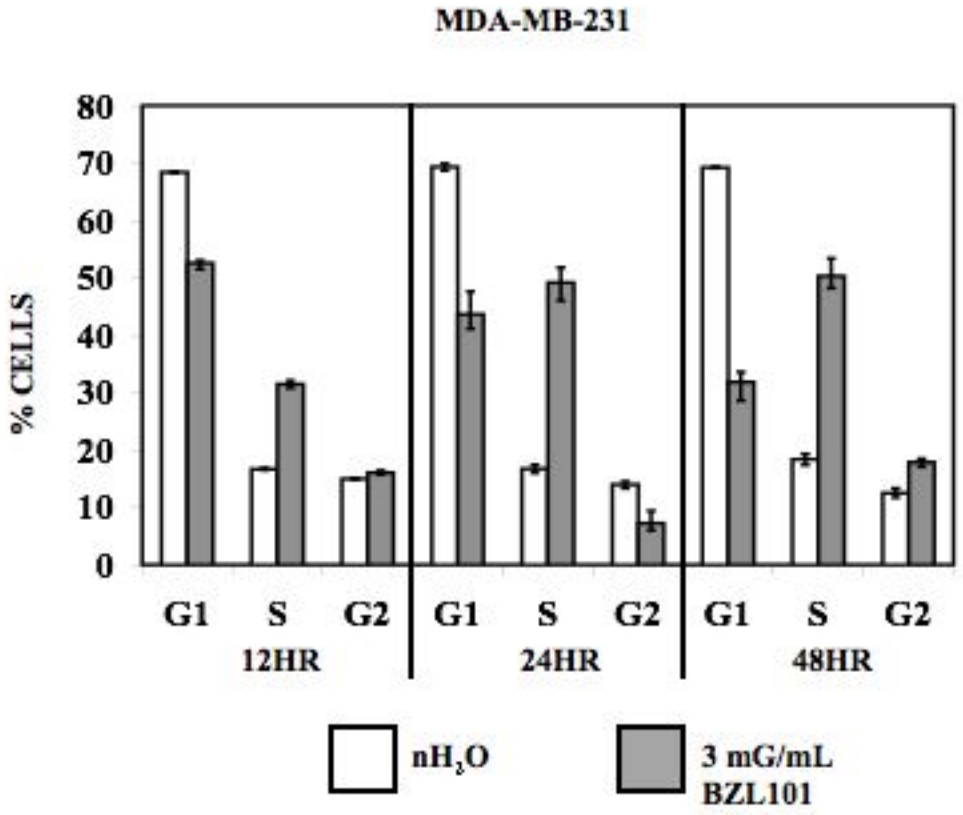
MDA-MB-231
% CELLS
80
70
60
50
40
30
20
10
0
G1
S
G2
12HR
24HR
48HR
nH2O
3 mG/mL
BZL101

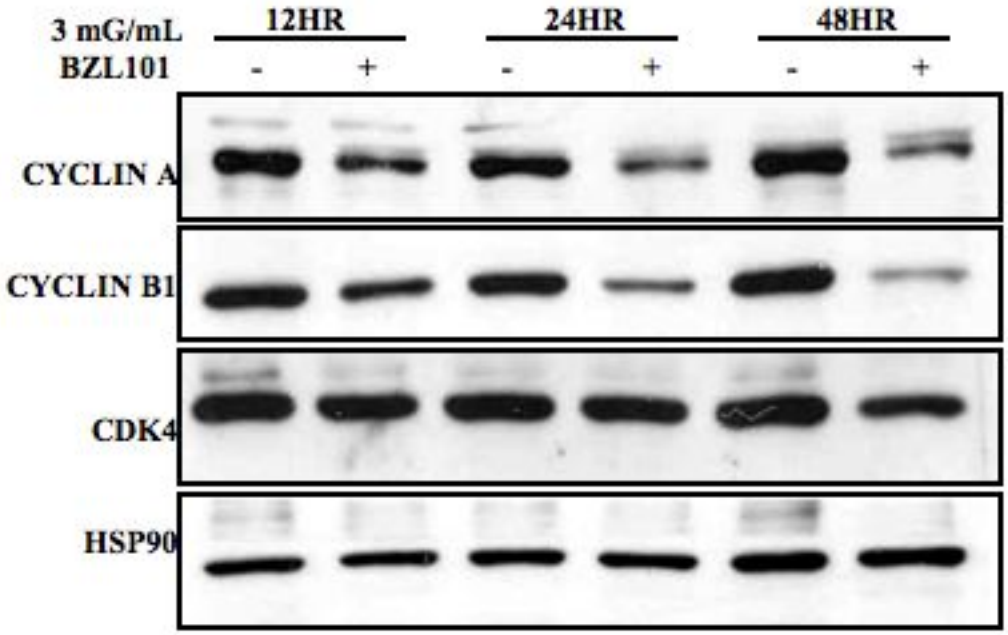
3 mG/mL
BZL101
12HR
24HR
48HR
-
+
CYCLIN A
CYCLIN B1
CDK4
HSP90

Hormone sensitivity confers a select growth advantage to cancer through the activation of downstream proliferative target genes. Loss of ERα expression in breast cancer results in a G1 cell cycle arrest. Because MCF7 cells display a G1 cell cycle arrest and also respond to BZL101 with ablation of ERα expression the kinetics of cell cycle arrest versus transcript ablation was studied in MCF7 cells with 2 mg/mL of BZL101 over a 48 hr time course and dose response. As shown in figure 39, BZL101 was able to ablate CDK2 and ERα transcript expression within 12 hr of treatment. CDK4 downregulation occurred at longer durations of exposure, again suggesting a secondary effect.

Regulation of RNA expression can occur through modulation of transcription factors to cis regulatory regions of DNA. In order to determine if the loss of RNA expression observed for CDK2, CDK4, and ERα observed in MCF7 cells were due to a loss of promoter activity MCF7 cells were transfected separately with promoter constructs containing the upstream regulatory regions hooked to a luciferase reporter gene. As shown in figure 39, BZL101 was able to decrease promoter activity of the CDK2 promoter fragment containing -2313 bp of upstream regulatory sequence, however BZL101 was unable to affect the truncated -101bp fragment, indicating BZL101 affects specific transcription factors who exert their transcriptional activity within this region. Similarly, transfection of CDK4 promoter fragments revealed the promoter region between -1767 and -687 as regulated by BZL101 and the region of ERα promoter regulated as between -860 and -550 upstream of the promoter A transcription start site.

Figure 39:

BZL101 sustained loss of cell cycle component and steroid receptor expression over time. (Upper panels) MCF7 cells were treated with 2 mg/mL of BZL101 over a 48 hr time course. RNA levels of cyclin A1, cyclin A2, CDK2, CDK4, and ERα were determined by RT-PCR. The PCR products were visualized on a 1.2 % agarose gel stained with ethidium bromide. GAPDH provided a gel loading control for the RT-PCR. Representative gels of three independent experiments are shown. (Lower panels) MCF-7 cells were transfected with the indicated CDK2, CDK4, or ERα promoter 5' deletion constructs linked to a luciferase reporter gene, and 24 hr post-transfection cells were treated for 24 hr with either the nH_20 vehicle control or with 2 mg/mL BZL101. Relative luciferase activity was evaluated in lysed cells using the Promega Luciferase Assay Kit and normalized to the reporter plasmid activity of the longest promoter fragment for each gene in cells treated with nH_2O. Two controls (data not shown) included CMV-luciferase to validate transfection efficiency (positive control) and pgl2 to measure background fluorescence (negative control). Bar graphs indicate relative luciferase activity normalized to the protein input and error bars were derived from the results of two independent experiments.

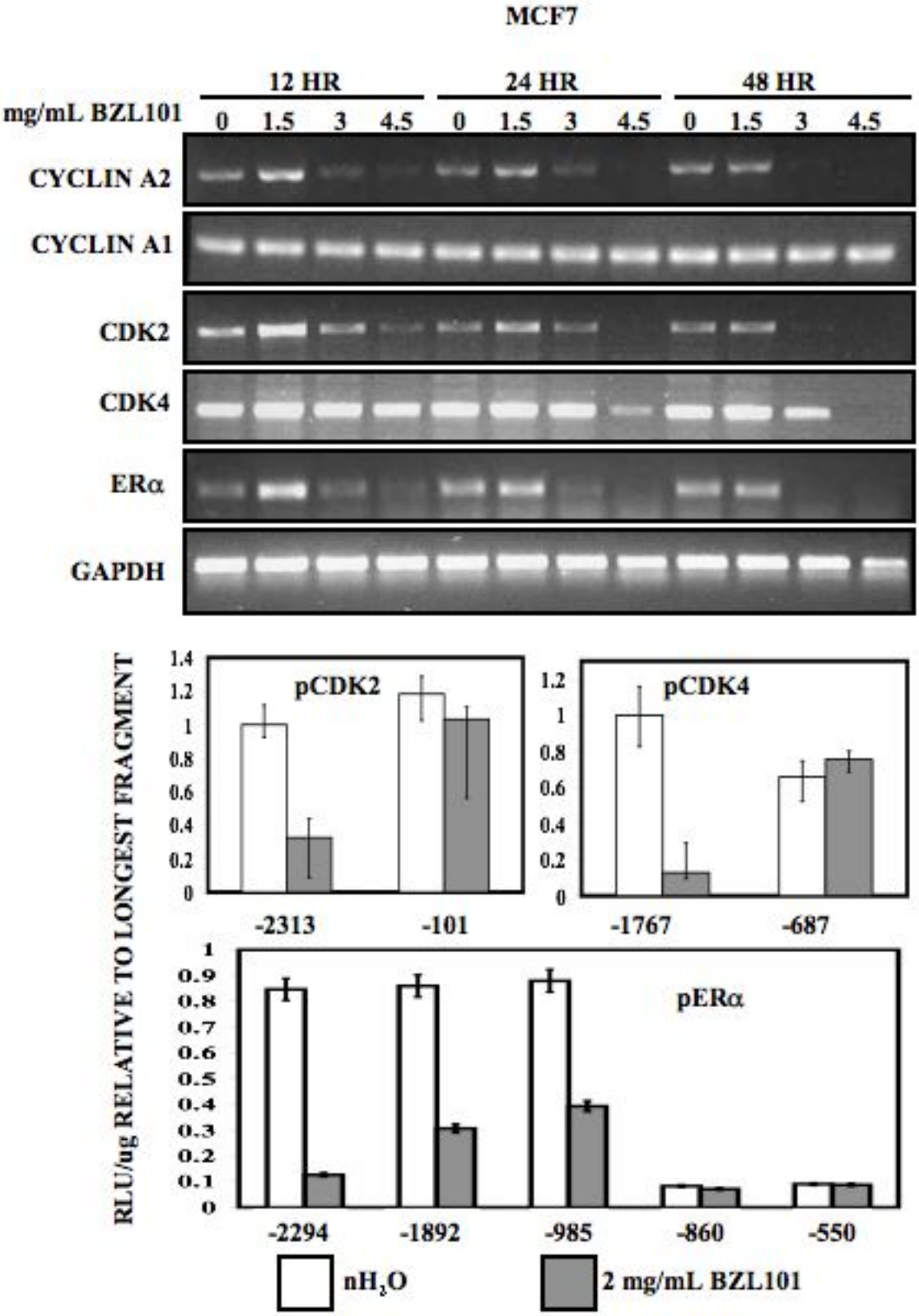
MCF7
12 HR
24 HR
48 HR
mg/mL BZL101
0 1.5 3 4.5 0 1.5 3 4.5 0 1.5 3 4.5
CYCLIN A2
CYCLIN A1
CDK2
CDK4
ERα
GAPDH
RLU/ug RELATIVE TO LONGEST FRAGMENT
pCDK2
-2313
-101
pCDK4
-1767
-687
pERα
-2294
-1892
-985
-860
-550
nH2O
2 mg/mL BZL101

BZL101 alters growth factor receptor expression and intracellular signaling in hormone sensitive MCF7 breast cancer cells

MCF7 human breast cancer cells respond to BZL101 with a G1 cell cycle arrest. Because growth factor pathways are the canonical method for stimulation of cell cycle progression through G1 into S phase, the potential involvement of growth factor signaling pathway disruption in the G1 cell cycle arrest was characterized. MCF7 cells were treated with 2mg/mL BZL101 for a 48 hr time course and total protein subjected to fractionation and western blot detection. As shown in figure 40, addition of BZL101 was able to disrupt the expression of several receptor tyrosine kinases involved in growth factor signaling, including members of the epidermal growth factor receptor family (EGFR, ERBB2, and ERBB3).

To determine if alterations in growth factor receptor (RTK) expression were a universal property of BZL101 or specific to hormone status or specific cell type hormone insensitive MDA-MB-231 cells were also subjected to 3 mg/mL BZL101 treatment for 24 hr and total protein lysate fractionation and detection. As shown in figure 40, expression of key growth factor receptors was also disrupted in MDA-MB-231 cells. Specifically, EGFR and HER2 expression decreased dramatically in response to BZL101. To determine what effect BZL101 may have on downstream signaling components members of the cellular survival signaling pathway, a downstream target of RTK signaling. As shown in figure 40, BZL101 abrogated expression of IRS1, the regulatory subunit of PI3K, and disrupted phosphorylation of AKT. Therefore the disruption of

Figure 40:

BZL101 alters growth factor receptor expression and intracellular signaling in hormone sensitive MCF7 breast cancer cells. (Upper panels) MDA-MB-231 cells were treated with 3 mg/mL of BZL101 for 48 hr. Total cell lysates were subjected to SDS-PAGE and the levels of growth factor signaling pathway components and HSP90 (loading control) protein was monitored by western blot analysis. (Lower panels) MCF7 cells were treated with either 2 mg/mL or 5 mg/mL of BZL101 over a 48 hr time course. Total cell lysates were subjected to SDS-PAGE and the levels of growth factor signaling pathway components and HSP90 (loading control) protein was monitored by western blot analysis.

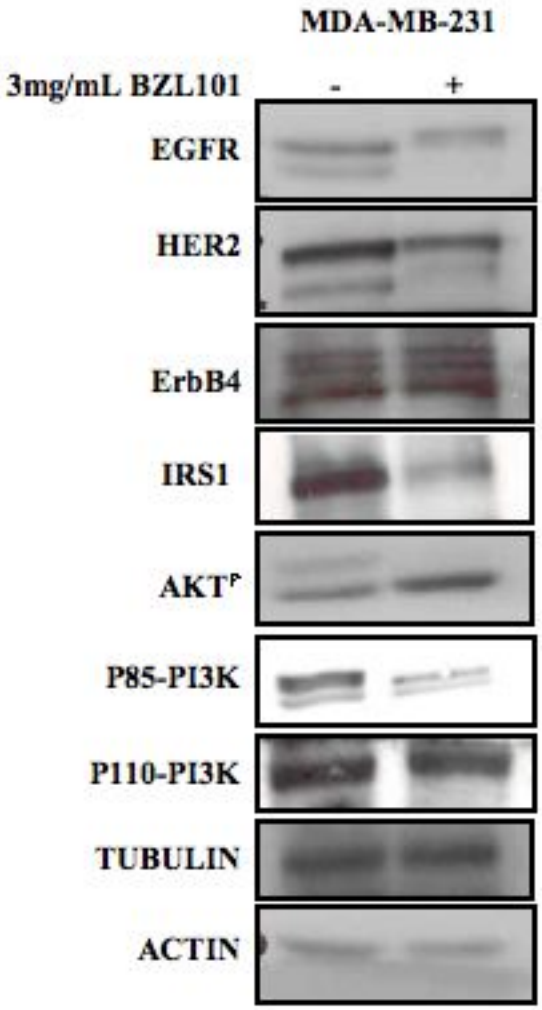
MDA-MB-231
3mg/mL BZL101
-
+
EGFR
HER2
ErbB4
IRS1
AKT
P85-PI3K
P110-PI3K
TUBULIN
ACTIN

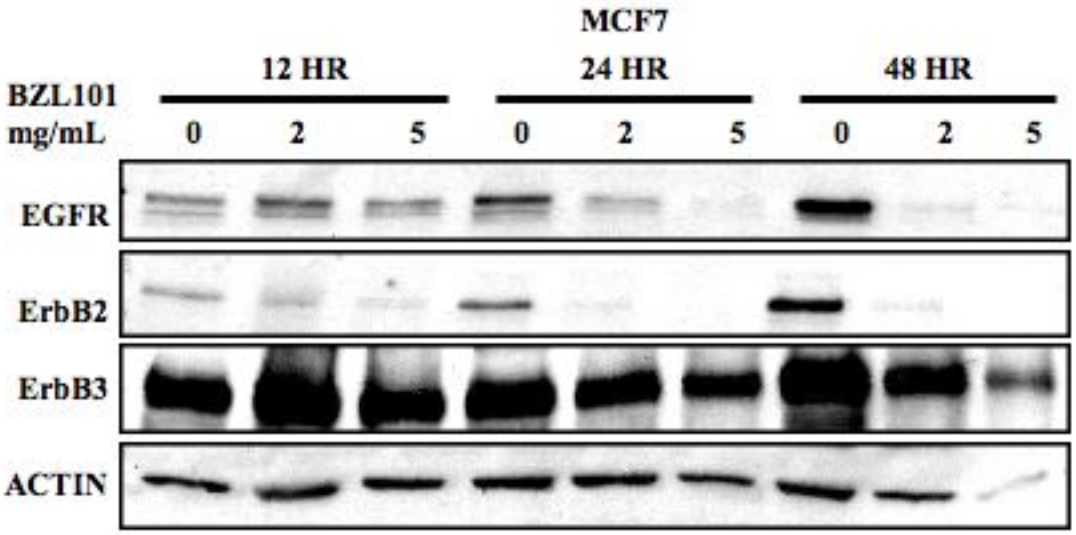
MCF7
12 HR
24 HR
48 HR
BZL101
mg/mL
0
2
5
0
2
5
0
2
5
EGFR
ErbB2
ErbB3
ACTIN

growth factor pathway signaling may be a more generalized response to BZL101, rather than a cell type specific occurance.

BZL101 alters MCF7 cellular morphology

G1 cell cycle arrest has been linked to the disruption of cellular morphology hrough the loss of cellular polarity and activation of the DNA damage pathway. In order to determine if BZL101 disrupted MCF7 cellular morphology cells were treated with or without 2 mg/mL BZL101 for 24 hr and subjected to indirect immunofluorescence. As shown in figure 41, BZL101 caused actin cytoskeletal rearrangement from the striated pattern normally observed in MCF7 to the formation of distinct punctae located on the nuclear periphery. While the cause of this rearrangement is unknown, gross morphological changes to cellular architecture could contribute to the overall effect of G1 cell cycle arrest in MCF7 human breast cancer cells.

Figure 41:

BZL101 alters MCF7 cellular morphology. MCF7 cells were treated with 2 mg/mL BZL101 for 24 hr ans crosslinked with formaldehyde to maintain cellular architecture. dIndirect immunofluorescence microscopy was used to visualize cytoplasmic actin localization. DAPI staining was used to visualize DNA (the nucleus).

.

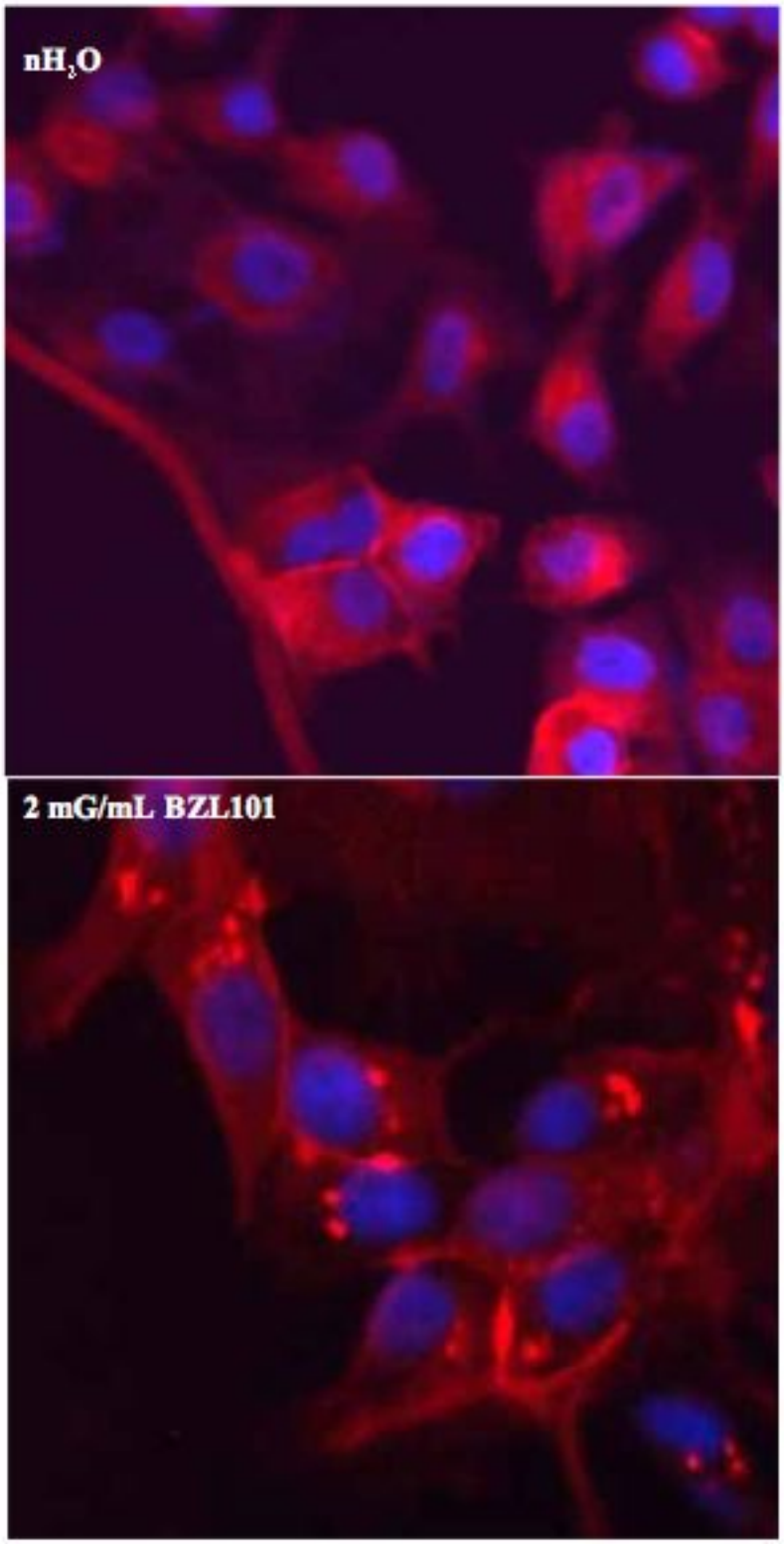

ACTIN DAPI

DISCUSSION:

We have determined that BZL101, an herbal mixture extracted from the *Scutellaria barbata* plant, is able to arrest the proliferation of hormone sensitive and insensitive human breast and prostate cancer cells. This was accompanied by distinct molecular changes in each cell type. As shown in figure 42, the specific phase of cell cycle arrest varied based on the individual characteristics of each cell line. In the less metastatic hormone sensitive cell lines tested, BZL101 was effective at slightly lower concentrations, namely 2mg/mL for MCF7 and 1.5mg/mL for LNCaP, as compared to the slightly higher concentration of 3mg/mL necessary for arrest in the metastatic hormone independent cancers MDA-MB-231 and PC3. The hormone insensitive lines responded to BZL101 by arresting in the S phase of the cell cycle. The hormone sensitive cell lines responded with arrest in either of the growth phases of the cell cycle, MCF7 arresting in G1 and LNCaP arresting in G2/M phase. In all cell lines tested BZL101 increased cellular debris indicative of cell death.

Distinct molecular changes in cell cycle regulatory components accompanied BZL101-induced cell cycle arrest. CDK1, CDK2, CDK4, and Cyclin A are downregulated by BZL101 in all cell lines tested. However, there were specific molecular changes corresponding to the observed cell cycle arrest observed in all cell lines. For instance, Cyclin B1 initiates G2/M progression by promoting anaphase. Cyclin

Figure 42:

Proposed Model for the BZL101 disruption of cell cycle progression in hormone sensitive and insensitive breast and prostate cancer cell lines. BZL101 blocks cell cycle progression at different phases of the cell cycle in each cell line tested. G1 cell cycle arrest was observed in hormone sensitive MCF7 breast cancer cells, with a decrease in G1 cell cycle regulators Cyclin D1, CDK2, and at later time points CDK4. Metastatic, hormone insensitive cell lines MDA-MB-231 and PC3 arrest in S phase upon BZL101 addition, with a corresponding decrease in Cyclin A and CDK2. In hormone sensitive LNCaP prostate cancer cells BZL101 induces a G2/M cell cycle arrest with a decreases in CyclinB1 and CDK1 expression.

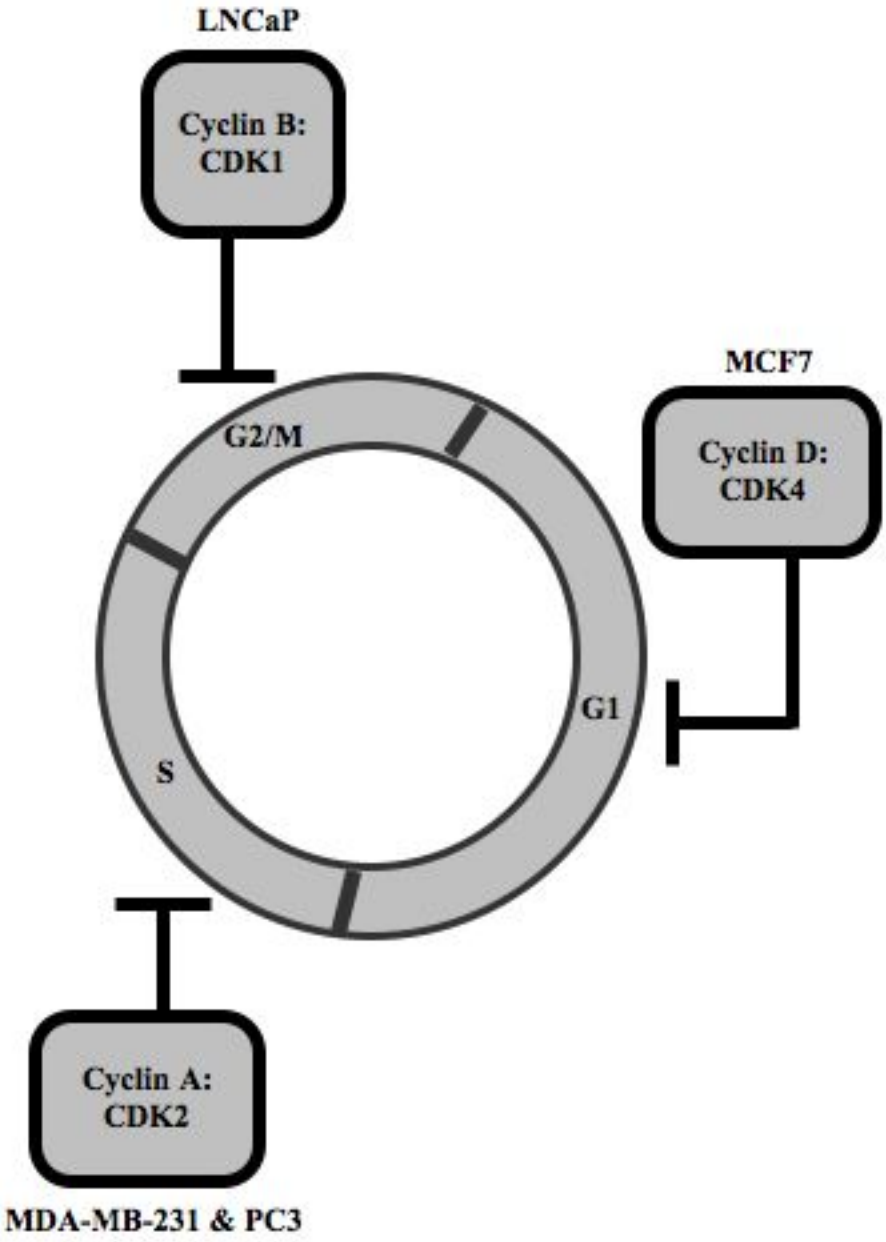
LNCaP
Cyclin B:
CDK1
MCF7
Cyclin D:
CDK4
G2/M
G1
S
Cyclin A:
CDK2
MDA-MB-231 & PC3

B1 expression is disrupted by BZL101 in LNCaP cells, and there is an observed G2/M cell cycle arrest with BZL101.

Hormone sensitive and insensitive reproductive cancer cells responded to BZL101 with decreased proliferation and increased cellular debris. BZL101 was able to ablate ERα expression in estrogen sensitive breast cancers, and androgen receptor (AR) expression in androgen sensitive prostate cancer cells. This disruption of steroid receptor expression implicates BZL101 as a potential therapeutic in the treatment of hormone sensitive breast can prostate cancers. BZL101 has demonstrated effectiveness in the Her2+ hormone insensitive SKBR3 breast cancer cell line (Fong *et al.*, 2008). We now show that additionally the hormone insensitive MDA-MB-231 breast cancer cell line is sensitive to BZL101 treatment. Additionally, we provide the first evidence that BZL101 is effective in prostate cancer cell models, both androgen sensitive and insensitive.

We have established that BZL101, an aqueous extract from the *Scutellaria barbata* plant, is an effective anticancer agent capable of inducing cell cycle arrest and increasing cellular debris in both breast and prostate cancer. BZL101 represents a promising therapeutic strategy, which, when combined with conventional treatments for reproductive cancer, could increase efficacy of treatment with reduced toxicity to patients.

Chapter IV

Conclusion and Future Directions

CONCLUSION

Hormone dependent breast cancer accounts for 70 % of newly diagnosed breast cancer and contributes to overall cancer incidence in the United States. The current therapeutic regimen includes aromatase inhibitors and selective estrogen receptor modulators (SERMs) to block estrogen dependent proliferation. In clinical development is a new wave of selective estrogen receptor downregulators (SERDs), capable of disrupting ERα protein expression.

I3C represents a natural phytochemical product with SERD activity. Being a natural component of the diet enables high toleration of I3C administration, as compared to other SERDs in development, namely fulvestrant which negatively affects heart and bone health. As established in chapter I, I3C activates AhR to induce nuclear translocation and recruitment of the Rbx1 E3 ligase, which results in the targeted degradation of ERα protein. This disruption of functional ERα protein in turn ablates expression of the GATA3 transcription factor, the loss of which feeds back onto ERα transcription, essentially enforcing the shutting off of ERα production. Loss of this critical oncogene in hormone sensitive breast cancer cells results in a dramatic halt to cell cycle progression, as evidenced by siRNA ablation of ERα or estrogen deprivation in hormone sensitive breast cancers cells induces a G1 cell cycle arrest (Sundar *et al.,* 2006).

The mechanism of G1 cell cycle arrest in hormone sensitive breast cancer cells is multipronged, with inhibition of G1-S progression occurring through multiple mechanisms, namely the altered localization of the cyclinE-CDK2 complex as a result of inhibited cyclin E processing and by the ablation of CDK6 expression through altered Sp1 activity. Chapter IIa describes the I3C dependent downregulation of IGF1R and IRS1 expression. IGF1R and IRS1 signaling activity through the MAPK and AKT pathways directly implicate these changes as direct contributors to the G1 cell cycle arrest induced by I3C.

Expression of telomerase induces cellular immortality through the extension of telomeric DNA sequence and DNA repair function, essentially blocking the cellular senescence seen in adult normal human tissues. Cancer is a disease of misregulated proliferation, and disruption of senescence is critical to the propagation of cancer. Chapter IIb establishes the mechanism I3C utilizes to disrupt expression of hTERT, the catalytic protein component of the telomerase ribonucleoprotein complex. I3C accomplishes this by disrupting hTERT transcription through alteration of Sp1 activity and ERα expression, two transcription factors critical to basal expression of telomerase in hormone sensitive breast cancers.

Disruption of cell cycle progression is key to blocking cancer cell proliferation. Chapter III demonstrated the effectiveness of the aqueous extract from the Ban Zhi Lian plant (BZL101), to disrupt hormone sensitive and insensitive breast and prostate cancer cell growth. BZL101 mediated cell cycle arrest was induced by cell type specific

changes in the expression of key cell cycle regulatory components. Prolonged exposure or high concentrations of BZL101 was able to induce cell death as evidenced by an increase in cellular debris upon BZL101 treatment. The effectiveness of BZL101 was within the range previously demonstrated as effective on hepatocarcinoma and leukemia, indicating the diversity of application for this emerging anticancer agent.

FUTURE DIRECTIONS

The aryl hydrocarbon receptor (AhR) is known to bind xenobiotic chemicals and induce cellular action. Interestingly, initial assays to discover an I3C target protein focused on this specific receptor. However, binding analysis and reporter assays were unclear as to the specificity of I3C for the ligand-binding domain (LBD). DIM, the acid condensation dimmer of I3C, has a much higher affinity for AhR, yet exerts completely opposite effects on ERα protein expression. Indeed the concentration of I3C needed to induce cell cycle arrest is almost ten times greater than DIM (200 μM I3C vs 30 μM DIM). In addition, TCDD, the highest affinity ligand known for AhR, is associated with endocrine disruption. TCDD was a component of Agent Orange, the manufacture of which was restricted in the United States after the discovery that this chemical mixture caused birth defects in rodents. More recently the endocrine disruption effect of TCDD on humans has been recognized through population studies on children of Vietnam veterans who were exposed to Agent Orange during the war.

This sets up an interesting biological question as to the activity of AhR ligands. Ligands such as TCDD and 3-methylchloranthrene (3-MC) are classified as agonists, while other ligands such as α-napthaflavone (αNAF) are classified as antagonists based on their activation of the classical AhR response pathway. With the discovery of new non-canonical signaling pathways for AhR the possibility that AhR ligands could operate under the same principals as ERα ligands becomes an exciting avenue of exploration. Partial agoinst and tissue-specific agoinsm have been seen for

several ERα ligands, which raises the potential for development of AhR specific ligands which have desirable agonist activity toward certain pathways in certain tissues and antagonist activity in tissues where negative phenotypes result. In addition, while the above mentioned data demonstrate the necessity of AhR in mediating I3C-dependent proteolytic degradation of ERα, they do not preclude the possibility that I3C actually binds to an alternate target protein. This binding could then recruit AhR to exploit its' signaling activity and coactivator associations.

This research demonstrated that one of the repercussions disruption of ERα expression has in hormone sensitive breast cancer cells is the ablation of GATA3 expression. GATA3 expression is intimately tied to ERα in breast cancer, which may be a result of normal endogenous regulation during mammary morphogenesis, as GATA3 is required during ductal elongation. GATA transcription factors are known for their involvement in regulation of gene expression in cell fate determination. Elucidation of their ultimate transcriptional targets would benefit the understanding of mammary carcinogenesis by allowing for a greater understanding of the molecular changes occurring in highly differentiated hormone sensitive breast cancer. This could aid in the discovery of new therapeutic targets, which could confer specificity to this class of breast cancer and represent a new wave of treatment options for women who have developed resistance to SERMs and SERDs.

Other targets of I3C-mdeiated disruption of ERα determined in these studies were IGF1R, IRS1, and hTERT. IGF signaling in hormone sensitive breast cancers is critical to

the proliferative potential of hormone sensitive breast cancers. However, IGF1R is a receptor tyrosine kinase which sequence similarity to Insulin Receptor (IR). IGF1R and IR are able to heterodimerize and induce intracellular phosphorylation. Therefore, the effect of I3C on IR expression and function should be evaluated. Also, the downregulation of IGF1R and IRS1 should result in change in the level of phosphorylated intracellular signaling components of the Ras-MAPK and AKT pathways. I3C is known to affect AKT signaling, which then directly affects NFkB activity, so determination of the role IGF1R and IRS1 downregulation plays in these events would be critical to establishing the overall mechanism of I3C induced G1 cell cycle arrest.

Telomerase activity in human cancer cells is critical to their immortalization and continued proliferation. As demonstrated in chapter IIb, I3C is able to block expression of hTERT, which results in a loss of telomerase activity toward telomeric extension. Determination of the effect I3C has on cellular senescence and DNA repair will help to identify the molecular mechanism of I3C action in hormone sensitive breast cancer cells. I3C-dependent ablation of hTERT expression was dependent on prior downregulation of ERα expression and Sp1 activity. While data presented here shows an increase in the levels of phosphoylated threonines on Sp1, it doe not preclude that alternate post-translational modifications take place in the presence of I3C. The site(s) of theronine phosphorylation are not established, and the kinase responsible for the increased phosphorylation is not identified, although if threonine-579 is the responsible site then the caesin kinase II enzyme would be a reasonable target for further characterization.

BZL101 is an aqueous extract from the scutellaria barbata plant which in chapter IV has been shown to have distinct molecular changes resulting in cell cycle arrest of human breast and prostate cancer cells regardless of hormone status. The active component responsible for BZL101 anticancer properties has yet to be identified, and indeed the different patterns of cell cycle arrest observed in multiple cell lines may be the result of differing susceptibility to individual components of this mixture. In addition, the ablation of individual cell cycle components may not necessarily result in cell cycle arrest, as CDK substitution occurs as an adaptive mechanism in cancer cells. Therefore, the actual involvement of each CDK and cyclin in the arrest of reproductive cancer cells should be examined.

REFERENCES

Adeyemo, O., Kallio, P.J., Palvimo, J.J., Kontula, K., and Janne, O.A. (1993). A single-base substitution in exon 6 of the androgen receptor gene causing complete androgen insensitivity: the mutated receptor fails to transactivate but binds to DNA in vitro. Hum Mol Genet *2*, 1809-1812.

Afouda, B.A., Martin, J., Liu, F., Ciau-Uitz, A., Patient, R., and Hoppler, S. (2008). GATA transcription factors integrate Wnt signalling during heart development. Development *135*, 3185-3190.

Aggarwal, B.B., and Ichikawa, H. (2005). Molecular targets and anticancer potential of indole-3-carbinol and its derivatives. Cell Cycle *4*, 1201-1215.

Ali, S., and Coombes, R.C. (2000). Estrogen receptor alpha in human breast cancer: occurrence and significance. J Mammary Gland Biol Neoplasia *5*, 271-281.

Aneja, R., Zhou, J., Zhou, B., Chandra, R., and Joshi, H.C. (2006). Treatment of hormone-refractory breast cancer: apoptosis and regression of human tumors implanted in mice. Mol Cancer Ther *5*, 2366-2377.

Antkiewicz, D.S., Burns, C.G., Carney, S.A., Peterson, R.E., and Heideman, W. (2005). Heart malformation is an early response to TCDD in embryonic zebrafish. Toxicol Sci *84*, 368-377.

Armstrong, S.A., Barry, D.A., Leggett, R.W., and Mueller, C.R. (1997). Casein kinase II-mediated phosphorylation of the C terminus of Sp1 decreases its DNA binding activity. J Biol Chem *272*, 13489-13495.

Asselin-Labat, M.L. (2007). [Mammary stem and progenitor cells: critical role of the transcription factor Gata-3]. Med Sci (Paris) *23*, 1077-1080.

Asselin-Labat, M.L., Sutherland, K.D., Barker, H., Thomas, R., Shackleton, M., Forrest, N.C., Hartley, L., Robb, L., Grosveld, F.G., van der Wees, J., Lindeman, G.J., and Visvader, J.E. (2007). Gata-3 is an essential regulator of mammary-gland morphogenesis and luminal-cell differentiation. Nat Cell Biol *9*, 201-209.

Asselin-Labat, M.L., Vaillant, F., Shackleton, M., Bouras, T., Lindeman, G.J., and Visvader, J.E. (2008). Delineating the epithelial hierarchy in the mouse mammary gland. Cold Spring Harb Symp Quant Biol *73*, 469-478.

Auborn, K.J., Fan, S., Rosen, E.M., Goodwin, L., Chandraskaren, A., Williams, D.E., Chen, D., and Carter, T.H. (2003). Indole-3-carbinol is a negative regulator of estrogen. J Nutr *133*, 2470S-2475S.

Badia, E., Oliva, J., Balaguer, P., and Cavailles, V. (2007). Tamoxifen resistance and epigenetic modifications in breast cancer cell lines. Curr Med Chem *14*, 3035-3045.

Baird, D.M. (2008). Mechanisms of telomeric instability. Cytogenet Genome Res *122*, 308-314.

Blasco, M.A., Rizen, M., Greider, C.W., and Hanahan, D. (1996). Differential regulation of telomerase activity and telomerase RNA during multi-stage tumorigenesis. Nat Genet *12*, 200-204.

Bocchinfuso, W.P., and Korach, K.S. (1997). Mammary gland development and tumorigenesis in estrogen receptor knockout mice. J Mammary Gland Biol Neoplasia *2*, 323-334.

Bosland, M.C. (2000). The role of steroid hormones in prostate carcinogenesis. J Natl Cancer Inst Monogr, 39-66.

Brenton, J.D., Carey, L.A., Ahmed, A.A., and Caldas, C. (2005). Molecular classification and molecular forecasting of breast cancer: ready for clinical application? J Clin Oncol *23*, 7350-7360.

Buchkovich, K.J., and Greider, C.W. (1996). Telomerase regulation during entry into the cell cycle in normal human T cells. Mol Biol Cell *7*, 1443-1454.

Campbell-Thompson, M., Lynch, I.J., and Bhardwaj, B. (2001). Expression of estrogen receptor (ER) subtypes and ERbeta isoforms in colon cancer. Cancer Res *61*, 632-640.

Carboni, J.M., Lee, A.V., Hadsell, D.L., Rowley, B.R., Lee, F.Y., Bol, D.K., Camuso, A.E., Gottardis, M., Greer, A.F., Ho, C.P., Hurlburt, W., Li, A., Saulnier, M., Velaparthi, U., Wang, C., Wen, M.L., Westhouse, R.A., Wittman, M., Zimmermann, K., Rupnow, B.A., and Wong, T.W. (2005). Tumor development by transgenic expression of a constitutively active insulin-like growth factor I receptor. Cancer Res *65*, 3781-3787.

Chang, E.C., Frasor, J., Komm, B., and Katzenellenbogen, B.S. (2006). Impact of estrogen receptor beta on gene networks regulated by estrogen receptor alpha in breast cancer cells. Endocrinology *147*, 4831-4842.

Charron, F., Paradis, P., Bronchain, O., Nemer, G., and Nemer, M. (1999). Cooperative interaction between GATA-4 and GATA-6 regulates myocardial gene expression. Mol Cell Biol *19*, 4355-4365.

Chen, I., Safe, S., and Bjeldanes, L. (1996). Indole-3-carbinol and diindolylmethane as aryl hydrocarbon (Ah) receptor agonists and antagonists in T47D human breast cancer cells. Biochem Pharmacol *51*, 1069-1076.

Chitnis, M.M., Yuen, J.S., Protheroe, A.S., Pollak, M., and Macaulay, V.M. (2008). The type 1 insulin-like growth factor receptor pathway. Clin Cancer Res *14*, 6364-6370.

Clarke, R., Liu, M.C., Bouker, K.B., Gu, Z., Lee, R.Y., Zhu, Y., Skaar, T.C., Gomez, B., O'Brien, K., Wang, Y., and Hilakivi-Clarke, L.A. (2003). Antiestrogen resistance in breast cancer and the role of estrogen receptor signaling. Oncogene *22*, 7316-7339.

Clarke, R.B., Howell, A., and Anderson, E. (1997). Type I insulin-like growth factor receptor gene expression in normal human breast tissue treated with oestrogen and progesterone. Br J Cancer *75*, 251-257.

Colozza, M., Califano, R., Minenza, E., Dinh, P., and Azambuja, E. (2008). Aromatase inhibitors: a new reality for the adjuvant endocrine treatment of early-stage breast cancer in postmenopausal women. Mini Rev Med Chem *8*, 564-574.

Cover, C.M., Hsieh, S.J., Cram, E.J., Hong, C., Riby, J.E., Bjeldanes, L.F., and Firestone, G.L. (1999). Indole-3-carbinol and tamoxifen cooperate to arrest the cell cycle of MCF-7 human breast cancer cells. Cancer Res *59*, 1244-1251.

Cover, C.M., Hsieh, S.J., Tran, S.H., Hallden, G., Kim, G.S., Bjeldanes, L.F., and Firestone, G.L. (1998). Indole-3-carbinol inhibits the expression of cyclin-dependent kinase-6 and induces a G1 cell cycle arrest of human breast cancer cells independent of estrogen receptor signaling. J Biol Chem *273*, 3838-3847.

Cram, E.J., Liu, B.D., Bjeldanes, L.F., and Firestone, G.L. (2001). Indole-3-carbinol inhibits CDK6 expression in human MCF-7 breast cancer cells by disrupting Sp1 transcription factor interactions with a composite element in the CDK6 gene promoter. J Biol Chem *276*, 22332-22340.

Cui, Y., Parra, I., Zhang, M., Hilsenbeck, S.G., Tsimelzon, A., Furukawa, T., Horii, A., Zhang, Z.Y., Nicholson, R.I., and Fuqua, S.A. (2006). Elevated expression of mitogen-activated protein kinase phosphatase 3 in breast tumors: a mechanism of tamoxifen resistance. Cancer Res *66*, 5950-5959.

Da Silva Xavier, G., Qian, Q., Cullen, P.J., and Rutter, G.A. (2004). Distinct roles for insulin and insulin-like growth factor-1 receptors in pancreatic beta-cell glucose sensing revealed by RNA silencing. Biochem J *377*, 149-158.

Dai, Z.J., Wang, X.J., Li, Z.F., Ji, Z.Z., Ren, H.T., Tang, W., Liu, X.X., Kang, H.F., Guan, H.T., and Song, L.Q. (2008). Scutellaria barbate extract induces apoptosis of hepatoma H22 cells via the mitochondrial pathway involving caspase-3. World J Gastroenterol *14*, 7321-7328.

Dutertre, M., and Smith, C.L. (2000). Molecular mechanisms of selective estrogen receptor modulator (SERM) action. J Pharmacol Exp Ther *295*, 431-437.

Eakin, C.M., Maccoss, M.J., Finney, G.L., and Klevit, R.E. (2007). Estrogen receptor alpha is a putative substrate for the BRCA1 ubiquitin ligase. Proc Natl Acad Sci U S A *104*, 5794-5799.

Eeckhoute, J., Keeton, E.K., Lupien, M., Krum, S.A., Carroll, J.S., and Brown, M. (2007). Positive cross-regulatory loop ties GATA-3 to estrogen receptor alpha expression in breast cancer. Cancer Res *67*, 6477-6483.

Enmark, E., and Gustafsson, J.A. (1999). Oestrogen receptors - an overview. J Intern Med *246*, 133-138.

Ewer, M.S., and Gluck, S. (2009). A woman's heart: the impact of adjuvant endocrine therapy on cardiovascular health. Cancer *115*, 1813-1826.

Fan, M., Bigsby, R.M., and Nephew, K.P. (2003). The NEDD8 pathway is required for proteasome-mediated degradation of human estrogen receptor (ER)-alpha and essential for the antiproliferative activity of ICI 182,780 in ERalpha-positive breast cancer cells. Mol Endocrinol *17*, 356-365.

Fang, S.H., Chen, Y., and Weigel, R.J. (2008). GATA-3 as a Marker of Hormone Response in Breast Cancer. J Surg Res.

Fong, S., Shoemaker, M., Cadaoas, J., Lo, A., Liao, W., Tagliaferri, M., Cohen, I., and Shtivelman, E. (2008). Molecular mechanisms underlying selective cytotoxic activity of BZL101, an extract of Scutellaria barbata, towards breast cancer cells. Cancer Biol Ther *7*, 577-586.

Fuqua, S.A., Fitzgerald, S.D., Chamness, G.C., Tandon, A.K., McDonnell, D.P., Nawaz, Z., O'Malley, B.W., and McGuire, W.L. (1991). Variant human breast tumor estrogen receptor with constitutive transcriptional activity. Cancer Res *51*, 105-109.

Garcia, H.H., Brar, G.A., Nguyen, D.H., Bjeldanes, L.F., and Firestone, G.L. (2005). Indole-3-carbinol (I3C) inhibits cyclin-dependent kinase-2 function in human breast cancer cells by regulating the size distribution, associated cyclin E forms, and subcellular localization of the CDK2 protein complex. J Biol Chem *280*, 8756-8764.

Garcia-Echeverria, C. (2006). Medicinal chemistry approaches to target the kinase activity of IGF-1R. IDrugs *9*, 415-419.

Garimella, R., Kacena, M.A., Tague, S.E., Wang, J., Horowitz, M.C., and Anderson, H.C. (2007). Expression of bone morphogenetic proteins and their receptors in the bone marrow megakaryocytes of GATA-1(low) mice: a possible role in osteosclerosis. J Histochem Cytochem *55*, 745-752.

Gomez, D.E., Tejera, A.M., and Olivero, O.A. (1998). Irreversible telomere shortening by 3'-azido-2',3'-dideoxythymidine (AZT) treatment. Biochem Biophys Res Commun *246*, 107-110.

Goya, M., Miyamoto, S., Nagai, K., Ohki, Y., Nakamura, K., Shitara, K., Maeda, H., Sangai, T., Kodama, K., Endoh, Y., Ishii, G., Hasebe, T., Yonou, H., Hatano, T., Ogawa, Y., and Ochiai, A. (2004). Growth inhibition of human prostate cancer cells in human adult bone implanted into nonobese diabetic/severe combined immunodeficient mice by a ligand-specific antibody to human insulin-like growth factors. Cancer Res *64*, 6252-6258.

Gregory, C.W., He, B., Johnson, R.T., Ford, O.H., Mohler, J.L., French, F.S., and Wilson, E.M. (2001). A mechanism for androgen receptor-mediated prostate cancer recurrence after androgen deprivation therapy. Cancer Res *61*, 4315-4319.

Happerfield, L.C., Miles, D.W., Barnes, D.M., Thomsen, L.L., Smith, P., and Hanby, A. (1997). The localization of the insulin-like growth factor receptor 1 (IGFR-1) in benign and malignant breast tissue. J Pathol *183*, 412-417.

Harris, H.A., Katzenellenbogen, J.A., and Katzenellenbogen, B.S. (2002). Characterization of the biological roles of the estrogen receptors, ERalpha and ERbeta, in estrogen target tissues in vivo through the use of an ERalpha-selective ligand. Endocrinology *143*, 4172-4177.

Higdon, J.V., Delage, B., Williams, D.E., and Dashwood, R.H. (2007). Cruciferous vegetables and human cancer risk: epidemiologic evidence and mechanistic basis. Pharmacol Res *55*, 224-236.

Hoch, R.V., Thompson, D.A., Baker, R.J., and Weigel, R.J. (1999). GATA-3 is expressed in association with estrogen receptor in breast cancer. Int J Cancer *84*, 122-128.

Howell, A., Cuzick, J., Baum, M., Buzdar, A., Dowsett, M., Forbes, J.F., Hoctin-Boes, G., Houghton, J., Locker, G.Y., and Tobias, J.S. (2005). Results of the ATAC (Arimidex, Tamoxifen, Alone or in Combination) trial after completion of 5 years' adjuvant treatment for breast cancer. Lancet *365*, 60-62.

Ito, H., Kyo, S., Kanaya, T., Takakura, M., Koshida, K., Namiki, M., and Inoue, M. (1998). Detection of human telomerase reverse transcriptase messenger RNA in voided urine samples as a useful diagnostic tool for bladder cancer. Clin Cancer Res *4*, 2807-2810.

Jellinck, P.H., Forkert, P.G., Riddick, D.S., Okey, A.B., Michnovicz, J.J., and Bradlow, H.L. (1993). Ah receptor binding properties of indole carbinols and induction of hepatic estradiol hydroxylation. Biochem Pharmacol *45*, 1129-1136.

Jemal, A., Siegel, R., Ward, E., Murray, T., Xu, J., and Thun, M.J. (2007). Cancer statistics, 2007. CA Cancer J Clin *57*, 43-66.

Jones, R.A., Campbell, C.I., Gunther, E.J., Chodosh, L.A., Petrik, J.J., Khokha, R., and Moorehead, R.A. (2007). Transgenic overexpression of IGF-IR disrupts mammary ductal morphogenesis and induces tumor formation. Oncogene *26*, 1636-1644.

Jones, R.A., Campbell, C.I., Wood, G.A., Petrik, J.J., and Moorehead, R.A. (2009). Reversibility and recurrence of IGF-IR-induced mammary tumors. Oncogene *28*, 2152-2162.

Jong, H.S., Park, Y.I., Kim, S., Sohn, J.H., Kang, S.H., Song, S.H., Bang, Y.J., and Kim, N.K. (1999). Up-regulation of human telomerase catalytic subunit during gastric carcinogenesis. Cancer *86*, 559-565.

Kallio, P.J., Palvimo, J.J., Mehto, M., and Janne, O.A. (1994). Analysis of androgen receptor-DNA interactions with receptor proteins produced in insect cells. J Biol Chem *269*, 11514-11522.

Kanaya, T., Kyo, S., Takakura, M., Ito, H., Namiki, M., and Inoue, M. (1998). hTERT is a critical determinant of telomerase activity in renal-cell carcinoma. Int J Cancer *78*, 539-543.

Kim, E.K., Kwon, K.B., Han, M.J., Song, M.Y., Lee, J.H., Ko, Y.S., Shin, B.C., Yu, J., Lee, Y.R., Ryu, D.G., Park, J.W., and Park, B.H. (2007). Induction of G1 arrest and apoptosis by Scutellaria barbata in the human promyelocytic leukemia HL-60 cell line. Int J Mol Med *20*, 123-128.

Kim, Y.S., and Milner, J.A. (2005). Targets for indole-3-carbinol in cancer prevention. J Nutr Biochem *16*, 65-73.

Kouros-Mehr, H., Bechis, S.K., Slorach, E.M., Littlepage, L.E., Egeblad, M., Ewald, A.J., Pai, S.Y., Ho, I.C., and Werb, Z. (2008a). GATA-3 links tumor differentiation and dissemination in a luminal breast cancer model. Cancer Cell *13*, 141-152.

Kouros-Mehr, H., Kim, J.W., Bechis, S.K., and Werb, Z. (2008b). GATA-3 and the regulation of the mammary luminal cell fate. Curr Opin Cell Biol *20*, 164-170.

Kouros-Mehr, H., Slorach, E.M., Sternlicht, M.D., and Werb, Z. (2006). GATA-3 maintains the differentiation of the luminal cell fate in the mammary gland. Cell *127*, 1041-1055.

Kushner, D.M., Paranjape, J.M., Bandyopadhyay, B., Cramer, H., Leaman, D.W., Kennedy, A.W., Silverman, R.H., and Cowell, J.K. (2000). 2-5A antisense directed

against telomerase RNA produces apoptosis in ovarian cancer cells. Gynecol Oncol *76*, 183-192.

Kyo, S., Takakura, M., Kanaya, T., Zhuo, W., Fujimoto, K., Nishio, Y., Orimo, A., and Inoue, M. (1999). Estrogen activates telomerase. Cancer Res *59*, 5917-5921.

Lee, A.V., Schiff, R., Cui, X., Sachdev, D., Yee, D., Gilmore, A.P., Streuli, C.H., Oesterreich, S., and Hadsell, D.L. (2003). New mechanisms of signal transduction inhibitor action: receptor tyrosine kinase down-regulation and blockade of signal transactivation. Clin Cancer Res *9*, 516S-523S.

Lee, W.L., Cheng, M.H., Chao, H.T., and Wang, P.H. (2008). The role of selective estrogen receptor modulators on breast cancer: from tamoxifen to raloxifene. Taiwan J Obstet Gynecol *47*, 24-31.

Li, S.L., Liang, S.J., Guo, N., Wu, A.M., and Fujita-Yamaguchi, Y. (2000). Single-chain antibodies against human insulin-like growth factor I receptor: expression, purification, and effect on tumor growth. Cancer Immunol Immunother *49*, 243-252.

Li, Z., Meng, Z.H., Sayeed, A., Shalaby, R., Ljung, B.M., and Dairkee, S.H. (2002). Genome-wide allelotyping of a new in vitro model system reveals early events in breast cancer progression. Cancer Res *62*, 5980-5987.

Liu, J.Y., Wang, Y.R., and Liu, Y. (2008). [Optimizing extraction process of Scutellaria barbata by golden section method]. Zhongguo Zhong Yao Za Zhi *33*, 896-899.

Liu, W., Ye, P., O'Kusky, J.R., and D'Ercole, A.J. (2009). Type 1 insulin-like growth factor receptor signaling is essential for the development of the hippocampal formation and dentate gyrus. J Neurosci Res *87*, 2821-2832.

Lynch, J.H., Batuello, J.T., Crawford, E.D., Gomella, L.G., Kaufman, J., Petrylak, D.P., and Joel, A.B. (2001). Therapeutic strategies for localized prostate cancer. Rev Urol *3 Suppl 2*, S39-48.

Manson, M.M., Farmer, P.B., Gescher, A., and Steward, W.P. (2005). Innovative agents in cancer prevention. Recent Results Cancer Res *166*, 257-275.

Maor, S., Mayer, D., Yarden, R.I., Lee, A.V., Sarfstein, R., Werner, H., and Papa, M.Z. (2006). Estrogen receptor regulates insulin-like growth factor-I receptor gene expression in breast tumor cells: involvement of transcription factor Sp1. J Endocrinol *191*, 605-612.

Mauro, L., Salerno, M., Panno, M.L., Bellizzi, D., Sisci, D., Miglietta, A., Surmacz, E., and Ando, S. (2001). Estradiol increases IRS-1 gene expression and insulin signaling in breast cancer cells. Biochem Biophys Res Commun *288*, 685-689.

Mercier, I., Mader, S., and Calderone, A. (2003). Tamoxifen and ICI 182,780 negatively influenced cardiac cell growth via an estrogen receptor-independent mechanism. Cardiovasc Res *59*, 883-892.

Miller, W.R. (1999). Biology of aromatase inhibitors: pharmacology/endocrinology within the breast. Endocr Relat Cancer *6*, 187-195.

Mohla, S., Stearns, V., Sathyamoorthy, N., Rosenfeld, M.G., and Nelson, P. (2009). The biology of hormone refractory breast and prostate cancer: An NCI workshop report. Cancer Biol Ther *8*.

Nagle, J.A., Ma, Z., Byrne, M.A., White, M.F., and Shaw, L.M. (2004). Involvement of insulin receptor substrate 2 in mammary tumor metastasis. Mol Cell Biol *24*, 9726-9735.

Newman, D.J., and Cragg, G.M. (2007). Natural products as sources of new drugs over the last 25 years. J Nat Prod *70*, 461-477.

Ociepa-Zawal, M., Rubis, B., Lacinski, M., and Trzeciak, W.H. (2007). The effect of indole-3-carbinol on the expression of CYP1A1, CYP1B1 and AhR genes and proliferation of MCF-7 cells. Acta Biochim Pol *54*, 113-117.

Ohtake, F., Baba, A., Takada, I., Okada, M., Iwasaki, K., Miki, H., Takahashi, S., Kouzmenko, A., Nohara, K., Chiba, T., Fujii-Kuriyama, Y., and Kato, S. (2007). Dioxin receptor is a ligand-dependent E3 ubiquitin ligase. Nature *446*, 562-566.

Ohtake, F., Fujii-Kuriyama, Y., and Kato, S. (2009). AhR acts as an E3 ubiquitin ligase to modulate steroid receptor functions. Biochem Pharmacol *77*, 474-484.

Osborne, C.K., Wakeling, A., and Nicholson, R.I. (2004). Fulvestrant: an oestrogen receptor antagonist with a novel mechanism of action. Br J Cancer *90 Suppl 1*, S2-6.

Paranjape, J.M., Xu, D., Kushner, D.M., Okicki, J., Lindner, D.J., Cramer, H., Silverman, R.H., and Leaman, D.W. (2006). Human telomerase RNA degradation by 2'-5'-linked oligoadenylate antisense chimeras in a cell-free system, cultured tumor cells, and murine xenograft models. Oligonucleotides *16*, 225-238.

Pasqualini, J.R., and Chetrite, G.S. (2005). Recent insight on the control of enzymes involved in estrogen formation and transformation in human breast cancer. J Steroid Biochem Mol Biol *93*, 221-236.

Rahman, K.M., Li, Y., and Sarkar, F.H. (2004). Inactivation of akt and NF-kappaB play important roles during indole-3-carbinol-induced apoptosis in breast cancer cells. Nutr Cancer *48*, 84-94.

Reddel, R.R., Alexander, I.E., Koga, M., Shine, J., and Sutherland, R.L. (1988). Genetic instability and the development of steroid hormone insensitivity in cultured T 47D human breast cancer cells. Cancer Res *48*, 4340-4347.

Richter, C.A., Tillitt, D.E., and Hannink, M. (2001). Regulation of subcellular localization of the aryl hydrocarbon receptor (AhR). Arch Biochem Biophys *389*, 207-217.

Roger, P., Sahla, M.E., Makela, S., Gustafsson, J.A., Baldet, P., and Rochefort, H. (2001). Decreased expression of estrogen receptor beta protein in proliferative preinvasive mammary tumors. Cancer Res *61*, 2537-2541.

Sachdev, D., Li, S.L., Hartell, J.S., Fujita-Yamaguchi, Y., Miller, J.S., and Yee, D. (2003). A chimeric humanized single-chain antibody against the type I insulin-like growth factor (IGF) receptor renders breast cancer cells refractory to the mitogenic effects of IGF-I. Cancer Res *63*, 627-635.

Safe, S., Papineni, S., and Chintharlapalli, S. (2008). Cancer chemotherapy with indole-3-carbinol, bis(3'-indolyl)methane and synthetic analogs. Cancer Lett *269*, 326-338.

Safi, R., Kovacic, A., Gaillard, S., Murata, Y., Simpson, E.R., McDonnell, D.P., and Clyne, C.D. (2005). Coactivation of liver receptor homologue-1 by peroxisome proliferator-activated receptor gamma coactivator-1alpha on aromatase promoter II and its inhibition by activated retinoid X receptor suggest a novel target for breast-specific antiestrogen therapy. Cancer Res *65*, 11762-11770.

Santen, R., Cavalieri, E., Rogan, E., Russo, J., Guttenplan, J., Ingle, J., and Yue, W. (2009). Estrogen mediation of breast tumor formation involves estrogen receptor-dependent, as well as independent, genotoxic effects. Ann N Y Acad Sci *1155*, 132-140.

Shaaban, A.M., O'Neill, P.A., Davies, M.P., Sibson, R., West, C.R., Smith, P.H., and Foster, C.S. (2003). Declining estrogen receptor-beta expression defines malignant progression of human breast neoplasia. Am J Surg Pathol *27*, 1502-1512.

Shay, J.W., and Bacchetti, S. (1997). A survey of telomerase activity in human cancer. Eur J Cancer *33*, 787-791.

Shekhar, P.V., Chen, M.L., Werdell, J., Heppner, G.H., Miller, F.R., and Christman, J.K. (1998). Transcriptional activation of functional endogenous estrogen receptor gene expression in MCF10AT cells: a model for early breast cancer. Int J Oncol *13*, 907-915.

Sisci, D., Morelli, C., Cascio, S., Lanzino, M., Garofalo, C., Reiss, K., Garcia, M., Russo, A., Ando, S., and Surmacz, E. (2007). The estrogen receptor alpha:insulin receptor substrate 1 complex in breast cancer: structure-function relationships. Ann Oncol *18 Suppl 6*, vi81-85.

Smith, L.L., Coller, H.A., and Roberts, J.M. (2003). Telomerase modulates expression of growth-controlling genes and enhances cell proliferation. Nat Cell Biol *5*, 474-479.

Staub, R.E., Feng, C., Onisko, B., Bailey, G.S., Firestone, G.L., and Bjeldanes, L.F. (2002). Fate of indole-3-carbinol in cultured human breast tumor cells. Chem Res Toxicol *15*, 101-109.

Stewart, A.J., Johnson, M.D., May, F.E., and Westley, B.R. (1990). Role of insulin-like growth factors and the type I insulin-like growth factor receptor in the estrogen-stimulated proliferation of human breast cancer cells. J Biol Chem *265*, 21172-21178.

Strissel, P.L., Ellmann, S., Loprich, E., Thiel, F., Fasching, P.A., Stiegler, E., Hartmann, A., Beckmann, M.W., and Strick, R. (2008). Early aberrant insulin-like growth factor signaling in the progression to endometrial carcinoma is augmented by tamoxifen. Int J Cancer *123*, 2871-2879.

Sundar, S.N., Kerekatte, V., Equinozio, C.N., Doan, V.B., Bjeldanes, L.F., and Firestone, G.L. (2006). Indole-3-carbinol selectively uncouples expression and activity of estrogen receptor subtypes in human breast cancer cells. Mol Endocrinol *20*, 3070-3082.

Surmacz, E., and Bartucci, M. (2004). Role of estrogen receptor alpha in modulating IGF-I receptor signaling and function in breast cancer. J Exp Clin Cancer Res *23*, 385-394.

Takada, Y., Andreeff, M., and Aggarwal, B.B. (2005). Indole-3-carbinol suppresses NF-kappaB and IkappaBalpha kinase activation, causing inhibition of expression of NF-kappaB-regulated antiapoptotic and metastatic gene products and enhancement of apoptosis in myeloid and leukemia cells. Blood *106*, 641-649.

Takakura, M., Kyo, S., Kanaya, T., Hirano, H., Takeda, J., Yutsudo, M., and Inoue, M. (1999). Cloning of human telomerase catalytic subunit (hTERT) gene promoter and identification of proximal core promoter sequences essential for transcriptional activation in immortalized and cancer cells. Cancer Res *59*, 551-557.

Traish, A.M., and Morgentaler, A. (2009). Epidermal growth factor receptor expression escapes androgen regulation in prostate cancer: a potential molecular switch for tumour growth. Br J Cancer.

Tremblay, J.J., and Viger, R.S. (2001). GATA factors differentially activate multiple gonadal promoters through conserved GATA regulatory elements. Endocrinology *142*, 977-986.

Van den Berg, C.L., Cox, G.N., Stroh, C.A., Hilsenbeck, S.G., Weng, C.N., McDermott, M.J., Pratt, D., Osborne, C.K., Coronado-Heinsohn, E.B., and Yee, D. (1997).

Polyethylene glycol conjugated insulin-like growth factor binding protein-1 (IGFBP-1) inhibits growth of breast cancer in athymic mice. Eur J Cancer *33*, 1108-1113.

Wang, T.T., Milner, M.J., Milner, J.A., and Kim, Y.S. (2006). Estrogen receptor alpha as a target for indole-3-carbinol. J Nutr Biochem *17*, 659-664.

Wang, Y., Hailey, J., Williams, D., Lipari, P., Malkowski, M., Wang, X., Xie, L., Li, G., Saha, D., Ling, W.L., Cannon-Carlson, S., Greenberg, R., Ramos, R.A., Shields, R., Presta, L., Brams, P., Bishop, W.R., and Pachter, J.A. (2005). Inhibition of insulin-like growth factor-I receptor (IGF-IR) signaling and tumor cell growth by a fully human neutralizing anti-IGF-IR antibody. Mol Cancer Ther *4*, 1214-1221.

Weng, J.R., Tsai, C.H., Kulp, S.K., and Chen, C.S. (2008). Indole-3-carbinol as a chemopreventive and anti-cancer agent. Cancer Lett *262*, 153-163.

Werner, H., and Bruchim, I. (2009). The insulin-like growth factor-I receptor as an oncogene. Arch Physiol Biochem *115*, 58-71.

Wittman, M., Carboni, J., Attar, R., Balasubramanian, B., Balimane, P., Brassil, P., Beaulieu, F., Chang, C., Clarke, W., Dell, J., Eummer, J., Frennesson, D., Gottardis, M., Greer, A., Hansel, S., Hurlburt, W., Jacobson, B., Krishnananthan, S., Lee, F.Y., Li, A., Lin, T.A., Liu, P., Ouellet, C., Sang, X., Saulnier, M.G., Stoffan, K., Sun, Y., Velaparthi, U., Wong, H., Yang, Z., Zimmermann, K., Zoeckler, M., and Vyas, D. (2005). Discovery of a (1H-benzoimidazol-2-yl)-1H-pyridin-2-one (BMS-536924) inhibitor of insulin-like growth factor I receptor kinase with in vivo antitumor activity. J Med Chem *48*, 5639-5643.

Wormke, M., Stoner, M., Saville, B., Walker, K., Abdelrahim, M., Burghardt, R., and Safe, S. (2003). The aryl hydrocarbon receptor mediates degradation of estrogen receptor alpha through activation of proteasomes. Mol Cell Biol *23*, 1843-1855.

Zhang, X., Mar, V., Zhou, W., Harrington, L., and Robinson, M.O. (1999a). Telomere shortening and apoptosis in telomerase-inhibited human tumor cells. Genes Dev *13*, 2388-2399.

Zhang, X.W., Liao, H.N., and Tong, T.J. (1999b). Telomere Shortening of MCF-7 Cells Caused by Antisense Telomerase cDNA. Sheng Wu Hua Xue Yu Sheng Wu Wu Li Xue Bao (Shanghai) *31*, 527-530.

Zhou, Q., Atadja, P., and Davidson, N.E. (2007). Histone deacetylase inhibitor LBH589 reactivates silenced estrogen receptor alpha (ER) gene expression without loss of DNA hypermethylation. Cancer Biol Ther *6*, 64-69.